Modelling for Flight Control

DANIEL JARRETT AUGER

MICHAELMAS 2004

FITZWILLIAM COLLEGE, CAMBRIDGE

THIS DISSERTATION IS SUBMITTED FOR THE DEGREE OF DOCTOR OF PHILOSOPHY

Summary

This dissertation considers model (in)validation in the context of closed-loop control. Real-world data invariably differs from that predicted by mathematical models. Discrepancies are due to modelling inaccuracy or exogenous noise. We address the question of whether given data is consistent with a member model set consisting of a 'ball' of systems in Vinnicombe's ν-gap metric. Existence can be determined using tangential Carathéodory-Fejér interpolation techniques, however the full necessary and sufficient conditions are non-convex in the presence of noise. In previous work, e.g. by Steele and Vinnicombe, these conditions are approximated to give sufficient conditions for consistency. This work proposes a technique for improving these approximations by successive relinearization about previous solutions, extends this to systems with non-zero initial conditions and proposes techniques for the construction of interpolants using Nevanlinna-Pick methods.

The work also considers an approach put forward by Smith, Dullerud and Miller in which the Yakubovich's $\mathcal{S}$-procedure is applied to problems with linear time-varying perturbations. A claimed necessary and sufficient condition for invalidation is shown to be sufficient only, a tighter sufficient condition is put forward, and a similar condition for non-causal perturbations is proposed.

Finally, model (in)validation techniques are applied to flight test data from QinetiQ's VAAC Harrier. Two experiments are performed on the longitudinal dynamics with different signal injection points. The techniques are seen to work effectively for both, though one experiment is considered more informative than the other. When the initial state is fixed at zero, causality and time-invariance are significant constraints, but when the initial state could vary, only time-invariance is significant. Two dynamic weighting strategies are considered, one based on the frequency-wise optimal stability margin, the other on a simplified 'proportional integral' approximation with the same all-frequency stability properties. These give consistent results. Interpolants are constructed and found to have unrealistically ragged frequency responses.

Preface

The primary funding for this work was supplied by the Engineering and Physical Sciences Research Council, with further support from QinetiQ. I am also grateful to have received additional support from AMS Radar Systems, the Isaac Newton Trust and Fitzwilliam College, Cambridge. I would like to express my thanks to all of these, without whom it would have been difficult or impossible for me to pursue graduate study here.

I would like to express my particular thanks to my supervisor, Dr Glenn Vinnicombe, whose support and advice have been stimulating and invaluable. I would also like to thank Dr Yoge Patel and Glenn De Mello of QinetiQ, in particular for supplying data from the VAAC Harrier (and advice on how to decode it!) and Professor Keith Glover for introducing us. Similarly, I would like to thank Professor David Cardwell for introducing me to AMS.

Members of the Department of Engineering's Control Group have given the opportunity for many interesting discussions, and I would like to thank Paresh Date, John Steele and Jonathan Paxman in particular. John's work, building on that of Rob Davis, laid the foundation for much that is here, and Jonathan and Paresh's insights have proved very useful. I would also like to thank Professor Roy Smith, whose visit to the Group was the starting point for the work of Chapter 6.

I would also like to thank my friends and family. There are a great many people deserving of a special mention and it wouldn't be possible to name them all. Particular thanks go to my parents, David and Kathryn Auger, and to my college-friends, John Bradbury, Isobel Hood, and Roman and Carrie Roth, for their excellent and

regular hospitality. A special mention must go to Paul Roberts, who, finding himself stuck up a very similar tree to the one I was in, has offered valuable moral support, encouragement and good coffee throughout our Ph.Ds.[1] Paul and I have a mutual friend who I shall not name here in case my examiners ask me to prove His existence. He is the one person—or perhaps I should say 'one of three persons of one substance'—who does have a perfect model for every system. All that is good in this dissertation I offer back to Him. The faults, though still offered, are entirely my own work.

This dissertation is dedicated to my parents. I shall of course pretend that it is necessary for them to read it cover to cover, but I shall not grumble too much if they simply read the introduction and then look at the colour pictures.

As a last minute addition, I would like to explicitly thank my proof-readers. Dr Glenn Vinnicombe 'did not proof read' my dissertation, but picked up a large portion of imaginative and innovative spellings none-the-less, and the job was well-completed over a single weekend by Dr Diana Galletly, Dr David Gillingham, Colin Jones, Ioannis Lestas, Dr Christos Papageorgiou, Dr Roman Roth, Carys Underdown and Oli Watkins. Many thanks to all!

[1] We have also encouraged each other to eat far too much chocolate and our 'Diet Coke' rota has almost certainly turned me into a borderline caffeine addict!

This dissertation is the result of my own work and includes nothing which is the outcome of work done in collaboration except where specifically indicated in the text. Including appendices, bibliography, footnotes, tables and equations, this dissertation contains approximately 40,000 words and just under fifty figures.[2] This is well within the limits specified by the Engineering Degree Committee.

[2]This word count was produced by parsing the relevant DVI file with `dvi2tty Thesis.dvi | wc -w` so it may well be an overestimate.

Contents

Chapter 1

Introduction

The real world is a complicated place and our attempts to describe it will inevitably fall short. This is immediately clear in the arts and humanities, but it is equally true of the applied sciences. Though our mathematics—given certain axioms—can be shown to be true in an absolute sense, any attempt to model a physical system, say, a car suspension or an aeroplane in flight—will result in something that is 'lesser' than the original system. Even if our estimates of all relevant physical quantities are correct, it is likely that we will have taken a simplified view of the system dynamics and ignored the potential for interaction with the rest of the world. The problem is concisely expressed in the introduction to [Vin01], the author of which is explaining the only two motivations for using feedback in control:

> 'There are two, and only two, reasons for using feedback. The first is to reduce the effect of any unmeasured disturbances acting on the system. The second is to reduce the effect of any uncertainty about the system dynamics.'

If we want a model that will perfectly capture all aspects of a physical system's behaviour, it is most unlikely that we shall ever be satisfied. However as control engineers, our real concern is to determine whether a given model captures the system's behaviour sufficiently well for us to achieve our given performance and stability objectives. Again from [Vin01],

> 'One of the key aims of feedback is to minimize the effects of lack of knowledge about a system which is to be controlled. Yet, one clearly needs to know *something* about the system in order to be able to design an effective feedback compensator for it ... "how much do we need to know about a system in order to design a feedback compensator that leaves the closed loop behaviour insensitive to that which we don't know?" '

In this work, we shall consider the problem of determining whether a model satisfactorily accounts for the measured behaviour of an actual system. This process is often called 'model validation'. After further developing existing techniques, we shall demonstrate their practical application using flight test data from QinetiQ's VAAC Harrier.

Model Validation and the Modelling Process

Model validation is part of the modelling process, a general framework for which follows:

1. Form a model based on physical insights and/or experimental data.
2. Test the model experimentally, taking measurements.
3. Compare the measurements with the model, and decide whether the model is good enough. If so FINISH; otherwise continue.
4. Refine the model based on further experimentation/insight.
5. Return to step 2.

There are plenty of variations on this. One source [Lju99a] caracatures a control-oriented modelling process as a 'game' involving the modeller and control designer: the modeller tries to produce a model that is as good as possible; the control engineer tries to design a controller that is robust as possible. The fundamental points,

however, are the same. Validation involves the comparison of models against new data, data from which they were not derived. The construction of a model that will accurately fit a given data set is often relatively straightforward, though the model may be complex; the true test of a model is its ability to predict the unknown.

An example of a practical application of 'validation ideas' is the notion of iterative control design by falsification. [VW00, Chapter 11]. In this scheme, a robust model set is progressively refined through experiment with controller designed for an 'optimistic' model chosen to give the best possible results from the unfalsified set. The control performance can be shown to converge to that 'best achievable performance and the practical potential has been demonstrated through published simulation results. [Ver00] There are differences between that scheme and the work presented herein, particularly parameterization of the model set. ('Robust control' is dealt with here in terms of coprime-factor perturbation model sets; in the iterative design schemes the model sets based on a parameter vector θ are reminiscent of those used in stochastic identification theory.[Lju99b])

There is a slight variation in terminology: some authors describe a model set that has not been shown inconsistent with reality (given certain assumptions, of course) as 'unfalsified'; others describe the set as 'not invalidated'. Both are, in a sense, ugly expressions involving an inherent double negation (at least if one regards 'false' as a negation). The body of published work that this most naturally follows on from uses the 'not invalidated' terminology. The choice to continue in this tradition is not intended to make a statement about the appropriateness of the alternatives.

Essentially, model validation always involves human decision making of some kind. In chapter 7, for example, 'trade off curves' are presented showing the amount of noise required for consistency plotted against the level of model perturbation required. There are no hard-and-fast rules for deciding what is acceptable. In some applications, large oscillations and near marginal stability may well be acceptable, but sluggish performance may be wholly so; in other applications, the rise time may be near irrelevant but solid stabilization of utmost importance. The techniques

presented herein offer tools to those who make decisions on model quality; it is beyond the scope of this work to judge exactly how these tools should be used.

Our Definition of Model Validation

The definition that follows shall be used universally throughout this work and is common in some parts of the literature. [Dav96, SV01]. [1]

Strictly speaking, a model P is *valid* if for all possible input-output pairs (u, y), the standard interpolation equation $y = Pu$ is satisfied. Similarly, a model set $\mathcal{P}$ is valid if there exists a single model $\hat{P} \in \mathcal{P}$ satisfying $y = \hat{P}u$. In practice, this is impossible to determine since we can never have access to all input pairs, merely a subset of them.

In practice, the problem considered is more usually one of invalidation or non-invalidation. Clearly, a model or model set is not valid if it does not account for any particular datum since it cannot account for the whole.

The robust control framework in which we are working is described in detail in Chapter 3. The model sets in which we are principally interested are described in terms of their robustness to coprime factor perturbations. Given a nominal model P_0 and a ν-gap radius beta, we shall attempt to establish the existence of a system $\hat{P} \in \{P_1 : \delta_\nu(P_0, P_1) < \beta\}$ that interpolates the measured data. We shall also allow exogenous noise.

Gap-based model validation was considered by Davis [Dav96], who derived necessary and sufficient conditions for validation in the gap and ν-gap metrics. These dealt with linear uncertainty, both time-invariant and time-varying, using tangential Carathéodory-Fejér interpolation techniques and their LTV equivalents [PKT$^+$92,

[1] In other published works the term valid is used to describe extended parameter vectors consistent with infinite time-horizon data sequences, with 'unfalsified' being used for time-truncated sequences. [Ver00]

PKT+94]. This resulted in constraints of the form

$$\begin{bmatrix} P^*P + P^*X + X^*P + X^*X & Q^* + Y^* \\ Q + Y & \gamma I \end{bmatrix} \geq 0 \tag{1.1}$$

where P and Q are related to the measurements, X represents the noise at the input to the uncertainty, Y represents the noise at the output of the uncertainty and $\gamma \in \mathbb{R}^+$. He noted that this was non-convex in X and Y, and simplified it by setting $X = 0$. The resulting constraint

$$\begin{bmatrix} P^*P & Q^* + Y^* \\ Q + Y & \gamma I \end{bmatrix} \geq 0$$

is a linear matrix inequality in Y (and γ) and is thus convex. The condition is an approximation, and neither sufficient nor necessary for validation. Davis's work is complemented by that of Chen [CW96], who showed that non-convexity occurred whenever a noise signal was present at the input to an uncertainty.

In more recent work, Steele and Vinnicombe [SV01] noted that the non-convex necessary and sufficient conditions would be convex were it not for the quadratic term in the (1,1) element of (1.1). Since noise signals are likely to be small, a convex constraint of the form

$$\begin{bmatrix} P^*P + P^*X + X^*P & Q^* + Y^* \\ Q + Y & \gamma I \end{bmatrix} \geq 0$$

would be a good approximation. More importantly, the Schur complement shows that it is a sufficient condition for validation: if a solution to the problem can be found, then the model is not invalidated. This was applied to the LTI and LTV ν-gap metric problems. Details are given in Chapter 4. New developments, including the accommodation of an initial state, iterative relinearization of the approximated perturbation block constraints to achieve something closer to the unapproximated

constraints and construction of interpolant plants are presented in Chapter 5. Chapter 6 considers invalidation methods using the S-procedure [Yak77], introducing a convex necessary and sufficient invalidation condition for LFT model sets with noncausal perturbation blocks and sufficient conditions for invalidation with LTV perturbations. A contradiction is noted with a claim in [SDM00].

Throughout this dissertation, we assume that the system is adequately approximated by discrete time systems. Alternative approaches based on 'lifting' are presented in [BP90, SD96, SDwn]. These allow systems to be 'h-anticipatory', i.e. non-causal within the inter-sample period, and may be more appropriate than our sample-and-hold approach in some applications.

The VAAC Harrier

The VAAC Harrier and its WEMSIM model is described in greater detail in Chapter 7, and is operated by QinetiQ (formerly DERA, etc.) to demonstrate advanced control law concepts. Rick Hyde and others [Hyd91, HGS95, Hyd00] carried out work on the application of McFarlane and Glover's $\mathcal{H}_\infty$ loopshaping robust control technique [MG90]. Davis [Dav96] carried out gap-metric validation on the VAAC Harrier (though with a different model) and some of his work has been implemented as a real-time Simulink model by Mathworks, Inc. A new investigation, based on validation in the ν-gap, is also presented in Chapter 7.

The ultimate aim of the application of (in)validation techniques in flight testing would be to allow real-time flight envelope expansion. At present, the problems are too complex for this though it may one day be a possibility.

Chapter 2

Mathematical Preliminaries

The notation in this dissertation is as far as possible consistent with that in standard text books, e.g. [CG00, ZDG95, Vin01], and the meaning is usually clear from the context. Note that a positive feedback convention has been used. There are many conventions for describing plant and controller; here, the symbols P and C denote plant and controller respectively. G will often be used to denote a 'general' system.

An underlying assumption we shall make is that our validation experiments involve data sampled at a constant rate, and we shall deal with discrete-time models only. The standard z is used for the inverse of the unit delay, although very occasionally $\lambda = z^{-1}$ has been used.

2.1 Norms and signal spaces

A detailed discussion of norms and signal spaces may be found in a standard text book [ZDG95]. The following reminders may be useful:

ℓ_p norm For a sequence $x = (x_0, x_1, \dots)$

$$\|x\|_p := \left(\sum_{i=0}^{\infty} |x_i|^p \right)^{1/p}$$

ℓ_∞ **norm** For a sequence $x = (x_0, x_1, \dots)$

$$\|x\|_\infty := \sup_i |x_i|$$

power For a sequence $x = (x_0, x_1, \dots, x_{N-1})$

$$\text{pow}(x) := \frac{1}{N} \sum_{i=0}^{N-1} |x_i|^2$$

The symbol $\mathcal{S}_k$ denotes a signal with k elements, i.e. $x = \{x_0, x_1\} \in \mathcal{S}_2$. ($\mathcal{S}_k^m$ indicates that each element of the sequence is a vector with m elements.)

$\mathcal{H}_\infty$ **norm** For a a system F

$$\|F\|_\infty := \sup_{|z^{-1}|<1} \overline{\sigma}[F(z^{-1})]$$

$\mathcal{H}_\infty$ **Space** $\mathcal{H}_\infty$ is a closed subspace of matrix-valued functions that are analytic and bounded inside the unit circle. $\mathcal{RH}_\infty$ is the subspace of real-rational functions in $\mathcal{H}_\infty$.

$\mathcal{L}_\infty$ **Space** $\mathcal{L}_\infty$ is a closed subspace of matrix-valued functions that are essentially bounded on the unit disc, with norm

$$\|F\|_\infty := \text{ess sup}_{\Omega \in (-2\pi, 2\pi]} \overline{\sigma} \left[F\left(e^{j\Omega}\right) \right]$$

$\mathcal{H}_\infty^-$ **Space** $\mathcal{H}_\infty^-$ is a (closed) subspace of $\mathcal{L}_\infty$ with functions that are analytic and bounded in the open unit disc. [ZDG95, Chapter 4].

$||G||_{i2}$ denotes the *induced 2-norm* of G, namely

$$\sup_u \frac{||G * u||_2}{||u||_2}$$

$\mathbb{D}$, $\delta\mathbb{D}$ $\mathbb{D}$ represents the open unit disk; $\delta\mathbb{D}$ represents the unit circle.

$\mathcal{S}_k^p$ represents the space of all real-valued finite-length signals of the form $\{u_0, u_1, \ldots, u_{k-1}\}$ where $u_i \in \mathbb{R}^p$

$\mathcal{L}_2$, $\mathcal{H}_2$, $\mathcal{H}_2^\perp$ $\mathcal{L}_2$ is the space of square integrable functions on $\delta\mathbb{D}$. $\mathcal{H}_2$ is the subspace of square integrable functions on $\delta\mathbb{D}$ analytic in the unit circle; $\mathcal{H}_2^\perp$ is the subspace of square integrable functions on $\delta\mathbb{D}$ analytic outside the unit circle.

$G^\sim$ $G^\sim(z) := G^T(z^{-1})$.

As indicated at the start of this chapter, notation is generally standard, following the pattern of texts such as [ZDG95].

2.2 Stacking and truncation of sequences

Consider a sequence $u = \{u_0, u_1, u_2, \ldots\}$. We define the vec operation as follows:

$$\text{vec}\,(u) = \begin{pmatrix} u_0 \\ u_1 \\ \vdots \end{pmatrix} \tag{2.1}$$

Remark 2.1 The vec notation is cumbersome, and will be dropped from time to time, the context (usually being an interpolation problem) dictating the meaning. ♡

The symbol Π_k is the k-step truncation operator, i.e. the operator that truncates a sequence to its first k elements. (When applied to a Toeplitz operator (see below) it works in the logical sense.)

2.3 Hankel and Toeplitz operators

The *Hankel Operator* is discussed in detail in Zhou et al [ZDG95] and Chen and Gu [CG00] and is in essence a mapping from past inputs to future outputs. It has

a number of applications in control theory, amongst these being the solution of the Nehari problem (Section 2.6.1).

The *Toeplitz Operator* is a mapping from inputs at and after some instant to outputs at and after that instant and is closely related to the impulse response of the system.

In order to define the operators, it is useful to define some orthogonal projections:

$$P_+ : l_2(-\infty, \infty) \mapsto l_2[0, \infty) \text{ or } \mathcal{L}_2(\partial\mathbb{D}) \mapsto \mathcal{H}_2(\partial\mathbb{D})$$

$$P_- : l_2(-\infty, \infty) \mapsto l_2(-\infty, 0) \text{ or } \mathcal{L}_2(\partial\mathbb{D}) \mapsto \mathcal{H}_2^\perp(\partial\mathbb{D})$$

The notation used in the following definitions is taken from [ZDG95, Section 8.1], where it is illustrated in diagramatic form.

Definition 2.2 (Hankel Operator) Consider a matrix function $G_d(\lambda) \in \mathcal{L}_\infty$. The discrete time Hankel Operator is defined as follows:

$$\Gamma_{G_d} : l_2(-\infty, 0) \mapsto l_2[0, \infty) \text{ or } \mathcal{H}_2^\perp(\partial\mathbb{D}) \mapsto \mathcal{H}_2(\partial\mathbb{D})$$

$$\Gamma_{G_d} = P_+ M_{G_d}|_{\mathcal{H}_2^\perp(\partial\mathbb{D})} \tag{2.2}$$

Definition 2.3 (Toeplitz Operator) The corresponding Toeplitz Operator is defined as

$$T_{G_d} : l_2[0, \infty) \mapsto l_2[0, \infty) \text{ or } \mathcal{H}_2(\partial\mathbb{D}) \mapsto \mathcal{H}_2(\partial\mathbb{D})$$

$$T_{G_d} = P_+ M_{G_d}|_{\mathcal{H}_2(\partial\mathbb{D})} \tag{2.3}$$

Let $G_d(\lambda) = \sum_{i=-\infty}^{\infty} G_i \lambda^i \in \mathcal{L}_\infty$. We can obtain the output sequence $\{y_i\}$ from the input $\{u_k\}$ by convolution:

$$y_k = \sum_{i=-\infty}^{\infty} G_i u_{k-i}$$

We can thus write an expression relating the input to the output:

$$\left(\begin{array}{c} y_0 \\ y_1 \\ \vdots \\ \hline y_{-1} \\ y_{-2} \\ \vdots \end{array}\right) = \left[\begin{array}{ccc|ccc} G_0 & G_{-1} & \bullet & G_1 & G_2 & \bullet \\ G_1 & G_0 & \bullet & G_2 & G_3 & \bullet \\ \bullet & \bullet & \bullet & \bullet & \bullet & \bullet \\ \hline G_{-1} & G_{-2} & \bullet & G_0 & G_1 & \bullet \\ G_{-2} & G_{-3} & \bullet & G_{-1} & G_0 & \bullet \\ \bullet & \bullet & \bullet & \bullet & \bullet & \bullet \end{array}\right] \left(\begin{array}{c} u_0 \\ u_1 \\ \vdots \\ \hline u_{-1} \\ u_{-2} \\ \vdots \end{array}\right)$$

$$=: \left[\begin{array}{c|c} T_1 & H_1 \\ \hline H_2 & T_2 \end{array}\right] \left(\begin{array}{c} u_0 \\ u_1 \\ \vdots \\ \hline u_{-1} \\ u_{-2} \\ \vdots \end{array}\right) \tag{2.4}$$

The 'purpose' of each of these blocks is as follows:

T_1	maps 'future' inputs to 'future' outputs;
T_2	maps 'past' inputs to 'past' outputs;
H_1	maps 'past' inputs to 'future' outputs; and
H_2	maps 'future' inputs to 'past' outputs.

T_1 and T_2 are called *block Toeplitz matrices*, and T_1 is the matrix representation of the Toeplitz operator. Similarly, H_1 and H_2 are called *block Hankel matrices* and H_1 is the matrix representation of the Hankel operator.

Some useful results relating to this form may be found in, for example, Zhou et al [ZDG95]: firstly,

$$\|G_d(\lambda)\|_\infty = \left\| \begin{bmatrix} T_1 & H_1 \\ H_2 & T_2 \end{bmatrix} \right\|, \ \|\Gamma_{G_d}\| = \|H_1\|, \text{ and } \|T_{G_d}\| = \|T_1\|$$

and, secondly, under the bilinear transformation, the discrete time and continuous time Hankel norms are unchanged.

Causality

For a causal system, $G_i = 0,\ \forall i < 0$. Consequently, we will find that $H_2 = 0$, i.e., no 'future' inputs are mapped to 'past' outputs. Equation (2.4) becomes:

$$\left(\begin{array}{c} y_0 \\ y_1 \\ \vdots \\ \hline y_{-1} \\ y_{-2} \\ \vdots \end{array}\right) = \left[\begin{array}{ccc|ccc} G_0 & 0 & 0 & G_1 & G_2 & \bullet \\ G_1 & G_0 & 0 & G_2 & G_3 & \bullet \\ \bullet & \bullet & \ddots & \bullet & \bullet & \bullet \\ \hline 0 & 0 & 0 & G_0 & G_1 & \bullet \\ 0 & 0 & 0 & 0 & G_0 & \bullet \\ 0 & 0 & 0 & 0 & 0 & \ddots \end{array}\right] \left(\begin{array}{c} u_0 \\ u_1 \\ \vdots \\ \hline u_{-1} \\ u_{-2} \\ \vdots \end{array}\right)$$

$$=: \left[\begin{array}{c|c} T_1 & H_1 \\ \hline H_2 & T_2 \end{array}\right] \left(\begin{array}{c} u_0 \\ u_1 \\ \vdots \\ \hline u_{-1} \\ u_{-2} \\ \vdots \end{array}\right) \tag{2.5}$$

The Toeplitz matrices have now taken on a triangular form: T_1 is a *lower block Toeplitz matrix* and T_2 is an *upper block Toeplitz matrix*.

Note that when we use the state space form $G_d(\lambda) = \left[\begin{array}{c|c} \Phi & \Gamma \\ \hline C & D \end{array}\right]$ we can find T_1 as follows:

$$T_1 = \begin{bmatrix} D & 0 & 0 & \cdots & 0 \\ C\Gamma & D & 0 & \cdots & 0 \\ C\Phi\Gamma & C\Gamma & D & \cdots & 0 \\ C\Phi^2\Gamma & C\Phi\Gamma & C\Gamma & \ddots & 0 \\ \vdots & \vdots & \vdots & & D \end{bmatrix} \tag{2.6}$$

Remark 2.4 Given a $p \times q$ system P, the notation 'T_P' indicates the lower block Toeplitz matrix corresponding to 'T_1' in the text above.

The notation $\Pi_l T_P$, denoting the $p\ell \times q\ell$ upper-left partition of the T_P is cumbersome. When working with finite data sequences, it will often be abbreviated to 'T_P'; it will be clear that a truncated matrix is meant by the context, and readability will be greatly improved.

The notation T_u applied to some infinite sequence $\{u_0, u_1, \dots\}$ indicates an infinite lower block Toeplitz matrix of the form

$$\begin{bmatrix} u_0 & 0 & \cdots \\ u_1 & u_0 & \cdots \\ \vdots & \vdots & \ddots \end{bmatrix}$$

Similarly, when dealing with finite-length sequences the same notation will indicate a *finite* matrix. ♡

2.4 The Schur complement and LMIs

Given the partitioned matrix

$$A := \begin{bmatrix} A_{11} & A_{21}^* \\ A_{21} & A_{22} \end{bmatrix} = A^*$$

the *Schur complement* of A_{11} in A is

$$X := A_{22} - A_{21}A_{11}^{-1}A_{21}^*;$$

and the Schur complement of A_{22} in A is

$$\widehat{X} := A_{11} - A_{21}^*A_{22}^{-1}A_{21}.$$

If $A_{11} > 0$, then $A \geq 0$ if and only if $X \geq 0$. Similarly, if $A_{22} > 0$, then $A \geq 0$ if and only if $\widehat{X} \geq 0$. (This is discussed in more detail in, for example, [ZDG95, Ch. 2 Sec. 3].)

This has applications in interpolation theory, where a common problem is to find the smallest feasible γ in

$$\gamma^2 T_s^* T_s - T_t^* T_t \geq 0.$$

This can be formulated as a Linear Matrix Inequality (LMI) minimization problem in $x = \gamma^2$: What is the smallest x for which

$$\begin{bmatrix} xT_s^*T_s & T_t^* \\ T_t & I \end{bmatrix} \geq 0 \ ? \tag{2.7}$$

or as an LMI minimisation problem in $\hat{x} = \gamma^2$: What is the largest $\hat{x}$ for which

$$\begin{bmatrix} T_s^*T_s & T_t^* \\ T_t & \hat{x}I \end{bmatrix} \geq 0 \ ? \tag{2.8}$$

Similarly, the constraint

$$A^2 - v^* T_P^* T_P v \geq 0$$

or

$$A - v^* T_P^* \frac{1}{A} T_P v \geq 0$$

with $A > 0$ may be represented as

$$\begin{bmatrix} A & v^* T_P^* \\ T_P v & AI \end{bmatrix} \geq 0$$

or equivalently

$$\begin{bmatrix} A^2 & v^* T_P^* \\ T_P v & I \end{bmatrix} \geq 0 \tag{2.9}$$

Convexity A function $f(x)$ is said to be convex in $[a, b]$ if for all $\lambda \in [0, 1]$,

$$f(\lambda a + (1 - \lambda)b) \leq \lambda f(a) + (1 - \lambda) f(b)$$

When a convex function is minimized over a convex set, any local minimum will turn out to be a global minimum. [CG00, Appendix B] Convex problems are considered to be computationally tractable. [Dav96] provides a number of results relating to the convexity of model validation problems, noting that many are 'NP hard'. Chapter 4 of [Dav96] discusses this in further detail. One property of NP hard problems is that the number of computations required to find the solution is not polynomially bounded in the problem size.[1]

If a problem can be formulated as an LMI, this implies convexity [CG00, Appendix B]. MATLAB's LMI Control Toolbox solves LMI problems efficiently using interior point algorithms, although they take much longer to solve than, say, a Riccati equation.

[1] Examples of non-polynomial bounds are factorials and exponentials.

2.5 The $\mathcal{S}$-procedure

The S-procedure is stated in the following form in [SDM00]:

Proposition 2.5 ($\mathcal{S}$-Procedure) *Let $Q_0(\chi), Q_1(\chi), \ldots Q_n(\chi)$ be quadratic matrix functions of vector $\chi \in \mathbb{R}^\ell$. If there exist scalars $\tau_i \geq 0$, $i = 1, \ldots, n$, such that*

$$Q_0(\chi) - \sum_{i=1}^{n} \tau_i Q_i(\chi) \geq 0, \text{ for all } \chi, \tag{2.10}$$

then, for all χ such that $Q_i(\chi) \geq 0$, $i = 1, \ldots, n$;

$$Q_0(\chi) \geq 0. \tag{2.11}$$

If $n = 1$ then this condition is necessary and sufficient.

The sufficiency of Proposition 2.5 is easy to see: if all $Q_i(\chi) \geq 0$, $i = 1, \ldots, n$ then (2.11) *must* hold true. The necessity when $n = 1$ is described in [Boy04] as 'not easy to prove' and the interested reader may wish to follow this up in the original sources [Yak77].[2]

2.6 Interpolation problems

2.6.1 The Nehari problem

The Nehari problem is discussed in detail by Zhou et al [ZDG95] and by Chen and Gu [CG00].

Nehari Problem Given $G \in \mathcal{L}_\infty$, determine

$$\inf_{Q \in \mathcal{H}_\infty} \|G - Q\|_\infty \tag{2.12}$$

and find a minimizer $Q \in \mathcal{H}_\infty$.

[2] The form when $n = 1$ the $\mathcal{S} - procedure$ is 'lossless'.

The solution is given by Nehari's Theorem:

Theorem 2.6 (Nehari's Theorem [ZDG95]) *Suppose $G \in \mathcal{L}_\infty$, then*

$$\inf_{Q \in \mathcal{H}_\infty^-} \|G - Q\|_\infty = \|\Gamma_G\|$$

and the infimum is achieved.

Corollary 2.7 *Suppose $G \in \mathcal{L}_\infty$ and let $\hat{\Gamma}_G = \Gamma^*_{G^\sim}$. Then*

$$\inf_{Q \in \mathcal{H}_\infty} \|G - Q\|_\infty = \|\hat{\Gamma}_G\|$$

and the infimum is achieved.

2.6.2 The Nevanlinna-Pick Interpolation Problem

The Nevanlinna-Pick Interpolation Problem is described for continuous SISO problems in Doyle et al [DFT92], and in the general discrete time case in Chen and Gu [CG00], for example.

Nevanlinna-Pick interpolation problem Let $\mathbb{D}$ and $\overline{\mathbb{D}}$ denote the open and closed unit discs respectively. Given $z_i \in \mathbb{D}$ and w_i in $\overline{\mathbb{D}}$, $i = 1, 2, \ldots, n$, where z_i are distinct, find an *interpolant*, i.e. a function $Q \in \overline{\mathcal{B}}\mathcal{H}_\infty(\mathbb{D})$ such that

$$Q(z_i) = w_i, \ i = 1, 2, \ldots, n \tag{2.13}$$

where $\overline{\mathcal{B}}\mathcal{H}_\infty(\mathbb{D})$ is the closed unit ball in $\mathcal{H}_\infty(\mathbb{D})$, i.e.

$$\overline{\mathcal{B}}\mathcal{H}_\infty(\mathbb{D}) := \{G \in \mathcal{H}_\infty(\mathbb{D}), \|G\|_\infty \leq 1\}$$

It is demonstrated in [CG00] that this interpolation problem can be reformulated as a Nehari problem. This can be seen by considering some polynomial $P \in \mathcal{H}_\infty(\mathbb{D})$

such that $P(z_i) = w_i$—this can always be obtained by Lagrange interpolation[3]—and observing that $Q - P$ must have zeros at all z_i. We can thus write

$$Q - P = BG$$

where $G \in \mathcal{H}_\infty(\mathbb{D})$ and $B = \prod_{i=1}^{n} \frac{\lambda - z_i}{1 - \bar{z}_i \lambda}$. The problem is thus to find a function satisfying

$$\left\| B^{-1}P + Q \right\|_\infty \leq 1$$

which is essentially the Nehari Problem.

Full details of the Nevanlinna-Pick algorithm, which gives the entire family of interpolants, are extensive and may be found in Chen and Gu [CG00]. One important theorem—that as to whether a solution exists—is reproduced here:

Theorem 2.8 *Given $z_i \in \mathbb{D}$ and $w_i \in \overline{\mathbb{D}}$, $i = 1, 2, \ldots, n$, where z_i are distinct, there exists an interpolant $Q \in \overline{\mathcal{B}}\mathcal{H}_\infty(\mathbb{D})$ such that (2.13) holds if and only if the* Pick matrix *Q defined by*

$$Q_{ij} = \left[\frac{1 - w_i \bar{w}_j}{1 - z_i \bar{z}_j} \right] \tag{2.14}$$

is positive semidefinite.

Furthermore, the solution is unique if and only if $\det Q = 0$.

2.6.3 Carathéodory-Fejér interpolation

The Carathéodory-Fejér problem is stated by Chen and Gu [CG00] as follows:

Carathéodory-Fejér Problem Given complex numbers c_i, $i = 0, 1, \ldots, n-1$, find a function $\hat{h} \in \overline{\mathcal{B}}\mathcal{H}_\infty(\mathbb{D})$ such that

$$\hat{h}(\lambda) = c_o + c_1\lambda + \cdots + c_n\lambda^{n-1} + \lambda^n \hat{g}(\lambda) \tag{2.15}$$

where $\hat{g} \in \overline{\mathcal{B}}\mathcal{H}_\infty(\mathbb{D})$.

[3] An explanation of this is given, for example, in [CG00, Ch. 2 Sec. 3.2]

In other words, the Carathéodory-Fejér problem is to find a function whose impulse response is the data sequence in question.

The first n coefficients of the Taylor expansion of $\hat{h}$ are required to match the given numbers, that is

$$\frac{\hat{h}^{(k)}(0)}{k!} = c_k, \;\; k = 0, 1, \ldots, n-1$$

This is similar to the Nevanlinna-Pick problem, but we have interpolation conditions repeated at the origin. Similarly, the Carathéodory-Fejér problem can also be posed as one of Nehari best approximation. This is not used in this work, but the interested reader may find more on the subject in a standard work on interpolation such as [Dym89].

To see how this relates to time-domain model validation, we need to write our transfer function in terms of $\lambda = z^{-1}$, the unit delay operator. The k-th derivative of the transfer function $G(\lambda)$ is thus

$$G^{(k)}(\lambda) = \begin{cases} D + C(I - \lambda A)^{-1}\lambda B, & k = 0, \\ k!C(I - \lambda A)^{-(k+1)}A^{(k-1)}B, & k = 1, 2, \ldots \end{cases}$$

this gives

$$\frac{G^{(k)}(0)}{k!} = \begin{cases} D, & k = 0, \\ CA^{(k-1)}B & , k = 1, 2, \ldots \end{cases}$$

This relates the norm-bounded impulse-response fitting problem directly to the Carathéodory-Fejér problem.

The condition for the existence of solutions to such problems is simple:

Theorem 2.9 ([CG00]) *Given c_i, $i = 0, 1, \ldots, n-1$, there exists a function $\hat{h} \in \overline{\mathcal{B}}\mathcal{H}_\infty(\mathbb{D})$ such that (2.15) is satisfied if and only if*

$$I - T_c^* T_c \geq 0 \tag{2.16}$$

where T_c is the lower triangular Toeplitz matrix

$$\begin{bmatrix} c_0 & 0 & \cdots & 0 \\ c_1 & c_0 & \ddots & \vdots \\ \vdots & \ddots & \ddots & 0 \\ c_{n-1} & c_{n-2} & \cdots & c_0 \end{bmatrix}$$

Moreover, this function is non-unique if and only if $I - T_c^* T_c > 0$ and unique if and only if $I - T_c^* T_c$ is rank deficient.

Chen and Gu also give a procedure for finding all interpolating functions.

There are a number of variations on the Carathéodory-Fejér theme. For model validation, the *tangential Carathéodory-Fejér interpolation problem*, which may be found in Foias et al [FF90] is of particular importance.

The Tangential Carathéodory-Fejér Interpolation Problem Given two vectors u and y of the form

$$u = \begin{pmatrix} u_1 \\ u_2 \\ \vdots \\ u_n \end{pmatrix} \qquad y = \begin{pmatrix} y_1 \\ y_2 \\ \vdots \\ y_n \end{pmatrix}$$

find the necessary and sufficient conditions for the existence of an infinite contractive Toeplitz matrix $\hat{A}_\infty$ satisfying $y = \hat{A}_n u$ where $\hat{A}_n$ is the $n \times n$ analytic Toeplitz matrix in the upper left hand corner of $\hat{A}_\infty$.

The condition for the existence of such a matrix is given in [FF90]. What follows is a generalized version, allowing for a non-unit norm constraint.

Theorem 2.10 ([PKT$^+$92]) *Given sequences $u \in \Pi_l \mathcal{S}_+^m$ and $y \in \Pi_l \mathcal{S}_+^n$, and a positive real number γ, there exists a stable, causal, linear, time-invariant operator*

Δ *satisfying*

$$\|\Delta\|_{i2} \leq \gamma$$
$$\Pi_l \Delta \begin{pmatrix} u_0 \\ u_1 \\ \vdots \\ u_{l-1} \end{pmatrix} = \begin{pmatrix} y_0 \\ y_1 \\ \vdots \\ y_{l-1} \end{pmatrix}$$

if and only if

$$T_y^T T_y \leq \gamma^2 T_u^T T_u \tag{2.17}$$

The same source provides a similar result for norm-bounded time-varying uncertainty, be it linear or not:

Theorem 2.11 ([PKT+92],[PKT+94]) *Given sequences* $u \in \Pi_l \mathcal{S}_+^m$ *and* $y \in \Pi_l \mathcal{S}_+^n$, *and a positive real number* γ, *there exists a stable, causal, time-varying operator* Δ *satisfying*

$$\|\Delta\|_{i2} \leq \gamma$$
$$\Pi_l \Delta \begin{pmatrix} u_0 \\ u_1 \\ \vdots \\ u_{l-1} \end{pmatrix} = \begin{pmatrix} y_0 \\ y_1 \\ \vdots \\ y_{l-1} \end{pmatrix}$$

if and only if

$$\|\Pi_k y\|_2 \leq \gamma \|\Pi_k u\|_2 \tag{2.18}$$

for all $k = \{1, 2, \ldots, l\}$.

These theorems can be applied to the uncertainty representations in Section 3.1. The applications of this form the basis of Chapter 4.

2.6.4 Construction of interpolants

The three interpolation problems discussed are closely interrelated and it is often possible to express them in terms of each other. To do so here would be lengthy, and the interested reader will find a full and detailed discussion in [Dym89] or a similar text book. Such texts provide methods of constructing interpolants functions, though many deal only with a one-sided Carathéodory-Fejér problem, neglecting the tangential variant. This limits the useful application to single-input problems.

Insights into the problem—and examples of the conversion between Nevanlinna-Pick and Carathéodory-Fejér problems in the context of multi-rate periodic systems—are given in [CQ04], who quotes a parameterization of *all* interpolant systems obtained from [FFGK91], of which the following result is part:

Let $u \in \mathcal{S}_k^q, y \in \mathcal{S}_k^p$ be input-output data sequences and define $U \in \mathrm{R}^{q\times k}, Y \in \mathrm{R}^{p\times k}$ as follows:

$$U := \begin{bmatrix} u_0 & u_1 & \cdots & u_{k-1} \end{bmatrix}$$
$$Y := \begin{bmatrix} y_0 & y_1 & \cdots & y_{k-1} \end{bmatrix}$$

Let $Z := \begin{bmatrix} 0_{k-1\times 1} & I_{k-1} \\ 0 & 0_{1\times k-1} \end{bmatrix}$ and let $Q, \tilde{Q} \in \mathbb{R}^{k\times k}$ be the solution to the Lyapunov equations

$$Z^*QZ - Q + U^*U = 0$$
$$Z^*\tilde{Q}Z - \tilde{Q} + Y^*Y = 0$$

Lemma 2.12 *Given sequences $u \in \mathcal{S}_k^q, y \in \mathcal{S}_k^p$ satisfying the tangential Carathéodory-Fejér type condition $T_y^*T_y \leq T_u^*T_u$, there exists a stable LTI system $G(z) = \left[\begin{array}{c|c} A & B \\ \hline C & D \end{array}\right]$*

such that $||G||_\infty \leq 1$ *and*

$$\begin{bmatrix} y_0 \\ y_1 \\ \vdots \\ y_{k-1} \end{bmatrix} = \begin{bmatrix} D & 0 & \cdots & 0 \\ CB & D & \cdots & 0 \\ \vdots & \vdots & & \vdots \\ CA^{k-2} & CA^{k-3} & \cdots & D_0 \end{bmatrix} \begin{bmatrix} u_0 \\ u_1 \\ \vdots \\ u_{k-1} \end{bmatrix}$$

and one such system is $G_1(z) = \left[\begin{array}{c|c} A_1 & A_1B_1 \\ \hline C_1 & C_1B_1 \end{array}\right]$ *where* $A_1 = (Q - Z^*\tilde{Q}Z)^{-1}Z^*(Q - \tilde{Q})$, $B_1 = (Q - Z^*\tilde{Q}Z)^{-1}U^*$, $C_1 = Y$.

Outline of proof. The existence of G is a direct consequence of Theorem 2.10 and requires no further proof. The rest may be found in [CQ04]. We can characterise all interpolant systems in terms of a LFT model set:

$$G(z) \in \{G_1(z) : \mathcal{F}_\ell(\Phi(z), \Delta(z)), ||\Delta||_\infty \leq 1)\}$$

where $\Phi(z) = \begin{bmatrix} \Phi_{11}(z) & \Phi_{12}(z) \\ \Phi_{21}(z) & \Phi_{22}(z) \end{bmatrix}$ and $\Phi_{11}(z) = C_1(I - z^{-1}A_1)^{-1}B_1$. The simplest solution $G_1 = \mathcal{F}_\ell(\Phi(z), 0) = \Phi_{11}(z)$ is as satisfactory as any other. The (non-standard) state-space description of $G_1(z)$ is

$$x(k+1) = A_1x(k) + B_1u(k+1)$$
$$y(k) = C_1x(k)$$

The state transformation $\xi(k) = x(k) - B_1u(k)$ gives a more conventional state-space form—

$$\xi(k+1) = A_1\xi(k) + A_1B_1u(k)$$
$$y(k) = C_1\xi(k) + C_1B_1u(k)$$

—which is as desired. □

Remark 2.13 A system constructed using Lemma 2.12 will contain q stable unobservable modes with poles at the origin, which may readily be removed from the system since they affect neither the input-output behaviour nor the $\mathcal{H}_\infty$-norm. A satisfactory way of eliminating these modes is balanced truncation. ♡

Corollary 2.14 *Given sequences $u \in \mathcal{S}_k^q, v \in \mathcal{S}_k^p$ satisfying the tangential Carathéodory-Fejér type condition $T_v^* T_v \leq \gamma^2 T_u^* T_u$ for $\gamma > 0$, let $y = \frac{1}{\gamma} v$. Then there exists a stable LTI system $G(z) = \left[\begin{array}{c|c} A & B \\ \hline C & D \end{array}\right]$ such that $||G||_\infty \leq \gamma$ and*

$$\begin{bmatrix} v_0 \\ v_1 \\ \vdots \\ v_{k-1} \end{bmatrix} = \begin{bmatrix} D & 0 & \cdots & 0 \\ CB & D & \cdots & 0 \\ \vdots & \vdots & & \vdots \\ CA^{k-2} & CA^{k-3} & \cdots & D_0 \end{bmatrix} \begin{bmatrix} u_0 \\ u_1 \\ \vdots \\ u_{k-1} \end{bmatrix}$$

and one such system is $G_1(z) = \left[\begin{array}{c|c} A_1 & A_1 B_1 \\ \hline \gamma C_1 & \gamma C_1 B_1 \end{array}\right]$ where A_1, B_1, C_1 are constructed to interpolate (u, y) using Lemma 2.12.

Outline of proof. This this follows trivially from Lemma 2.12. The problem is simplified by re-scaling, and the re-scaling is removed from the final system. □

2.6.5 Parameterization of all degree-N interpolants

Interpolants constructed using the above methods have the potential to be very 'ragged' in the frequency domain. An obvious question to ask is whether there are other interpolants of the same degree with smoother frequency responses. There is a body of work including, for example, [Geo01] which considers the construction of all solutions to the Nevanlinna-Pick problem with degree N. Essentially, the idea is that where interpolants exists, it is possible to find degree-N polynomials $a(z)$, $b(z)$

such that

$$f(z) = \frac{b(z)}{a(z)}$$

is an interpolant and

$$a(z)b^*(z) + a^*(z)b(z) = \sigma(z)\sigma^*(z)$$

for any N-degree polynomial $\sigma(z)$ with all its roots in the unit disk. The work of [BN02] provides an algorithm for solving the degree-constrained Nevanlinna-Pick interpolation problem with derivative constraints. (This problem is often referred to as the 'NPDC' problem.) This paper provides further insight into the theory, and the authors have also developed software to solve this problem, avaliable on the Internet at http://www.math.kth.se/∼andersb/software.html. The problem description in [BN02] supposes that we have two sets of complex numbers:

$$\mathcal{Z} := \{z_j : j = 0, 1, \ldots, n, z_i \neq z_j \text{ if } i \neq j\}$$

and

$$\mathcal{W} := \{w_{jk} : j = 0, 1, \ldots, n,\ k = 0, 1, \ldots, m_j - 1\}$$

where all elements of $\mathcal{Z}$ satisfy $|z_j| < 1$. The algorithm given attempts to construct an interpolant that satisfies three conditions:

1. Interpolation:
$$\frac{f^{(k)}(z_j)}{k!} = w_{jk}, \quad \begin{matrix} j = 0, 1, \ldots, n \\ k = 0, 1, \ldots, m_j - 1 \end{matrix}$$

2. Strict positive realness, i.e. f is analytic in an open region containing the closed unit disc, and $\mathrm{Re}(f(z)) > 0$ for all z in the closed unit disc.

3. f is rational and $\deg f \leq m := \sum_{j=0}^{n} m_j - 1$

The second condition may be converted into norm-bound by applying an appropriate bilinear range transformation, e.g. $g(z) = (-f(z) + 1)/(f(z) + 1)$, as described in

[BN02, Lemma A2]. Choosing $\mathcal{Z} = \{0\}$ and $\mathcal{W}$ to be the first part of the impulse response of the system to be constructed—uniquely determinable from single-input data—gives the usual Carathéodory-Fejér problem.

Chapter 3

Uncertainty, Stabilization and Performance

3.1 Representing unstructured uncertainty

A detailed discussion of representations of uncertainty may be found in a standard textbook on robust control [ZDG95]. This section looks at two representations: the linear fractional transformation, which can accommodate most standard problems, and the normalized coprime factorization.

3.1.1 Linear Fractional Transformations (LFTS)

Linear Fractional Transformations (LFTs) can be used to represent many forms of unstructured uncertainty. The *upper* LFT (Fig. 3.1(a)) is commonly used to represent uncertainty; the *lower* LFT (Fig. 3.1(b)) is generally used to represent interconnections with controllers. If $P = \begin{bmatrix} P_{11} & P_{12} \\ P_{21} & P_{22} \end{bmatrix}$, the resulting closed-loop transfer functions are usually denoted $\mathcal{F}_u(P, \Delta)$ and $\mathcal{F}_l(P, C)$.

The LFTs implicitly give a mapping from $\begin{pmatrix} u \\ t \end{pmatrix}$ to $\begin{pmatrix} y \\ s \end{pmatrix}$. It is often useful to

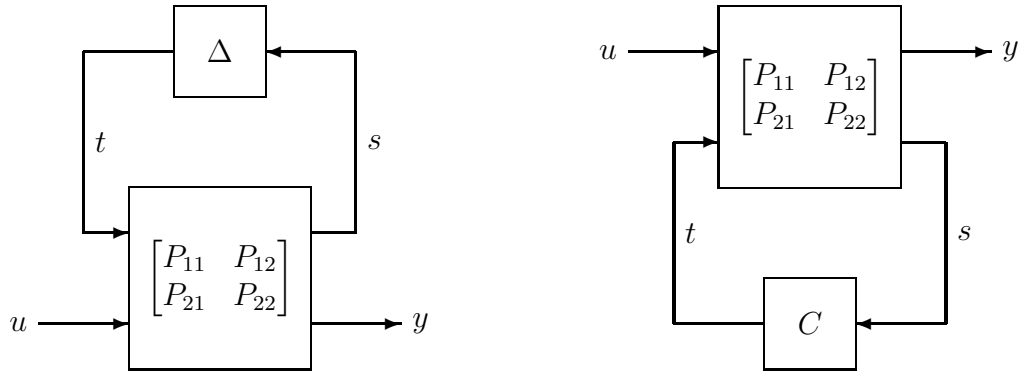

(a) Upper LFT

(b) Lower LFT

Figure 3.1: Linear Fractional Transformations

know the relationship between $\begin{pmatrix} u \\ y \end{pmatrix}$ and $\begin{pmatrix} s \\ t \end{pmatrix}$. For the upper LFT,

$$\begin{pmatrix} s \\ t \end{pmatrix} = \begin{bmatrix} P_{12} - P_{11}P_{21}^{-1}P_{22} & P_{11}P_{21}^{-1} \\ -P_{21}^{-1}P_{22} & P_{21}^{-1} \end{bmatrix} \begin{pmatrix} u \\ y \end{pmatrix} \qquad \text{if } P_{21} \text{ is invertible} \qquad (3.1)$$

$$\begin{pmatrix} u \\ y \end{pmatrix} = \begin{bmatrix} P_{12}^{-1} & -P_{12}^{-1}P_{11} \\ P_{22}P_{12}^{-1} & P_{21} - P_{22}P_{12}^{-1}P_{11} \end{bmatrix} \begin{pmatrix} s \\ t \end{pmatrix} \qquad \text{if } P_{12} \text{ is invertible} \qquad (3.2)$$

and for the lower LFT

$$\begin{pmatrix} s \\ t \end{pmatrix} = \begin{bmatrix} P_{21} - P_{22}P_{12}^{-1}P_{11} & P_{22}P_{12}^{-1} \\ -P_{12}^{-1}P_{11} & P_{12}^{-1} \end{bmatrix} \begin{pmatrix} u \\ y \end{pmatrix} \qquad \text{if } P_{12} \text{ is invertible} \qquad (3.3)$$

$$\begin{pmatrix} u \\ y \end{pmatrix} = \begin{bmatrix} P_{21}^{-1} & -P_{21}^{-1}P_{22} \\ P_{11}P_{21}^{-1} & P_{12} - P_{11}P_{21}^{-1}P_{22} \end{bmatrix} \begin{pmatrix} s \\ t \end{pmatrix} \qquad \text{if } P_{21} \text{ is invertible} \qquad (3.4)$$

The invertability of P_{12} and P_{21} is not in general guaranteed. Table 3.1 gives the upper LFT form of some standard unstructured uncertainty representations. It can be seen that for the last form (a left coprime factorization), $P_{21} = \tilde{M}^{-1}$: this is always invertible so it is always possible to find s and t from u and y.

$W_1 \in \mathcal{RH}_\infty\ W_2 \in \mathcal{RH}_\infty,\ \Delta \in \mathcal{RH}_\infty$	
Model Set $\mathcal{P}$	Upper LFT Form
$(I + W_1 \Delta W_2)P$	$\mathcal{F}_u\left(\begin{bmatrix} 0 & W_2 P \\ W_1 & P \end{bmatrix}, \Delta\right)$
$P(I + W_1 \Delta W_2)$	$\mathcal{F}_u\left(\begin{bmatrix} 0 & W_2 \\ P W_1 & P \end{bmatrix}, \Delta\right)$
$(I + W_1 \Delta W_2)^{-1} P$	$\mathcal{F}_u\left(\begin{bmatrix} W_2 & 0 \\ -W_2 W_1 & W_2 P \end{bmatrix}, \Delta\right)$
$P + W_1 \Delta W_2$	$\mathcal{F}_u\left(\begin{bmatrix} 0 & W_2 \\ W_1 & P \end{bmatrix}, \Delta\right)$
$(\tilde{M} + \Delta_{\tilde{M}})^{-1}(N + \Delta_{\tilde{N}})\ P = \tilde{M}^{-1}\tilde{N}$ $\Delta = \begin{bmatrix} \Delta_{\tilde{N}} & \Delta_{\tilde{M}} \end{bmatrix}$	$\mathcal{F}_u\left(\begin{bmatrix} 0 & \begin{bmatrix} I \\ -P \end{bmatrix} \\ \begin{bmatrix} -\tilde{M}^{-1} \\ \tilde{M}^{-1} \end{bmatrix} & P \end{bmatrix}, \Delta\right)$

Table 3.1: Some Unstructured Uncertainties and their LFT Representations

3.1.2 Normalized Coprime Factorizations (NCFs)

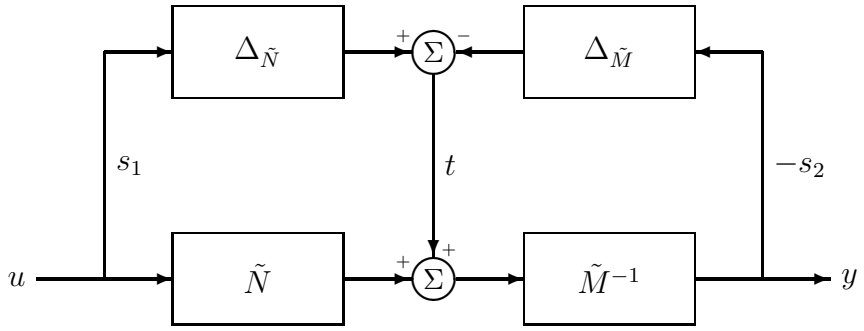

Figure 3.2: Left Coprime Factor Uncertainty

Normalized Coprime Factorizations (NCFs) are a convenient way of representing uncertainty. The well-known left normalized coprime factorization is:

$$P = \tilde{M}^{-1}\tilde{N}$$

where $\tilde{M}\tilde{M}^{\sim} + \tilde{N}\tilde{N}^{\sim} = I$.

Uncertainty may be represented by perturbations of the coprime factors (Fig. 3.2):

$$\mathcal{P} = \left\{ P : P = \left(\tilde{M} + \Delta_{\tilde{M}}\right)^{-1} \left(\tilde{N} + \Delta_{\tilde{N}}\right), \Delta = \begin{bmatrix} \Delta_{\tilde{N}} & \Delta_{\tilde{M}} \end{bmatrix} \in \mathbf{\Delta} \right\} \tag{3.5}$$

Remark 3.1 The left normalized coprime factorization fits into the LFT framework: see Table 3.1. ♡

Remark 3.2 For convenience, the set of plants described by (3.5), with the additional constraint $\|\Delta\|_{i2} < \gamma$ will be denoted by

$$\mathcal{P} = \mathcal{NCF}\left(\tilde{N}, \tilde{M}, \mathbf{\Delta}, \gamma\right) \tag{3.6}$$

♡

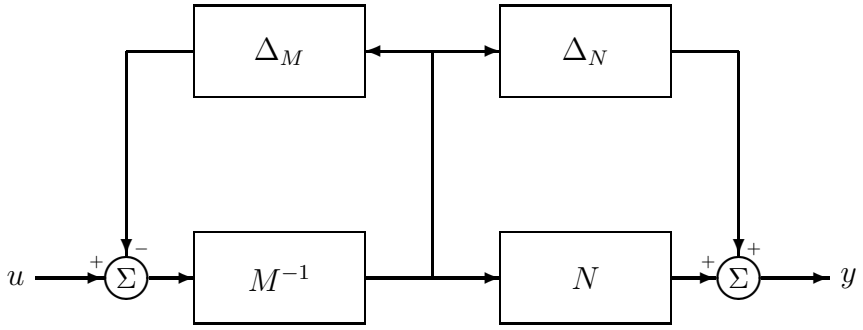

Figure 3.3: Right Coprime Factorization

The right normalized coprime factorization is:

$$P = NM^{-1}$$

where $M^{\sim}M + N^{\sim}N = I$.

Uncertainty may be represented by perturbations of the coprime factors (Fig. 3.2):

$$\mathcal{P} = \left\{ P : P = (N + \Delta_N), (M + \Delta_M)^{-1} \Delta = \begin{bmatrix} \Delta_N \\ \Delta_M \end{bmatrix} \in \mathbf{\Delta} \right\} \tag{3.7}$$

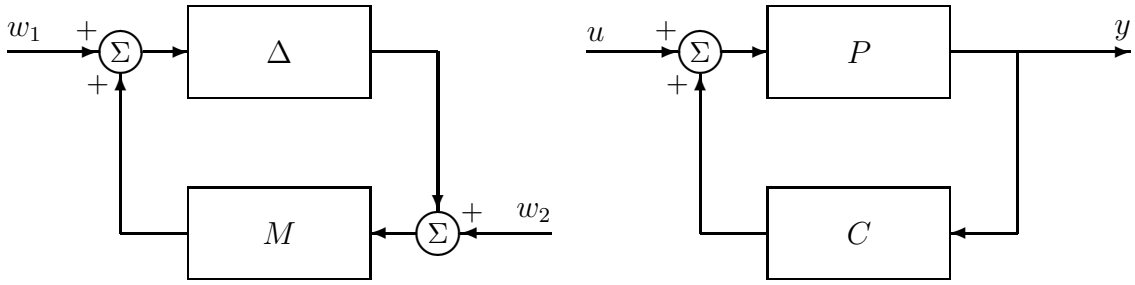

(a) Small Gain Theorem

(b) Controlled System

Figure 3.4: Small Gain Theorem and Robust Stability Margin

Remark 3.3 For convenience, the set of plants described by (3.7), with the additional constraint $\|\Delta\|_{i2} < \gamma$ will be denoted by

$$\mathcal{P} = \mathcal{NCF}\left(N, M, \mathbf{\Delta}, \gamma\right) \tag{3.8}$$

♡

3.2 Stabilization and robust performance

Stabilization of an uncertain system may be determined using the well-known small gain theorem.

Theorem 3.4 (Small Gain Theorem [ZDG95]) *Consider the interconnected system of Fig. 3.4(a) Suppose $M \in \mathcal{RH}_\infty$ and let $\gamma > 0$. Then the system is well-posed and internally stable for all $\Delta \in \mathcal{RH}_\infty$ with*

1. $\|\Delta\|_\infty \leq 1/\gamma$ *if and only if* $\|M\|_\infty < \gamma$;
2. $\|\Delta\|_\infty < 1/\gamma$ *if and only if* $\|M\|_\infty \leq \gamma$.

Definition 3.5 The robust performance of a system is described by the robust

stability margin:

$$b_{P,C} := \begin{cases} \left(\left\| \begin{bmatrix} I \\ C \end{bmatrix} (I - PC)^{-1} \right)^{-1} \begin{bmatrix} I & -P \end{bmatrix} \right\|_\infty \Bigg)^{-1} & \text{if } C \text{ stabilizes } P \\ \\ 0 & \text{otherwise} \end{cases}$$

and

$$b_{\text{opt}} := \sup_C b_{P,C}$$

Remark 3.6 These quantities are derived from the application of the Small Gain Theorem to an NCF-perturbed plant. A detailed derivation and methods of calculation may be found in a standard text [ZDG95] [Zho98].

The same sources also show that $b_{P,C}$ is a good measure of controller performance.

♡

3.2.1 The gap metric, δ_g

The gap metric $\delta_g(P_1, P_2)$ is a measure of the smallest perturbation of the coprime factors of P_1 producing P_2.

The formal definition [Zho98] uses the notion of a graph: the graph of the operator P is the subspace of $\mathcal{H}_2$ consisting of all pairs (u, y) such that $y = Pu$:

$$\begin{bmatrix} M \\ N \end{bmatrix} \mathcal{H}_2$$

which is a closed subspace of $\mathcal{H}_2$. The gap between P_1 and P_2 is defined by

$$\delta_g(P_1, P_2) = \left\| \Pi \begin{bmatrix} M_1 \\ N_1 \end{bmatrix}_{\mathcal{H}_2} - \Pi \begin{bmatrix} M_2 \\ N_2 \end{bmatrix}_{\mathcal{H}_2} \right\|$$

where M_i, N_i are the right normalized coprime factors of P_i, and $\Pi_{\mathcal{H}_2}$ denotes the orthogonal projection onto $\mathcal{H}_2$.

Theorem 3.7 *([QD92]) Suppose the feedback system with the pair (P_0, C_0) is stable. Let $\mathcal{P} := \{P : \delta_g(P, P_0) < r_1\}$ and $\mathcal{C} := \{C : \delta_g(C, C_0) < r_2\}$. Then*

1. *The feedback system with the pair (P,K) is stable for all $P \in \mathcal{P}$ and $C \in \mathcal{C}$ if and only if*

$$\arcsin b_{P_o,C_o} \geq \arcsin r_1 + \arcsin r_2.$$

2. *The worst possible performance resulting from these sets of plants and controllers is given by*

$$\inf_{P\in\mathcal{P},C\in\mathcal{C}} \arcsin b_{P,C} = \arcsin b_{P_0,C_0} - \arcsin r_1 - \arcsin r_2$$

Note that this theorem still holds if either $\mathcal{P}$ or $\mathcal{C}$ is taken as a closed ball.

Note that a 'ball' in the gap metric centred on some system P and satisfying $\delta_g(P, P_1) \leq \gamma$ is identical to $\mathcal{NCF}(\tilde{N}, \tilde{M}, \Delta, \gamma)$.

3.2.2 The ν-gap metric, δ_ν

The ν-gap metric, δ_ν, is defined as follows:

Definition 3.8 ([Vin01])

$$\delta_\nu(P_1, P_2) = \begin{cases} \|\tilde{G}_2 G_1\|_\infty & \text{if } \det(G_2^* G_1(e^{j\Omega}) \neq 0 \ \forall\ \Omega \in (-\pi, \pi] \\ & \text{and wno } \det(G_2^* G_1) = 0 \\ 1 & \text{otherwise} \end{cases}$$

where $G_i := \begin{bmatrix} M_i \\ N_i \end{bmatrix}$ and $\tilde{G}_i := \begin{bmatrix} -\tilde{N}_i & \tilde{M}_i \end{bmatrix}$, and $P_i = N_i M_i^{-1} = \tilde{M}_i^{-1}\tilde{N}_i$ are normalized coprime factorizations.

The ν-gap metric, δ_ν, is less conservative than the gap metric, δ_g. An in-depth analysis can be found in Vinnicombe's book [Vin01]. Some of the important properties follow:

Remark 3.9 The ν-gap between two systems is never greater than the gap between them, i.e.

$$\delta_\nu(P_1, P_2) \leq \delta_g(P_1, P_2)$$

♡

Remark 3.10

1. Given a nominal system $P_1 \in \mathcal{P}^{p\times q}$, a compensator $C \in \mathcal{P}^{q\times p}$ then:
   $[P_2, C]$ is stable for all systems $[P_2]$ satisfying $\delta_\nu(P_1, P_2) \leq \beta$ if, and only if, $b_{P_1,C} > \beta$

2. Given a nominal system P_1, a perturbed system $P_2 \in \mathcal{P}^{p\times q}$ and a number $\beta < b_{\text{opt}}(P_1)$ then:
   $[P_2, C]$ is stable for all compensators C satisfying $b_{P_1,C} > \beta$ if, and only if, $\delta_\nu(P_1, P_2) \leq \beta$

♡

δ_ν is thus less conservative than δ_g, since if $b_{P_1,C} = \gamma$ and $\delta_\nu(P_1, P_2) > \gamma$, there exists at least one controller that will achieve the $b_{P_1,C}$ but will not stabilize P_2.

Definition 3.11 For convenience, the set of models lying within a ν-gap radius β about P shall be denoted by $\mathcal{B}_\nu(P, \beta)$. Formally,

$$\mathcal{B}_\nu(P, \beta) := \{P_1 : \delta_\nu(P, P_1) < \beta\}$$

3.2.3 Parameterization of a ball in the ν-gap metric

Given a nominal system P, and some $\beta < b_{\text{opt}}(P)$ it is possible to synthesize a 'central controller'

$$M = \begin{bmatrix} M_{11} & M_{12} \\ M_{21} & M_{22} \end{bmatrix}$$

such that $b_{P,C} > \beta \; \forall \; C \in \mathcal{C}_{P,\beta}$ where

$$\mathcal{C}_{P,\beta} = \{C_1 : C_1 = \mathcal{F}_\ell(M, Q), Q \in \mathcal{RH}_\infty, ||Q||_\infty < 1\}$$

and the inverses M^{-1} and M_{21}^{-1} exist [GGLD90]. Computation using the small gain theorem is straightforward, either using readily-available $\mathcal{H}_\infty$ synthesis software[1] or by directly solving the relevant Riccati equations [Can01]. The inverse of $\begin{bmatrix} 0 & I \\ I & 0 \end{bmatrix} M \begin{bmatrix} 0 & I \\ I & 0 \end{bmatrix}$, which we shall denote as G, forms the basis for an LFT parameterization of a ball of systems in the ν-gap. This was first shown in [VG94], and discussed in [Dav96, Chapter 5.3]. Defining

$$\mathcal{B}_\nu^{\text{LTI}}(P, \beta) := \{P_1 : P_1 = \mathcal{F}_u(G, \Delta), \Delta \in \mathcal{RH}_\infty, \|\Delta\|_\infty < 1\}$$

it is shown in [Vin01, Chapter 9] that $\mathcal{B}_\nu(P, \beta) \equiv \mathcal{B}_\nu^{\text{LTI}}(P, \beta)$.

Remark 3.12 The perturbation block in the set $\mathcal{B}_\nu^{\text{LTI}}(P, \beta)$ is linear and time-invariant uncertainty. We can use the same G as the basis for similar sets

$$\mathcal{B}_\nu^{\text{LTV}}(P, \beta) := \left\{ P_1 : P_1 = \mathcal{F}_u(G, \Delta), \sup_{||s||_2=1} ||\Delta s||_2 < 1, \Delta \text{ LTV} \right\}$$

and

$$\mathcal{B}_\nu^{\text{NC}}(P, \beta) := \left\{ P_1 : P_1 = \mathcal{F}_u(G, \Delta), \sup_{||s||_2=1} ||\Delta s||_2 < 1, \Delta \text{ may be non-causal} \right\}$$

[1] e.g. MATLAB's `hinfsyne command`

$\mathcal{B}_\nu^{\mathrm{LTI}}(P,\beta) \subset \mathcal{B}_\nu^{\mathrm{LTV}}(P,\beta) \subset \mathcal{B}_\nu^{\mathrm{NC}}(P,\beta)$. ♡

3.3 Optimal weighting for stability analysis

The frequency-wise ν-gap between any two systems varies according to scaling. Given some constant $k \neq 1$ and two systems P_1 and P_2 it will usually be the case that

$$\delta_\nu(P_1, P_2) \neq \delta_\nu(kP_1, kP_2)$$

Likewise, given some controller C it is often the case that

$$b(P_1, C) \neq b\left(kP_1, \frac{1}{k}C\right)$$

The robust stability margin is different, yet the properties of the closed loop characteristic equation have not changed. This begs the question of whether there is some 'optimal' scaling giving meaningful results. Such a strategy is proposed in [SV02].

The frequency-wise robust stability margin is defined as follows in [SV02]:

Definition 3.13 (Frequency-wise generalized stability margin $\rho(P(e^{j\Omega}), C(e^{j\Omega}))$

$$\rho(P(e^{j\Omega}), C(e^{j\Omega})) := \frac{1}{\overline{\sigma}\left(\begin{bmatrix} P(e^{j\Omega}) \\ I \end{bmatrix} (I - C(e^{j\Omega})P(e^{j\Omega}))^{-1} \begin{bmatrix} -C(e^{j\Omega}) & I \end{bmatrix}\right)}$$

In [SV02] it is noted that provided $[P, C]$ is stable,

$$b(P, C) = \min_{\Omega \in [0, 2\pi)} \rho(P(e^{j\Omega}), C(e^{j\Omega}))$$

An optimally-scaled variant is also given:

Definition 3.14 (Frequency-wise optimally-scaled input/output stability margin) A frequency-wise measure of closed-loop stability to input/output gain and phase

offsets is given by

$$\rho_{\text{scaled}}\left(P(e^{j\Omega}), C(e^{j\Omega})\right) := \max_{W_{\text{i}}, W_{\text{o}} \text{ diagonal}} \rho\left(W_{\text{o}} P W_{\text{i}}, W_{\text{i}}^{-1} C W_{\text{o}}^{-1}\right)(e^{j\Omega})$$

In effect, this defines 'optimal' dynamic weights $W_{\text{i}}^{\circ}(e^{j\Omega})$ and $W_{\text{o}}^{\circ}(e^{j\Omega})$, which may prove useful for stability analysis.

Similarly, also from [SV02] we have the non frequency-wise equivalent:

Definition 3.15 (Optimally-scaled input/output stability margin) When $[P, C]$ is stable,

$$b_{\text{scaled}}(P, C) := \min_{\Omega \in [0, 2\pi)} \rho_{\text{scaled}}(P(e^{j\Omega}), C(e^{j\Omega}))$$

otherwise $b_{\text{scaled}}(P, C) = 0$.

Note that could be possible to find non-optimal weights $\hat{W}_{\text{o}}, \hat{W}_{\text{i}}$ achieving the same stability margin, providing that

$$\rho\left(\hat{W}_{\text{o}} P \hat{W}_{\text{i}}, \hat{W}_{\text{i}}^{-1} C \hat{W}_{\text{o}}^{-1}\right)(e^{j\Omega}) \geq b_{\text{scaled}}(P, C)$$

for all $\Omega \in [0, 2\pi)$.

Chapter 4

$\mathcal{H}_\infty$ Model Validation

In the previous chapter, the subject of robust stabilization and performance has been considered. The techniques represented are part of a body of control theory that exploits the concept of robust stability margins: providing that the system does not deviate from some nominal one by more than a definite, measurable amount, an acceptable level of performance and stabilization can be guaranteed. Thus, for any given control design, there is a set of models which can be guaranteed to give satisfactory results.

The framework described is an example of *model based control design*. The starting point is a nominal model, and the end point is a controller stabilizing that model and a model set around it. The techniques presented in this chapter compare observed data from post-design experiments to such model sets. With certain assumptions about exogenous noise entering the system, it is possible to make judgements about the size of the largest model set consistent with the observed data. It is not guaranteed that a model set that is not invalidated by observed experimental data will hold good for all data, but our confidence in it is increased.

In the modelling/control design process, model validation follows control design: the effectiveness of the model/controller combination in practice is considered. If a controller which was expected to work in conjunction with a given model does not work in reality, then the model is not adequate to the design, and it must be refined

through further experimentation and/or insight.

The methods of this chapter are computationally intensive and unlikely to be of use in real-time applications, e.g. on-line envelope expansion. Those looking for more computationally efficient methods may find better results with parameter-vector model structures in the context of an 'iterative falsification and control' schem [VW00], though this does not have the direct applicability to our school of robust control design.

4.1 The $\mathcal{H}_\infty$ model validation problem

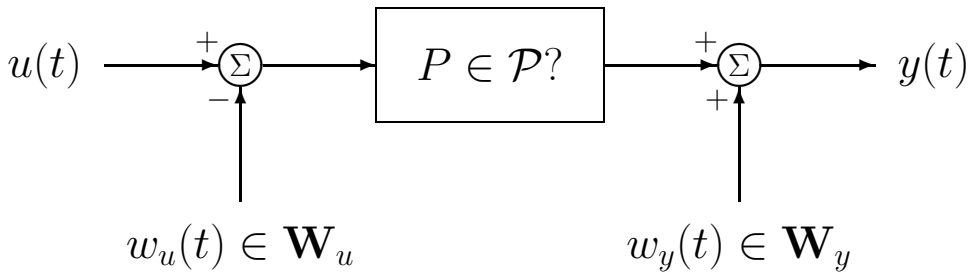

Figure 4.1: The $\mathcal{H}_\infty$ Model Validation Problem

The block diagram for a generic time domain model validation problem is shown in Fig. 4.1: it consists of

- a plant P (unknown);
- a model set $\mathcal{P}$ to which P is supposed to belong;
- a test input, u, which has been applied to the P experimentally; and
- the resulting measured output, y.

In real applications, is inevitable that there will be some noise in the system. This is taken into account by introducing

- 'plant input noise', w_u, belonging to some noise set $\mathbf{W}_u$; and

- 'plant output noise', 'sensor noise' or 'measurement noise', w_y taken into account, belonging to some noise set $\mathbf{W}_y$

(The noise sets will typically consist of all suitably-dimensioned sequences satisfying some bound, e.g. an ℓ_2 norm bound. More will be said about these noise sets in section 4.5.)

The time domain model validation problem is:

> **Given $\mathcal{P}$, u, y, $\mathbf{W}_u$ and $\mathbf{W}_y$, do there exist $P \in \mathcal{P}$, $w_u \in \mathbf{W}_u$ and $w_y \in \mathbf{W}_y$ such that** $y(t) = P * (u(t) - w_u(t)) + w_y(t)$?

In practice, $u, y \in \mathcal{S}_k$ where $k < \infty$ so, strictly, a model can only be considered validated for the particular data used. It cannot be said for certain that $P \in \mathcal{P}$ as the following example shows:

Example 4.1 *Suppose we have the system*

$$P_{\text{true}}(z) = 1 - 0.8z^{-1} + 0.6z^{-2} - 0.2z^{-3} \tag{4.1}$$

the noise sets $\mathbf{W}_u = \mathbf{W}_y = 0$*, the input sequence* $u = \{1, 0, 0\}$*. The first three elements of the resulting output sequence will be* $y = \{1, -0.8, 0.6\}$*.*

Now suppose we have postulated a model set of the form

$$\mathcal{P} = \left\{P : P(z) = a + bz^{-1} + cz^{-2}\right\} \tag{4.2}$$

It is clear that setting $a = 1, b = -0.8, c = 0.6$*, giving*

$$P_{\text{nom}}(z) = 1 - 0.8z^{-1} + 0.6z^{-2}$$

will produce output data consistent with y *from* u*. This means that the model is valid for this data, but* $P_{\text{true}} \notin \mathcal{P}$

Note that, had our the impulse response in Example 4.1 been one sample longer, we could not have found a $P \in \mathcal{P}$ consistent with the input-output data. Thus:

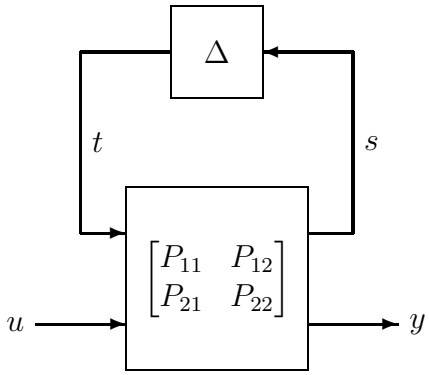

Figure 4.2: Linear Fractional Transformation

It is not possible to demonstrate conclusively that a given system $P_{\text{true}} \in \mathcal{P}$. However, if no $P_{\text{true}} \in \mathcal{P}$ which is consistent with the input-output data and noise conditions exists, then the model set $\mathcal{P}$ has been invalidated.

Specific problem definitions

There are two variations of the $\mathcal{H}_\infty$ validation problem:

- The Model Validation Decision Problem (MVDP). 'Given a model set and some data, are the two consistent?'
- The Model Validation Optimization Problem (MVOP). 'Given a model set parameterized on some uncertainty Δ with an unknown bound in size. e.g., $\|\Delta\|_{i2} \leq \gamma$ with γ unknown, what is the tightest bound for which the model is consistent?'

4.2 Validation in LFT model sets

A model set $\mathcal{P}$ in the form of Fig. 4.2 with Δ linear and $\|\Delta\|_{i2} < \gamma$ can be shown to be consistent with input-output sequences (u, y) using either Theorem 2.10 or 2.11, depending on whether Δ is time-invariant or not. In the time-invariant case, this

means that

$$T_t^T T_t \leq \gamma^2 T_s^T T_s$$

However this is only a simple problem if sequences (s, t) can be calculated from (u, y): as shown in previous work [Dav96], in general there are a set of s satisfying

$$T_{P_{21}} t = y - T_{P_{22}} u$$

and for each t there is a corresponding s given by

$$t = T_{P_{11}} s + T_{P_{12}} u$$

This **general model validation problem** would involve a search over all (s, t) satisfying the above equations: the computational complexity of the general model validation problem incorporating noise has been shown to be NP hard [Dav96].

It is immediately clear that the problem will be much simpler when there is a unique mapping from (u, y) to (s, t): as shown in equation (3.1), this can be done whenever P_{21}^{-1} exists.

This method, the incorporation of noise, is illustrated for the specific case of the left normalized coprime factorization, but the ideas are directly transferable to other cases.

4.3 Non-invalidation/validation in the gap metric, δ_g

A left normalized coprime factorization (Fig. 4.3) can be represented as an upper linear fractional transform $P = \mathcal{F}_u\left(R, \begin{bmatrix}\Delta_{\tilde{N}} & \Delta_{\tilde{M}}\end{bmatrix}\right)$ where

$$\left(\begin{bmatrix}s_1\\ s_2\end{bmatrix}\right) = \underbrace{\left[\begin{pmatrix}0\\ -\tilde{M}^{-1}\end{pmatrix} \quad \begin{pmatrix}I\\ -\tilde{M}^{-1}\tilde{N}\end{pmatrix}\right]}_{R} \begin{pmatrix}t\\ u\end{pmatrix} \tag{4.3}$$

$\tilde{M}^{-1}$ is, by definition, invertible, yielding a unique mapping from u and y to s and t:

$$s(k) = \begin{pmatrix}+u(k)\\ -y(k)\end{pmatrix} \tag{4.4}$$

$$t(k) = \left(\tilde{M} * y\right) - \left(\tilde{N} * u\right) \tag{4.5}$$

Theorems 2.10 and 2.11 can now be applied:

Figure 4.3: Left Normalized Coprime Factorization

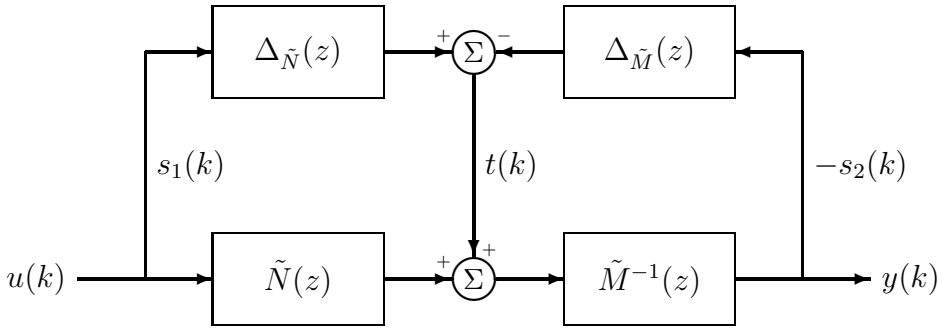

Proposition 4.1 ([Dav96]) *Given a model set $\mathcal{P}$ with the structure of Fig. 4.3, with $\Delta = \begin{bmatrix} \Delta_{\tilde{N}} & \Delta_{\tilde{M}} \end{bmatrix} \in \mathbf{\Delta}$ and $\|\Delta\|_{i2} < \gamma$, and a set of input-output data $u \in \Pi_l \mathcal{S}_+^m$ and $y \in \Pi_l \mathcal{S}_+^n$, let*[1]

$$s = \text{vec} \left[\begin{pmatrix} u \\ y \end{pmatrix} \right] \tag{4.6}$$

$$t = T_{\tilde{M}} \text{vec}\,(y) - T_{\tilde{N}} \text{vec}\,(u) \tag{4.7}$$

then:

1. *if Δ is* linear *and* time invariant*, there exists some plant $P_1 \in \mathcal{P}$ satisfying*

$$y = \Pi_l T_{P_1} u$$

if and only if

$$T_t{}^T T_t \leq \gamma^2 T_s{}^T T_s \tag{4.8}$$

or, equivalently (by the Schur complement)

$$\begin{bmatrix} \gamma^2 T_s{}^T T_s & T_t{}^T \\ T_t & I \end{bmatrix} \geq 0 \tag{4.9}$$

2. *if Δ is* linear *but* time varying*, there exists some plant $P_1 \in \mathcal{P}$ satisfying*

$$y = \Pi_l T_{P_1} u$$

if and only if

$$\|\Pi_k t\|_2 \leq \gamma \|\Pi_k s\|_2 \tag{4.10}$$

[1]The more alert reader may notice that the sign of y in the expression for s is reversed. This does not matter, since the sense is still correct in $T_s^T T_s$.

for all $k = 1, 2, \ldots, l$*, or, equivalently (by the Schur complement)*

$$\begin{bmatrix} \gamma^2 (\Pi_{k(p+q)} s)^T (\Pi_{k(p+q)} s) & (\Pi_{kq} t)^T \\ (\Pi_{kq} t) & I \end{bmatrix} \geq 0 \tag{4.11}$$

for all $k = 1, 2, \ldots, l$ *(where* q *is the output dimension of* $\tilde{N}$*)*

The following remarks are drawn from material in [Dav96].

Remark 4.2 Validation of a right-coprime factor model set does not yield the same results (due to the difference between the gap and T-gap metrics). ♡

Remark 4.3 The induced 2-norm of a system is equal to the infinity norm:

$$\sup_u \|\Delta\|_{i2} = \frac{\|\Delta * u\|_2}{\|u\|_2} = \|\Delta\|_\infty = \sup_{|z|>1} \overline{\sigma}[\Delta(z)] \tag{4.12}$$

Finding the minimum value of γ is the same as attempting to find the smallest $\mathcal{H}_\infty$ perturbation to the coprime factors: it is thus a lower bound on the gap $\delta_g(P_{\text{nom}}, P_{\text{true}})$, where and $P_{\text{nom}} = \tilde{M}^{-1}\tilde{N}$ and $P_{\text{true}} = (\tilde{M} + \Delta_{\tilde{M}})^{-1}(\tilde{N} + \Delta_{\tilde{N}})$. ♡

Remark 4.4 The minimum value of γ often tends to δ_g as the length of the data record increases, provided that exitation is persistent. ♡

Remark 4.5 The LMIs in γ given for the two cases can be solved using commands from MATLAB's LMI Toolbox: `gevp` and `mincx`. ♡

4.3.1 Non-invalidation/invalidation with a central noise input

Existing approaches to gap validation [Dav96] model noise as entering 'in the middle' of the NCF as shown in Fig. 4.4. This entry point guarantees convexity, and achieves a compromise between placing the noise at the input or the output. (See pp. 45–48 of [Dav96] for details.) Effectively, the noise is not subject to model perturbations.

Proposition 4.6 ([Dav96]) *Given a model set $\mathcal{P}$ with the structure of Fig. 4.4, with $\Delta = \begin{bmatrix} \Delta_{\tilde{N}} & \Delta_{\tilde{M}} \end{bmatrix} \in \mathbf{\Delta}$ and $\|\Delta\|_{i2} < \gamma$, and a set of input-output data $(u, y) \in (\mathcal{S}_\ell^q, \mathcal{S}_\ell^p)$, and a noise set $\mathbf{W}_t$ consisting of all $w_t \in \mathcal{S}_\ell^p$ satisfying some given constraint) let*

$$s = \text{vec}\left[\begin{pmatrix} u \\ v \end{pmatrix}\right] \tag{4.13}$$

$$t = T_{\tilde{M}}\text{vec}\,(y) - T_{\tilde{N}}\text{vec}\,(u) \tag{4.14}$$

then:

1. *If Δ is* linear *and* time invariant*, there exist $(P_1, \hat{w}_t) \in (\mathcal{P}, \mathbf{W}_t)$ satisfying the interpolation condition*

$$y = T_{P_1} u + T_{\tilde{M}^{-1}} \hat{w}_t \tag{4.15}$$

if and only if there exists $w_t \in \mathbf{W}_t$ satisfying

$$(T_t - T_{w_t})^T (T_t - T_{w_t}) \leq \gamma^2 {T_s}^T T_s \tag{4.16}$$

or, equivalently (by the Schur complement)

$$\begin{bmatrix} \gamma^2 {T_s}^T T_s & T_t^T - T_{w_t}^T \\ T_t - T_{w_t} & I \end{bmatrix} \geq 0 \tag{4.17}$$

This is an LMI in $\begin{bmatrix} \gamma^2 \\ w_t \end{bmatrix}$. If any such w_t exist, then $\hat{w}_t = w_t$ is a solution of (4.15).

2. *if Δ is* linear *but* time varying*, there exist $(P_1, \hat{w}_t) \in (\mathcal{P}, \mathbf{W}_t)$ satisfying (4.15) if and only if there exists $w_t \in \mathbf{W}_t$ such that*

$$\|\Pi_k(t - w_t)\|_2 \leq \gamma \|\Pi_k s\|_2 \;\; \forall k = 1, 2, \ldots, \ell \tag{4.18}$$

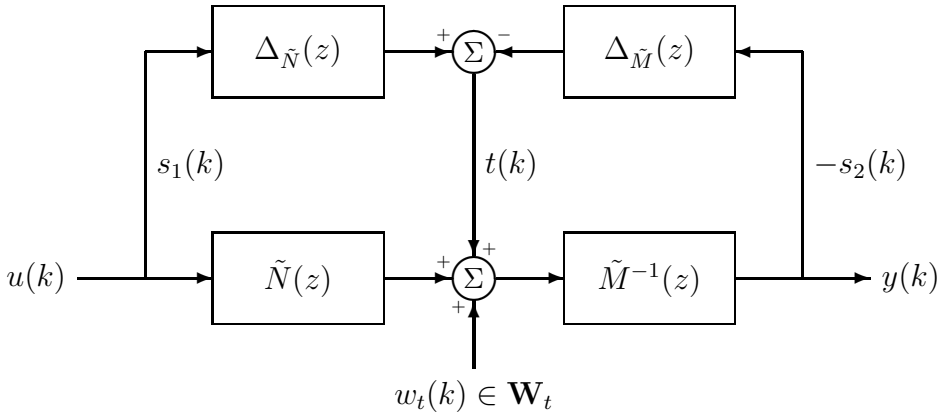

Figure 4.4: Left Normalized Coprime Factorization with Noise

or, equivalently,

$$\begin{bmatrix} \gamma^2(\Pi_{k(p+q)}(s))^T(\Pi_{k(p+q)}s) & (\Pi_{kp}(t-w_t))^T \\ (\Pi_{kp}(t-w_t) & I \end{bmatrix} \geq 0 \ \forall \ k = 1, 2, \ldots, \ell \quad (4.19)$$

Again, should such w_t exist, then $\hat{w}_t = w_t$ is a solution of (4.15)

4.3.2 Non-invalidation with input-output noise

The noise injection points shown in Fig. 4.5 are more realistic, but have been avoided in previous work because they do not necessarily result in convex problems. Subsequent work on ν-gap validation [SV01] has got round this difficulty by approximating the validation problem. Similar ideas can be applied to gap validation techniques.

Consider the equation relating the input to the output:

$$(y - w_y) = \left(\tilde{M} + \Delta_{\tilde{M}}\right)^{-1} \left(\tilde{N} + \Delta_{\tilde{N}}\right)(u - w_u) \quad (4.20)$$

$$\left(\tilde{M} + \Delta_{\tilde{M}}\right)(y - w_y) = \left(\tilde{N} + \Delta_{\tilde{N}}\right)(u - w_u) \quad (4.21)$$

This can be rearranged with all the uncertain terms on the RHS

$$-\begin{bmatrix}\tilde{N} & \tilde{M}\end{bmatrix}\begin{bmatrix}+(u-w_u)\\-(y-w_y)\end{bmatrix}=\begin{bmatrix}\Delta_{\tilde{N}} & \Delta_{\tilde{M}}\end{bmatrix}\begin{bmatrix}+(u-w_u)\\-(y-w_y)\end{bmatrix} \tag{4.22}$$

$$-\begin{bmatrix}\tilde{N} & \tilde{M}\end{bmatrix}\left(\begin{bmatrix}+u\\-y\end{bmatrix}-\begin{bmatrix}+w_u\\-w_y\end{bmatrix}\right)=\begin{bmatrix}\Delta_{\tilde{N}} & \Delta_{\tilde{M}}\end{bmatrix}\left(\begin{bmatrix}+u\\-y\end{bmatrix}-\begin{bmatrix}+w_u\\-w_y\end{bmatrix}\right) \tag{4.23}$$

Now define $\Delta=\begin{bmatrix}\Delta_{\tilde{N}} & \Delta_{\tilde{M}}\end{bmatrix}$, $s=\begin{bmatrix}+u\\-y\end{bmatrix}$ and $w_s=\begin{bmatrix}+w_u\\-w_y\end{bmatrix}$. The equation now becomes

$$-\begin{bmatrix}\tilde{N} & \tilde{M}\end{bmatrix}(s-w_s)=\Delta(s-w_s) \tag{4.24}$$

Now define $t=-\begin{bmatrix}\tilde{N} & \tilde{M}\end{bmatrix}s$ and $w_t=-\begin{bmatrix}\tilde{N} & \tilde{M}\end{bmatrix}w_s$. This gives a useful result:

$$(t-w_t)=\Delta(s-w_s) \tag{4.25}$$

Note that it is easy to recover recover w_u and w_y from w_s since

$$\begin{bmatrix}w_u\\w_y\end{bmatrix}=\begin{bmatrix}I_q & 0\\0 & -I_p\end{bmatrix}w_s \tag{4.26}$$

where q and p are the input and output dimensions of the plant.

Proposition 4.7 *Given a model set $\mathcal{P}$ with the structure of Fig. 4.5, with $\Delta=\begin{bmatrix}\Delta_{\tilde{N}} & \Delta_{\tilde{M}}\end{bmatrix}\in\mathbf{\Delta}$ and $\|\Delta\|_{i2}<\gamma$, and a set of input-output data $u\in\Pi_l\mathcal{S}_+^m$ and*

$y \in \Pi_l \mathcal{S}_+^n$, *and noise sets* $\mathbf{W}_u$ *and* $\mathbf{W}_y$, *let*

$$s = \text{vec} \begin{bmatrix} +u \\ -y \end{bmatrix} \tag{4.27}$$

$$t = T_{-[\tilde{N}\ \tilde{M}]} s \tag{4.28}$$

then:

1. *if* Δ *is* linear *and* time invariant, *there exists some plant* $P_1 \in \mathcal{P}$ *and some noise sequences* $w_u \in \mathbf{W}_u$ *and* $w_y \in \mathbf{W}_y$ *satisfying*

$$y = \Pi_l T_{P_1}(u - w_u) + w_y$$

if and only if

$$(T_t - T_{w_t})^T (T_t - T_{w_t}) \leq \gamma^2 (T_s - T_{w_s})^T (T_s - T_{w_s}) \tag{4.29}$$

where w_s, w_t *are the 'vec' forms of the corresponding signals defined earlier in the section. From the definitions, it is clear that* $T_{w_t} = -T_{[\tilde{N}\ \tilde{M}]} T_{w_s}$. *By the*

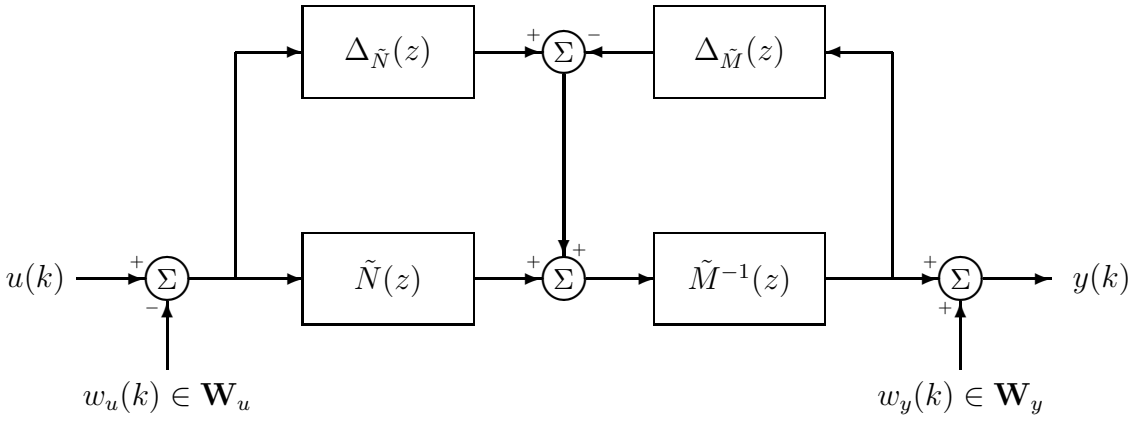

Figure 4.5: Left Normalized Coprime Factorization with Noise

Schur complement:

$$\begin{bmatrix} \left(T_s^T T_s - T_{w_s}^T T_s - T_s^T T_{w_s} + T_{w_s}^T T_{w_s}\right) & T_t^T - (T_{-[\tilde{N}\ \tilde{M}]} T_{w_s})^T \\ T_t - T_{-[\tilde{N}\ \tilde{M}]} T_{w_s} & \gamma^2 \end{bmatrix} \geq 0 \qquad (4.30)$$

2. *if* Δ *is* linear *but* time varying*, there exists some plant* $P_1 \in \mathcal{P}$ *and some noise sequence* $w_t \in \mathbf{W}_t$ *satisfying*

$$y = \Pi_l T_{P_1}(u - w_u) + w_y$$

if and only if

$$\|\Pi_k(t - w_t)\|_2 \leq \gamma \|\Pi_k(s - w_s)\|_2 \qquad (4.31)$$

or, equivalently,

$$\left\|\Pi_k(t + [\tilde{N}\ \tilde{M}] * w_s)\right\|_2 \leq \gamma \|\Pi_k(s - w_s)\|_2 \qquad (4.32)$$

for all $k = 1, 2, \ldots, l$*, or, equivalently (by the Schur complement)*

$$\begin{bmatrix} \left(\Pi_{k(m+n)}(s - w_s)\right)^T \left(\Pi_{k(m+n)}(s - w_s)\right) & \left(\Pi_{kq}\left(t + [\tilde{N}\ \tilde{M}] * w_s\right)\right)^T \\ \left(\Pi_{kq}(t + [\tilde{N}\ \tilde{M}] * w_s\right) & \gamma^2 \end{bmatrix} \geq 0 \qquad (4.33)$$

for all $k = 1, 2, \ldots, l$ *(where* q *is the output dimension of* $\tilde{N}$*).*

Proof. This is a simple application of Theorems 2.10 and 2.11. □

Note that (4.30) and (4.33) cannot be expressed as LMIs in $\begin{bmatrix} \gamma^2 \\ w_s \end{bmatrix}$. It is straightforward to approximate these conditions to get LMI problems:

Proposition 4.8 (Sufficient Conditions for Validation) *Given a model set* $\mathcal{P}$ *with the structure of Fig. 4.5, with* $\Delta = \begin{bmatrix} \Delta_{\tilde{N}} & \Delta_{\tilde{M}} \end{bmatrix} \in \mathbf{\Delta}$ *and* $\|\Delta\|_{i2} < \gamma$*, and a set*

of input-output data $u \in \Pi_l \mathcal{S}_+^m$ *and* $y \in \Pi_l \mathcal{S}_+^n$*, and noise sets* $\mathbf{W}_u$ *and* $\mathbf{W}_y$*, let*

$$s = \text{vec} \begin{bmatrix} u \\ -y \end{bmatrix} \tag{4.34}$$

$$t = T_{-[\tilde{N}\ \tilde{M}]} s \tag{4.35}$$

then:

1. *if* Δ *is* linear *and* time invariant*, there exists some plant* $P_1 \in \mathcal{P}$ *and some noise sequences* $w_u \in \mathbf{W}_u$ *and* $w_y \in \mathbf{W}_y$ *satisfying*

$$y = \Pi_l T_{P_1}(u - w_u) + w_y$$

if (but not *only if)*

$$(T_t - T_{w_t})^T (T_t - T_{w_t}) \leq \gamma^2 \left(T_s^T T_s - T_{w_s}^T T_s - T_s^T T_{w_s} \right) \tag{4.36}$$

Now $T_{w_t} = -T_{-[\tilde{N}\ \tilde{M}]} T_{w_s}$*. By the Schur complement:*

$$\begin{bmatrix} T_s^T T_s - T_{w_s}^T T_s - T_s^T T_{w_s} & T_t^T - \left(T_{-[\tilde{N}\ \tilde{M}]} T_{w_s} \right)^T \\ T_t - T_{-[\tilde{N}\ \tilde{M}]} T_{w_s} & \gamma^2 \end{bmatrix} \geq 0 \tag{4.37}$$

2. *if* Δ *is* linear *but* time varying*, there exists some plant* $P_1 \in \mathcal{P}$ *and some noise sequence* $w_t \in \mathbf{W}_t$ *satisfying*

$$y = \Pi_l T_{P_1}(u - w_u) + w_y$$

if (but not *only if)*

$$\begin{bmatrix} (\Pi_k s)^T (\Pi_k s) - (\Pi_k w_s)^T (\Pi_k s) - (\Pi_k s)^T (\Pi_k w_s) & \left(\Pi_{kq} \left(t + [\tilde{N}\ \tilde{M}] * w_s \right) \right)^T \\ \left(\Pi_{kq} (t + [\tilde{N}\ \tilde{M}] * w_s \right) & \gamma^2 \end{bmatrix} \geq 0 \tag{4.38}$$

for all $k = 1, 2, \ldots, l$ (where q is the output dimension of $\tilde{N}$).

Proof. This is exactly as before, except that the interpolation condition is approximate. In the LTI case, we observe that

$$(T_t - T_{w_t})^T (T_t - T_{w_t}) \leq \gamma^2 (T_s - T_{w_s})^T (T_s - T_{w_s})$$

is the same as

$$(T_t - T_{w_t})^T (T_t - T_{w_t}) \leq \gamma^2 \left(T_s^T T_s - T_{w_s}^T T_s - T_s^T T_{w_s} + T_{w_s}^T T_{w_s} \right)$$

Writing this as

$$(T_t - T_{w_t})^T (T_t - T_{w_t}) - \gamma^2 \left(T_s^T T_s - T_{w_s}^T T_s - T_s^T T_{w_s} \right) \leq \gamma^2 T_{w_s}^T T_{w_s}$$

it is immediately clear that, since $\gamma \geq 0$ and $T_{w_s}^T T_{w_s} \geq 0$, this will always be true if

$$(T_t - T_{w_t})^T (T_t - T_{w_t}) - \gamma^2 \left(T_s^T T_s - T_{w_s}^T T_s - T_s^T T_{w_s} \right) \leq 0$$

Thus we have a sufficient condition for validation. Similar manipulations apply to the LTV case. □

(4.37) and (4.38) *are* an LMIs in $\begin{bmatrix} \gamma^2 \\ w_s \end{bmatrix}$.

Remark 4.9 It has been observed by Steele and Vinnicombe [SV01] that it is reasonable to assume that the effect of $T_{w_s}^T T_{w_s}$ will be substantially smaller than that of $T_{w_s}^T T_s$ and its transpose. ♡

Remark 4.10 There is no scope for simplifying the problem by assuming that $w_s = 0$ as may be done for the ν-gap problem because $w_s = \begin{pmatrix} +w_u \\ -w_y \end{pmatrix}$. ♡

Remark 4.11 These approximate conditions are implicitly formulated as MVOPs. ♡

4.4 Non-invalidation in the ν-gap metric, δ_ν

The basic framework for validation in the ν-gap metric was laid down in [Dav96]; it was extended in [SV01] to allow more realistic noise constraints at the cost of approximation of the interpolation constraints.

Let P be some nominal plant and let $\beta < b_{\text{opt}}(P)$ be a ν-gap radius. Recall from section 3.2.3 the parameterization of a 'ball' of radius β in the ν-gap centred on P is:

$$\mathcal{B}_\nu^{\text{LTI}}(P,\beta) = \left\{P_1 : P_1 = \mathcal{F}_u(M^{-1},\Delta), \Delta \in \mathcal{RH}_\infty, \|\Delta\|_\infty < 1\right\}$$

where M is the *central controller* acheving $b_{P,C} > \beta$ for all $C \in \{C_1 : C_1 = \mathcal{F}_\ell(M,Q), Q \in \mathcal{RH}_\infty, \|Q\|_\infty < 1\}$. (See section 3.2.3 for details.)

Taking u as the system input, y as the corresponding output, t as the perturbation block output and s as the perturbation block input, any model in the above set can be described with the equations

$$\begin{bmatrix} y \\ s \end{bmatrix} = M^{-1} \begin{bmatrix} u \\ t \end{bmatrix}$$

$$t = \Delta s$$

An important property of this set is that given any (u,y) the corresponding (s,t) are unique; similarly, given any (s,t) the corresponding (u,y) are unique. The relationship between the two pairs is given by the *chain scattering form* of M:

$$\text{ch}(M) := \begin{bmatrix} M_{12} - M_{11}M_{21}^{-1}M_{22} & M_{11}M_{21}^{-1} \\ -M_{21}^{-1}M_{22} & M_{21}^{-1} \end{bmatrix} \tag{4.39}$$

The existence of M_{21}^{-1}, $M^{-1} \in \mathcal{R}$ and $\text{ch}(M)^{-1} \in \mathcal{RH}_\infty$ are demonstrated in

[GGLD90]. The chain scattering form gives the following relationship:

$$\begin{pmatrix} s \\ t \end{pmatrix} = \mathrm{ch}(M)^{-1} \begin{pmatrix} u \\ y \end{pmatrix} \tag{4.40}$$

If noise sequences (w_u, w_y) are subtracted from the system input and output, linearity gives the perturbation block input and output as $\begin{pmatrix} s - w_s \\ t - w_t \end{pmatrix}$ where

$$\begin{pmatrix} w_s \\ w_t \end{pmatrix} := \mathrm{ch}(M)^{-1} \begin{pmatrix} w_u \\ w_y \end{pmatrix} \tag{4.41}$$

These ideas will be useful in the following sections.

4.4.1 Non-convex conditions for non-invalidation/validation

This gives rise to the following propositions [SV01]:

Proposition 4.12 (LTI Non-Invalidation) *Given some nominal model P, noise sets $\mathbf{W}_u$ and $\mathbf{W}_y$ and a ν-gap radius β, and the corresponding central controller M as described in section 3.2.3, the following statements are equivalent.*

1. *there exist noise sequences $w_u \in \mathbf{W}_u$ and $w_y \in \mathbf{W}_y$, and a linear, time-invariant $\hat{P} \in \mathcal{B}_\nu(P, \beta)$ such that $y = \hat{P} * (u - w_u) + w_y$;*
2. *there exist sequences (w_s, w_t) such that $\begin{pmatrix} w_u \\ w_y \end{pmatrix} := \mathrm{ch}(M) * \begin{pmatrix} w_s \\ w_t \end{pmatrix} \in \mathbf{W}_u \times \mathbf{W}_y$ and*

$$(T_t - T_{w_t})^* (T_t - T_{w_t}) \leq (T_s - T_{w_s})^* (T_s - T_{w_s}), \tag{4.42}$$

3. *(by the Schur complement) there exist sequences (w_s, w_t) such that $\begin{pmatrix} w_u \\ w_y \end{pmatrix} :=$*

$$\mathrm{ch}(M) * \begin{pmatrix} w_s \\ w_t \end{pmatrix} \in \mathbf{W}_u \times \mathbf{W}_y \text{ and}$$

$$0 \leq \begin{bmatrix} T_s^* T_s - T_{w_s}^* T_s - T_s^* T_{w_s} + T_{w_s}^* T_{w_s} & T_t^* - T_{w_t}^* \\ T_t - T_{w_t} & I \end{bmatrix} \tag{4.43}$$

Any values of (w_s, w_t) *and their equivalent* (w_u, w_y) *satisfying one of the conditions will satisfy the others.*

There is a corresponding result for linear time-varying uncertainty:

Proposition 4.13 (LTV Non-invalidation) *Given some nominal model* P*, noise sets* $\mathbf{W}_u$ *and* $\mathbf{W}_y$ *and a* ν*-gap radius* β*, and the corresponding central controller* M *as described in section 3.2.3, the following statements are equivalent.*

1. *there exist noise sequences* $w_u \in \mathbf{W}_u$ *and* $w_y \in \mathbf{W}_y$*, and a linear, time-varying* $\hat{P} \in \mathcal{P}_\nu(P, \beta)$ *such that* $y = \hat{P} * (u - w_u) + w_y$*;*
2. *there exist sequences* (w_s, w_t) *such that* $\begin{pmatrix} w_u \\ w_y \end{pmatrix} := \mathrm{ch}(M) * \begin{pmatrix} w_s \\ w_t \end{pmatrix} \in \mathbf{W}_u \times \mathbf{W}_y$ *and*
$$\|\Pi_k(t - w_t)\|_2 \leq \|\Pi_k(s - w_s)\|_2 \ \forall \ k \in [0, N-1] \tag{4.44}$$
3. *(by the Schur complement) there exist sequences* (w_s, w_t) *such that* $\begin{pmatrix} w_u \\ w_y \end{pmatrix} :=$ $\mathrm{ch}(M) * \begin{pmatrix} w_s \\ w_t \end{pmatrix} \in \mathbf{W}_u \times \mathbf{W}_y$ *and*

$$0 \leq \begin{bmatrix} (\Pi_k(s - w_s))^* \Pi_k(s - w_s) & (\Pi_k(t - w_t))^* \\ \Pi_k(t - w_t) & I \end{bmatrix} \tag{4.45}$$

Any values of (w_s, w_t) *and their equivalent* (w_u, w_y) *satisfying one of the conditions will satisfy the others.*

Unfortunately, the presence of quadratic terms in the Schur complement makes these non-convex.

4.4.2 Convex sufficient conditions for non-invalidation

Steele and Vinnicombe [SV01] approximated these conditions to give sufficient conditions for validation:

Proposition 4.14 (LTI Non-invalidation—Sufficient Condition [SV01]) *Given some nominal model P, a ν-gap radius β and the corresponding central controller M as described in section 3.2.3, and noise sets $\mathbf{W}_u$ and $\mathbf{W}_y$, there exist noise sequences $w_u \in \mathbf{W}_u$ and $w_y \in \mathbf{W}_y$, and a linear, time-invariant $\hat{P} \in \mathcal{P}_\nu(P, \beta)$ such that $y = \hat{P} * (u - w_u) + w_y$ if, but* not *only if, there exist sequences (w_s, w_t) such that* $\mathrm{ch}(M) * \begin{pmatrix} w_s \\ w_t \end{pmatrix} \in \mathbf{W}_u \times \mathbf{W}_y$ *and*

$$(T_t - T_{w_t})^* (T_t - T_{w_t}) \leq \left(T_s^* T_s - T_{w_s}^* T_s - T_{w_s}^* T_s\right), \tag{4.46}$$

or equivalently, by the Schur complement,

$$0 \leq \begin{bmatrix} T_s^* T_s - T_{w_s}^* T_s - T_s^* T_{w_s} & T_t^* - T_{w_t}^* \\ T_t - T_{w_t} & I \end{bmatrix} \tag{4.47}$$

When (w_s, w_t) exist, values of (w_u, w_y) satisfying the original condition are given by $\begin{pmatrix} w_u \\ w_y \end{pmatrix} = \mathrm{ch}(M) * \begin{pmatrix} w_s \\ w_t \end{pmatrix}$.

Proposition 4.15 (LTV Validation—Sufficient Condition [SV01]) *Given some nominal model P, a ν-gap radius β and the corresponding central controller M as described in section 3.2.3, and noise sets $\mathbf{W}_u$ and $\mathbf{W}_y$, there exist noise sequences $w_u \in \mathbf{W}_u$ and $w_y \in \mathbf{W}_y$, and a linear, time-varying $\hat{P} \in \mathcal{P}_\nu(P, \beta)$ such that $y = \hat{P} * (u - w_u) + w_y$ if, but* not *only if, there exist sequences (w_s, w_t) such that*

$$\mathrm{ch}(M) * \begin{pmatrix} w_s \\ w_t \end{pmatrix} \in \mathbf{W}_u \times \mathbf{W}_y \text{ and}$$

$$0 \leq \begin{bmatrix} (\Pi_k s)^* \Pi_k s - (\Pi_k w_s)^* \Pi_k s - (\Pi_k s)^* \Pi_k w_s & (\Pi_k (t - w_t))^* \\ \Pi_k (t - w_t) & I \end{bmatrix} \tag{4.48}$$

When (w_s, w_t) exist, values of (w_u, w_y) satisfying the original condition are given by $\begin{pmatrix} w_u \\ w_y \end{pmatrix} = \mathrm{ch}(M) * \begin{pmatrix} w_s \\ w_t \end{pmatrix}$.

The authors of [SV01] also provide sufficient and necessary conditions for (non)-invalidation when $w_s = 0$. This idea will not be developed further, but is included for completeness in Appendix A.

4.5 Constraining exogenous noise

Having dealt with constraints relating to model perturbations, it is time to address the nature of the 'noise sets' governing the exogenous noise. At the start of this chapter, it was mentioned that these typically take the form of a bound such as a maximum ℓ_2-norm. Other possibilites might include a ℓ_∞ norm or the mean of the absolute value. Key in the usefulness of these bounds is our ability to implement them as linear constraints.

In the case of the ℓ_2-norm, if $\|w_u\|_2$ is constrained to be less than than A,

$$(\mathrm{vec}\,(w_u))^T \mathrm{vec}\,(w_u) < A^2 \tag{4.49}$$

which is, in LMI form,

$$\begin{bmatrix} A^2 & (\mathrm{vec}\,(w_u))^T \\ \mathrm{vec}\,(w_u) & I \end{bmatrix} > 0 \tag{4.50}$$

This makes it very easy to constrain the ℓ_2-norm of a sequence of decision variables. Linear mappings are possible:

If w_u is a function of some other noise set, e.g. $w_u = G * w_s$, where G is a linear system, this can be re-written as

$$\begin{bmatrix} A^2 & (\text{vec}\,(w_s))^T T_G^T \\ T_G \text{vec}\,(w_s) & I \end{bmatrix} > 0 \tag{4.51}$$

where T_G is the finite lower-block Toeplitz operator corresponding to G. This means that it is possible to apply bounds to 'filtered' versions of the decision variable sequences. This is of practical usefulness in some LFT model sets where the effects of noise sequences applied at the system input/output are modelled by decision variable sequences representing the sequences' effects at the perturbation block input/output; an example of this may be seen in Propositon 4.12 where the constraint on noise is expressed as:

$$\begin{pmatrix} w_u \\ w_y \end{pmatrix} := \text{ch}(M) * \begin{pmatrix} w_u \\ w_y \end{pmatrix} \in \mathbf{W}_u \times \mathbf{W}_y$$

Recall that $\text{ch}(M)$ is a linear mapping; nothing else about it is presently important. Suppose that the desired bound on the exogenous noise sequences is an ℓ_2-norm bound on the combined input-output sequences:

$$\mathbf{W}_u \times \mathbf{W}_y := \{(w_u, w_y) : ||w_u||_2^2 + ||w_y||_2^2 < \gamma^2, w_u \in \mathcal{S}_k^q, w_y \in \mathcal{S}_k^p\}$$

It is easy to see how this bound may be expressed using (4.51).

There are plenty of variations on this: it is also possible to bound noise according to the mean of the absolute sum of the samples [SV01]:

$$-N\epsilon_{\text{mean}} < b^T w_y < N\epsilon_{\text{mean}} \tag{4.52}$$

for N samples and a maximum mean value ϵ_{mean}, where b is a vector of ones.[2] This may be trivially implemented as a pair of inequality constraints.

[2]If we used $\begin{pmatrix} w_u \\ w_y \end{pmatrix}$ in the equation, b would select the right elements.

An ℓ_∞ bound is implemented by applying a similar pair of constraints to each term.

None of the bounds outlined above prevents unrealistic cross-correlations between inputs, outputs and noise models: this could make the results overly optimistic, because a model error could be 'covered up' if it happened to result in an admissibl 'noise' sequence. Sources such as [Pag96] suggest methods of constraining the cross correlation, though preliminary experiments did not yield promising results: owing to the difficulty in implementing nonlinear constraints, it was found to be difficult to place appropriate restrictions on the autocorrelation of a supposedly random noise sequence.

4.6 Issues in implementation

LMI problems may be implemented using MATLAB's LMI Control Toolbox or other non-comercial solvers such as SeDuMi. In practice, this has been found to be quite slow. Earlier work [Dav96] quotes the following claim from [BVG94]:

> ...we are able to solve convex optimization problems with over 1,000 variables and 10,000 constraints in around 10 minutes on a workstation.

This level of performance was not achieved. It was found that problems with roughly 350 decision variables implemented in MATLAB, an LTI/LTV interpolation constraint and a noise-norm constraint took several hours to solve using a modern Pentium processor. Improvement here would be desirable.

MATLAB's LMI Control Toolbox has the following commands:

- `feasp` – determines whether a convex problem is strictly feasible, i.e. minimize t subject to

$$L(x) < R(x) + t \times I \tag{4.53}$$

- `gevp` – solves a generalised minimum eigenvalue problem, i.e. finds the smallest

value of t for which

$$C(x) < 0 \tag{4.54}$$

$$0 < B_j(x) \qquad j = 1, \ldots, M \tag{4.55}$$

$$A_j(x) < t \times B_j(x) \qquad j = 1, \ldots, M \tag{4.56}$$

- `mincx` – minimizes $c^T x$ subject to

$$L(x) < R(x) \tag{4.57}$$

Remark 4.16 `mincx` is the obvious choice where a MVOP can be formulated suitably. `feasp` seems at first glance to be the most appropriate for MVDPs. ♡

Remark 4.17 `mincx` can be used to 'do' `feasp`-type problems. Given the fact that the LMI Lab routines assume *strict* inequalities, `feasp` can complain bitterly about marginally-feasible problems. With `mincx` it is possible to avoid this: it is also possible to set the problem to find the minimum eigenvalue of the interpolation matrix whilst ensuring that the noise constraints are met. ♡

Remark 4.18 It was observed that sometimes the 'full' interpolation matrix—with the non-linear terms included—'passed' the validation test using the noise sets obtained from non-feasible approximate problems. (This makes sense, since the approximate problems provide *sufficient* conditions for validation.) In the light of this, `mincx` could sometimes be preferred for MVDPs. However it is difficult to see exactly how small eigenvalue perturbations relate to the interpolation conditions, so this may be unhelpful. This problem does not arise using SeDuMi. ♡

Remark 4.19 (Weighted Plants) The above techniques can be applied to weighted plants, but care should be taken to use appropriate noise constraints: noise sequences are unlikely to enter at the inputs and outputs of the *weighted* plant. ♡

Chapter 5

Extensions to Model Validation Theory

This chapter describes refinements to model validation theory. In particular, the following methods are proposed:

1. The linear approximations to the standard quadratic non-invalidation conditions are refined by successive relinearization about the optimal solution to the previous approximation. (Section 5.1)

2. Non-zero initial states are dealt with using 'initializing sequences' appended to the data before the start of the time record. (Section 5.2.)

3. A constrained tangential Nevanlinna-Pick method is used to construct interpolant systems from noise-corrected data. (Section 5.3.)

5.1 Improving results obtained through approximation

All the gap and ν-gap non-invalidation problems considered so far share a common difficulty: nonconvexity. (This was shown for the gap and ν-gap problems by [Dav96] and it was shown in [CG00] that similar problems arise whenever the input to a

perturbation block is unknown.) Two ways round this have been put forward. In [Dav96], simplifying assumptions are made about the noise: it acts only on the nominal plant, rather than the perturbed system. A slightly more sophisticated approach was given in [SV01] where the problem was made convex—and sufficient but non-necessary for non-invalidation—by dropping any unknown quadratic terms.

In [SV01] the unknown variables corresponded exactly with the noise variables, recall from Section 4.4 that when testing for a system satisfying

$$y + w_y = P(u + w_u)$$

the known part of the input and output to the uncertainty block were taken as

$$\begin{pmatrix} s \\ t \end{pmatrix} = \mathrm{ch}\,(M)^{-1} \begin{pmatrix} u \\ y \end{pmatrix}$$

and the unknown part corresponded directly to the noise signals

$$\begin{pmatrix} w_s \\ w_t \end{pmatrix} = \mathrm{ch}\,(M)^{-1} \begin{pmatrix} w_u \\ w_y \end{pmatrix}$$

We could, however, linearize the problem about *any* suitably dimensioned signals.

Algorithm Inputs: a $(p \times q)$ model set $\mathcal{P}$ and input-output sequences ($u \in \mathcal{S}_k^q, y \in \mathcal{S}_k^p$) and an objective function $c(w_u, w_y)$ and the required tolerance for the result τ_γ.

Outputs: $\hat{\gamma}$, which is an upper bound on the smallest value of $c(w_u, w_y)$ achievable under the constraint $(y + w_y) = P(u + w_u)$, and sequences $(\hat{w}_u, \hat{w}_y)$ which achieve it. (We hope that the bound will be better than that obtainable without iteration, and it can be proved that it will be no worse.)

BEGIN.

1. Define counter i and let $i = 0$.

2. Linearize the full non-invalidation problem, and use the linear approximation to find sequences (w_{u0}, w_{y0}) consistent with the problem such that $c(w_{u0}, w_{y0})$ is minimized; denote the minimum γ_0

3. Increment the counter i by 1.

4. Re-linearize the full non-invalidation problem about $(w_{u(i-1)}, w_{y(i-1)})$, and and use the linear approximation to find sequences $(w_{ui} \in \mathcal{S}_k^q, w_{yi})$ consistent with the problem such that $c(w_{ui}, w_{yi})$ is minimized; denote the minimum γ_i.

5. If $\gamma_{i-1} - \gamma_i > \tau_\gamma$, go to step 3; otherwise continue.

6. Let $\hat{\gamma} = \gamma_i$, $\hat{w}_u = w_{ui}$ and $\hat{w}_y = w_{yi}$.

END.

There are many variations on this algorithm, and it is intended to be illustrative rather than definitive; there are many ways of finding an initial solution, for example, and in practice one normally restricts the number of iterations that may be performed before termination.

The mathematics below provides the machinery for the application of such algorithms to the ν-gap non-invalidation problem. Theorems 5.1 and 5.3 provide the necessary problem relinearizations; the main result is given in Remark 5.2. (The latter is stated as a remark because it adds context but no further mathematics.)

5.1.1 Sufficient condition: non-invalidation with LTI uncertainty

Theorem 5.1 *Given a linear time-invariant $p \times q$ model P, a ν-gap radius β, the corresponding central controller M, noise sets $\mathbf{W}_u$ and $\mathbf{W}_y$, measured data sequences $u \in \mathcal{S}_k^q$, $y \in \mathcal{S}_k^p$, and sequences $w_{u0} \in \mathcal{S}_k^q$, $w_{y0} \in \mathcal{S}_k^p$, then there exist $\hat{P} \in \mathcal{B}_\nu^{\mathrm{LTI}}(P, \beta)$ and sequences $w_u \in \mathbf{W}_u$, $w_y \in \mathbf{W}_y$ such that*

$$(y + w_y) = \hat{P}\,(u + w_u) \tag{5.1}$$

if there exist sequences $w_s \in \mathcal{S}_k^q, w_t \in \mathcal{S}_k^p$ satisfying

$$\mathrm{ch}\,(M) \begin{pmatrix} w_s \\ w_t \end{pmatrix} + \begin{pmatrix} w_{u0} \\ w_{y0} \end{pmatrix} \in \mathbf{W}_u \times \mathbf{W}_y \tag{5.2}$$

and either of the following (equivalent) conditions:

(i)

$$(T_t + T_{w_t})^*(T_t + T_{w_t}) \leq (T_s^* T_s + T_{w_s}^* T_s + T_s^* T_{w_s})$$

(ii)

$$0 \leq \begin{bmatrix} T_s^* T_s + T_{w_s}^* T_s + T_s^* T_{w_s} & T_t^* + T_{w_t}^* \\ T_t + T_{w_t} & I \end{bmatrix}$$

where

$$\begin{pmatrix} s \\ t \end{pmatrix} = \mathrm{ch}\,(M)^{-1} \begin{pmatrix} u + w_{u0} \\ y + w_{y0} \end{pmatrix} \tag{5.3}$$

The corresponding (w_u, w_y) are given by (5.2).

Outline of proof. The proof is more-or-less identical to that of Proposition 4.14. The standard LTI interpolation condition of Theorem 2.10 requires that the perturbation block's input $\hat{s} = s + w_s$ and output $\hat{t} = t + w_t$ satisfy $T_{\hat{t}}^* T_{\hat{t}} \leq T_{\hat{s}}^* T_{\hat{s}}$. Clearly, if $0 \leq M - A^* A$, then $0 \leq M$ hence condition (i). By the Schur complement this is

equivalent to condition (ii). The equivalent plant output signals are given by

$$\begin{pmatrix} \hat{u} \\ \hat{y} \end{pmatrix} = \mathrm{ch}\,(M) \begin{pmatrix} s + w_s \\ t + w_t \end{pmatrix} = \underbrace{\begin{pmatrix} u \\ y \end{pmatrix}}_{\text{measured}} + \underbrace{\mathrm{ch}\,(M) \begin{pmatrix} w_s \\ w_t \end{pmatrix} + \begin{pmatrix} w_{u0} \\ w_{y0} \end{pmatrix}}_{\text{exogenous noise}}$$

giving the constraint on the noise sequences w_s, w_t. □

The philosophy here is not greatly different from that in [SV01], but it enables an iterative approach to some optimization problems. This is summed up by the following remark.

Remark 5.2 Given P, β, M, u, y as for Theorem 5.1, and a feasible starting point $(w_{u0},\ w_{y0}) \in \mathbf{W}_u \times \mathbf{W}_y$ let $c(w_u, w_y) = \|\Pi_k C_u w_u\|_2^2 + \|\Pi_k C_y w_y\|_2^2$, where C_u and C_y are (possibly dynamic) weighing functions. If we attempt to minimize $c(\dots)$ using the approximated LTI constraint of Theorem 5.1, then we can guarantee the resulting 'minimum' will be at least as small as $c(w_{u0}, w_{y0})$, and it is quite possible that it will be smaller. (This is obvious, seen by setting $w_u = w_{u0}$ and $w_y = w_{y0}$). This result can be applied iteratively, though there is no guarantee that the final result will be the global minimum for the full (i.e. non-approximated) problem. ♡

5.1.2 Sufficient condition: non-invalidation with LTV uncertainty

Theorem 5.1 deals with unstructured LTI perturbations. There is of course an analogous result for unstructured LTV perturbations.[1]

Theorem 5.3 *Given a linear time-invariant $p \times q$ model P, a ν-gap radius β, the corresponding central controller M, noise sets $\mathbf{W}_u$ and $\mathbf{W}_y$, measured data sequences*

[1] There are of course a great many more variations on the theme: non-causal uncertainties, other non-convex LFT structures, etc. These differ only in trivialities, and there is no need for explicit discussion of them here.

$u \in \mathcal{S}_k^q$, $y \in \mathcal{S}_k^p$, and sequences $w_{u0} \in \mathcal{S}_k^q$, $w_{y0} \in \mathcal{S}_k^p$, let s, t be as defined in (5.3).

Then there exist $\hat{P} \in \mathcal{B}_\nu^{\mathrm{LTV}}(P, \beta)$ and sequences $w_u \in \mathbf{W}_u$, $w_y \in \mathbf{W}_y$ satisfying the interpolation condition (5.1) if there exist sequences $w_s \in \mathcal{S}_k^q, w_t \in \mathcal{S}_k^p$ satisfying (5.2) and either of the following (equivalent) conditions:

(i)

$$\|\Pi_j(t + w_t)\|_2^2 \leq \|\Pi_j s\|_2^2 + \mathrm{vec}\,(\Pi_j w_s)^* \mathrm{vec}\,(\Pi_j s) + \mathrm{vec}\,(\Pi_j s)^* \mathrm{vec}\,(\Pi_j w_s)$$

for all $j = 1, 2, \ldots, k$.

(ii)

$$0 \leq \begin{bmatrix} \|\Pi_j s\|_2^2 + \mathrm{vec}\,(\Pi_j w_s)^* \mathrm{vec}\,(\Pi_j s) + \mathrm{vec}\,(\Pi_j s)^* \mathrm{vec}\,(\Pi_j w_s) & \mathrm{vec}\,(\Pi_j(t + w_t))^* \\ \mathrm{vec}\,(\Pi_j(t + w_t)) & I \end{bmatrix}$$

for all $j = 1, 2, \ldots, k$.

The corresponding (w_u, w_y) are given by (5.2).

Apart from the form of the perturbation-block constraint this is identical to Theorem 5.1 and the **proof** is directly analogous. The ideas of Remark 5.2 apply equally here.

5.1.3 Improvement by iteration: a numerical example

As a numerical example, we shall consider the problem addressed in [SV01]: invalidation data of length $k = 60$ is generated from the impulse response of

$$P_{\mathrm{true}}(z) = \frac{-0.1157z^2 + 0.2671z + 0.002967}{z^2 - 1.893z + 0.905}$$

and this is compared to a nominal model

$$P(z) = \frac{0.0625z^2 + 0.125z + 0.0625}{z^2 - 2z + 1}$$

The following optimization problem is considered: minimize

$$\gamma_w := \left\{ ||w_u||_2^2 + ||w_y||_2^2 \right\}^{1/2}$$

subject to the constraint

$$(y + w_y) = \hat{P}(u + w_u)$$

for some $\hat{P} \in \mathcal{B}_\nu(P, \beta)$, considering the LTI and LTV cases separately.

For each of the LTI and LTV cases, three quantities are calculated for a range of β values:

(i) the upper bound on the smallest consistent $\|w\|_2$ from the initial relinearization; the same quantity as that investigated in [SV01]

(ii) the upper bound on the smallest consistent $\|w\|_2$ obtained from two further relinearizations

(iii) a final upper bound obtained by applying MATLAB's `fmincon` function to the full non-invalidation problem using the results of (ii) as a starting point. (This uses a 'brute force' optimization method, fully documented in [Mat00].)

The results are shown in Figures 5.1 (page 68) and 5.2 (page 69). In both cases we observe that the three-iteration relinearization method provides a slight improvement on the initial linearization, and that the nonlinear optimization is not able to do noticeably better.

5.1.4 Offsets and trends

The ideas developed in this section may help circumvent one limitation in [SV01]: the assumption that w_s and w_t are small compared to s and t. Whilst this is a perfectly reasonable assumption to make when dealing with small random noise sequences, it begins to break down when dealing with larger perturbations such as offsets and trends. In the case of a constant-but unknown output offset y_0, the noise

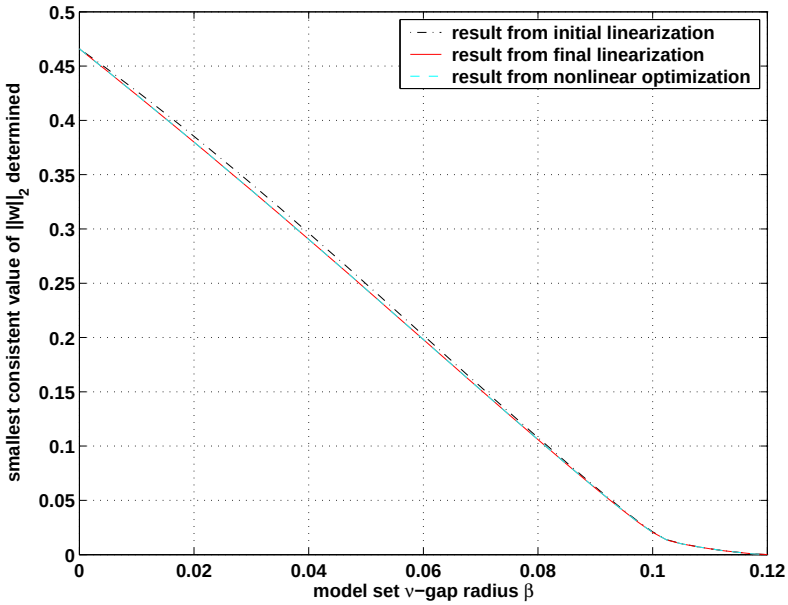

(a) Smallest consistent values $\|w\|_2$ for the first and final iterations and the nonconvex optimization

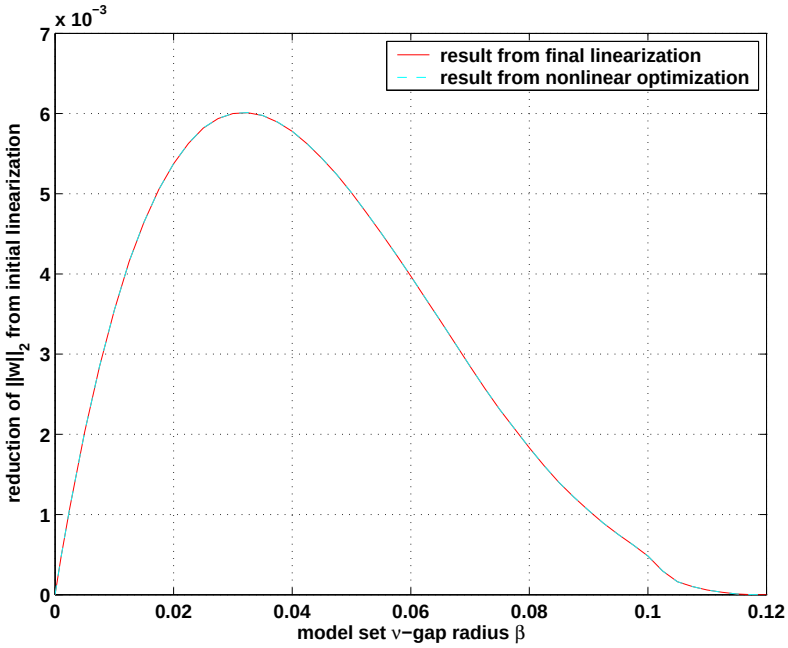

(b) Reduction in the smallest $\|w\|_2$ achieved for the final iteration and the nonconvex optimization

Figure 5.1: Applying the method of relinearizations to the example in [SV01] with LTI uncertainty. The zero ν-gap radius values were calculated analytically using a least-squares method.

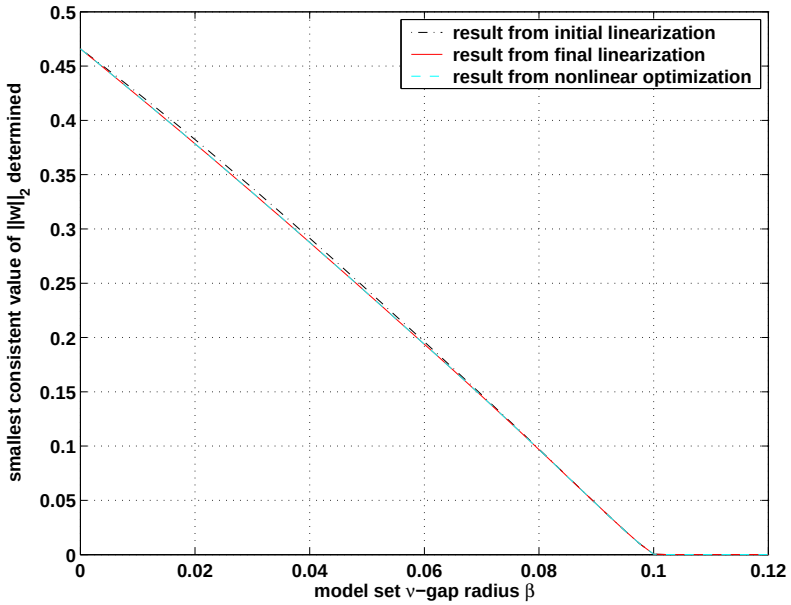

(a) Smallest consistent values $\|w\|_2$ for the first and final iterations and the nonconvex optimization

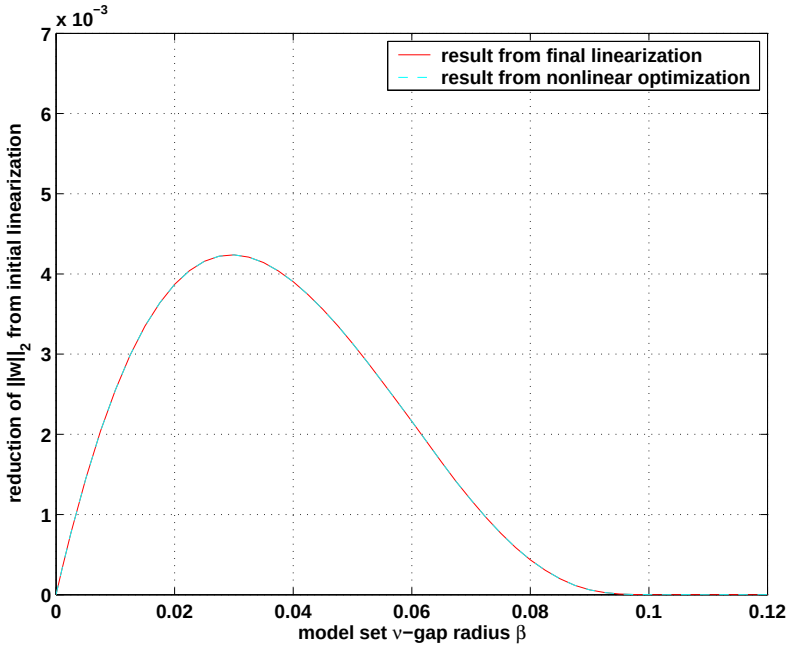

(b) Reduction in the smallest $\|w\|_2$ achieved for the final iteration and the nonconvex optimization

Figure 5.2: Applying the method of relinearizations to the example in [SV01] with LTV uncertainty. The zero ν-gap radius values were calculated analytically using a least-squares method.

set might take the following form:

$$\mathbf{W}_u \times \mathbf{W}_y := \left\{ (w_u, w_y) : \ \exists\, y_0 \text{ s.t. } \|w_u\|_2^2 + \|w_y - y_0\|_2^2 \leq \gamma_w \right\}$$

The w_s, w_t required to match the data in such cases might well be quite large and the approximation of the full perturbation block constraint may be poor. Improvement by iteration will often be possible.

5.1.5 Choice of starting point

The most obvious application of Theorems 5.1 and 5.3 is to use as (w_{u0}, w_{y0}) the 'optimal' (w_u, w_y) obtained from Proposition 4.14 or 4.15. Other choices of w_{u0}, w_{y0} are equally possible: one such might be the optimal solution for a zero-perturbation problem (this is easily solved using least-squares techniques), or the solution for a different (but close) ν-gap radius β.

5.2 Accounting for non-zero initial states

The simple Carathéodory-Fejér and energy-bound constraints demonstrate the existence or otherwise of $\mathcal{H}_\infty$-norm bounded systems mapping a given input to a given output. An implicit assumption is made that the systems are initially in equilibrium. In practical situations, this is rarely the case. A conceptually simple idea proposed (though not developed) in [Ste01] is to account for the non-zero initial state by pre-padding the input and output data with unknown variables. Any interpolation constraints are set up to take these sequences into account, but the constraints on exogenous noise need not do so. This section develops these ideas.

The most intuitive method of applying the initial sequences idea is illustrated in Fig. 5.3(a). The validation data has been pre-padded with zeros. All parts of the extended sequences are allowed to be subject to variation, which will be included in the perturbation-block constraints, but the noise constraints are only applied to the parts of the signals in 'measured time'. The aim here is that the initial part of

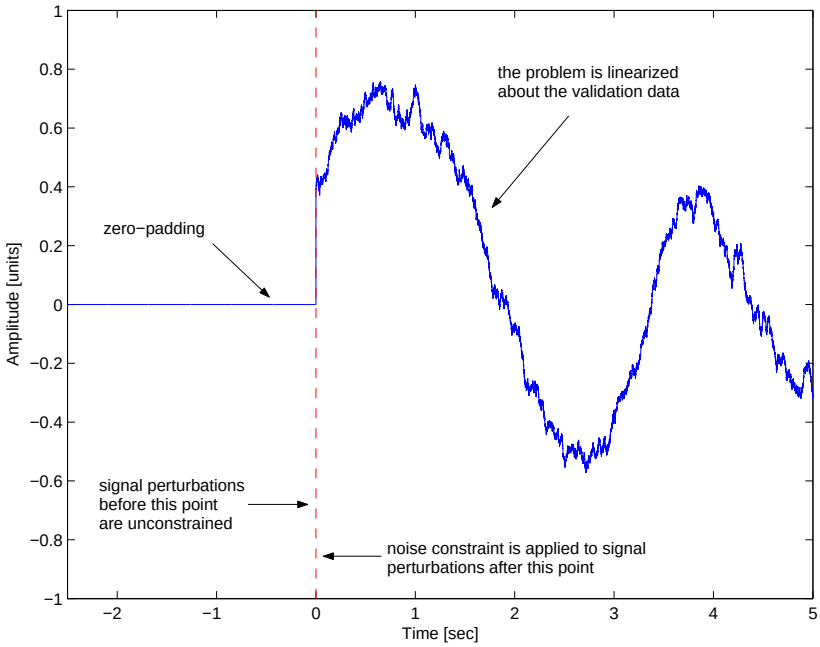

(a) Zero-padding approach

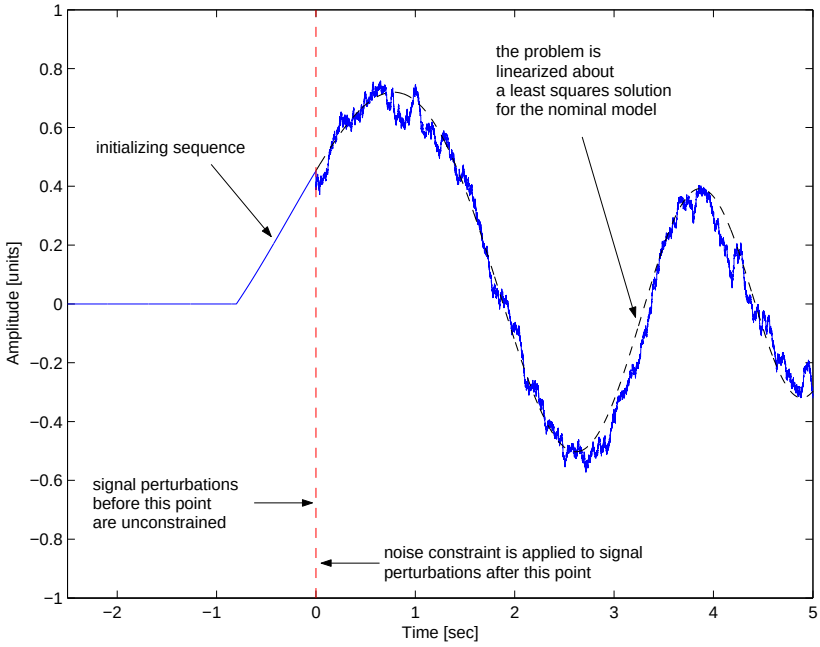

(b) Modified approach

Figure 5.3: Accounting for initial state using pre-record sequences. The approach of Fig. 5.3(a) gains no advantage when the quadratic perturbation-block constraints are approximated. The method of Fig. 5.3(b) is not subject to this problem.

the sequence is wholly unconstrained and will automatically yield a suitable initial state at the start of 'measured time'. Unfortunately, this does not work when the quadratic constraints are approximated. Section 5.2.2 shows that the perturbation-block constraints applied across the extended sequences gains little (LTV case) or nothing (LTI case): the linearization about a zero-signal causes variable pre-zero terms to 'drop out' of the problem.

An alternative approach, illustrated in Fig. 5.3(b), is to linearize the problem about some nominal 'pre-data' sequences. A method of doing this is described in Section 5.2.3. A numerical example is given in Section 5.2.4.

5.2.1 A non-invalidation problem with non-zero initial state

The general model validation decision problem (MVDP) for systems initially in motion may be stated as follows:

Definition 5.4 (MVDP for systems initially in motion) Given a finite-dimensional $p \times q$ model set $\mathcal{P}$, input-output data $\tilde{u} \in \mathcal{S}_k^q$, $\tilde{y} \in \mathcal{S}_k^p$, and input-output noise constraints $\mathbf{W}_{\tilde{u}} \times \mathbf{W}_{\tilde{y}}$, do there exist a system $\hat{P} \in \mathcal{P}$, an initial state x_0 and noise sequences $w_{\tilde{u}}, w_{\tilde{y}} \in \mathbf{W}_{\tilde{u}} \times \mathbf{W}_{\tilde{y}}$ such that the input-output pair $(y + w_y)$ is consistent with the first k elements of the response of $\hat{P}$ to $(u + w_u)$ when the initial state is x_0.

For LTI systems this is of course equivalent to finding the existence of $\hat{P} = \left[\begin{array}{c|c} \hat{A} & \hat{B} \\ \hline \hat{C} & \hat{D} \end{array}\right] \in \mathcal{P}$ such that

$$\begin{pmatrix} \hat{y}_0 \\ \hat{y}_1 \\ \vdots \\ \hat{y}_{k-1} \end{pmatrix} = \begin{bmatrix} \hat{D} & 0 & \cdots & 0 \\ \hat{C}\hat{B} & \hat{D} & \cdots & 0 \\ \vdots & \vdots & \ddots & \vdots \\ \hat{C}\hat{A}^{k-2}\hat{B} & \hat{C}\hat{A}^{k-3}\hat{B} & \cdots & \hat{D} \end{bmatrix} \begin{pmatrix} \hat{u}_0 \\ \hat{u}_1 \\ \vdots \\ \hat{u}_{k-1} \end{pmatrix} + \begin{bmatrix} \hat{C} \\ \hat{C}\hat{A} \\ \vdots \\ \hat{C}\hat{A}^{k-1} \end{bmatrix} x_0 \qquad (5.4)$$

where $\hat{y} = \tilde{y} + w_{\tilde{y}}$ and $\hat{u} = \tilde{u} + w_{\tilde{u}}$. In the context of closed-loop control $\mathcal{P}$ will typically be either $\mathcal{B}_\nu^{\mathrm{LTI}}(P, \beta)$ or $\mathcal{B}_\nu^{\mathrm{LTV}}(P, \beta)$ for some nominal LTI system P and some $\beta \in (0, b_{\mathrm{opt}}(P))$.

5.2.2 Why simple zero-padding won't work

Given a model set $\mathcal{B}_\nu^{\mathrm{LTI}}(P, \beta)$, measured sequences $\tilde{u} \in \mathcal{S}_k^q, \tilde{y} \in \mathcal{S}_k^p$ and noise constraints $\mathbf{W}_{\tilde{u}} \times \mathbf{W}_{\tilde{y}}$, the simplest approach to 'padding out' a sequence is to define extended sequences

$$\{y\}_j = \begin{cases} 0, & j = 0, \ldots, n-1 \\ \{\tilde{y}\}_{j-n}, & j = n, \ldots, (n+k-1) \end{cases} \tag{5.5}$$

$$\{u\}_j = \begin{cases} 0, & j = 0, \ldots, n-1 \\ \{\tilde{u}\}_{j-n}, & j = n, \ldots, (n+k-1) \end{cases} \tag{5.6}$$

and a modified noise set encompassing all sequences whose 'tails' are within $\mathbf{W}_{\tilde{u}} \times \mathbf{W}_{\tilde{y}}$:

$$\mathbf{W}_u \times \mathbf{W}_y := \left\{ (w_u, w_y) : \{w_u\}_{n,\ldots,(n+k-1)} \times \{w_y\}_{n,\ldots,(n+k-1)} \in \mathbf{W}_{\tilde{u}} \times \mathbf{W}_{\tilde{y}} \right\} \tag{5.7}$$

The natural thing to do next would be to test for non-invalidation using Proposition 4.14. Similarly, we might apply Proposition 4.15 for the LTV case. Unfortunately this will not work as expected.

Theorem 5.5 (LTI Equivalence Theorem) *Given sequences $s \in \mathcal{S}_k^q$, $t \in \mathcal{S}_k^p$ with $t_0 \neq 0$, define $\sigma \in \mathcal{S}_\ell^q$ such that $\sigma_i = 0$ and $\tau \in \mathcal{S}_\ell^p$ such that $\tau_i = 0$, with $\hat{s}$ and $\hat{t}$ given by*

$$\hat{s} = \{\sigma_0, \sigma_1, \ldots \sigma_{\ell-1}, s_0, s_1, \ldots s_{k-1}\} \tag{5.8}$$

$$\hat{t} = \{\tau_0, \tau_1, \ldots \tau_{\ell-1}, t_0, t_1, \ldots t_{k-1}\} \tag{5.9}$$

Then there exist sequences $w_\sigma \in \mathcal{S}_\ell^q$, $w_\tau \in \mathcal{S}_\ell^p$ *and* $w_s, w_t \in \mathbf{W}_s \times \mathbf{W}_t$ *such that*

$$\begin{bmatrix} T_{\hat{s}}^* T_{\hat{s}} + T_{w_{\hat{s}}}^* T_{\hat{s}} + T_{\hat{s}}^* T_{w_{\hat{s}}} & T_{\hat{t}}^* + T_{w_{\hat{t}}}^* \\ T_{\hat{t}} + T_{w_{\hat{t}}} & I \end{bmatrix} \geq 0 \tag{5.10}$$

where $w_{\hat{s}} = \{w_\sigma, w_s\}$ *and* $w_{\hat{t}} = \{w_\tau, w_t\}$, *if and only if there exist sequences* $w_s, w_t \in \mathbf{W}_s \times \mathbf{W}_t$ *such that*

$$\begin{bmatrix} T_s^* T_s + T_{w_s}^* T_s + T_s^* T_{w_s} & T_t^* + T_{w_t}^* \\ T_t + T_{w_t} & I \end{bmatrix} \geq 0 \tag{5.11}$$

and the only w_σ *and* w_τ *satisfying (5.10) are* $w_\sigma = \{0, 0, \ldots, 0\}$ *and and* $w_\tau = \{0, 0, \ldots, 0\}$.

A rather tedious proof is given in Appendix B.

Theorem 5.6 (LTV Equivalence Theorem) *Given sequences* $s \in \mathcal{S}_k^q$, $t \in \mathcal{S}_k^p$ *with* $t_0 \neq 0$, *define* $\sigma \in \mathcal{S}_\ell^q$ *such that* $\sigma_i = 0$ *and* $\tau \in \mathcal{S}_\ell^p$ *such that* $\tau_i = 0$, *with* $\hat{s}$ *and* $\hat{t}$ *from (5.8) and (5.9). Let*

$$V_z^n := \operatorname{vec} \Pi_n z$$

Then there exist sequences $w_\sigma \in \mathcal{S}_\ell^q$, $w_\tau \in \mathcal{S}_\ell^p$ *and* $w_s, w_t \in \mathbf{W}_s \times \mathbf{W}_t$ *such that*

$$\begin{bmatrix} V_{\hat{s}}^{j\,*} V_{\hat{s}}^j + V_{\hat{s}}^{j\,*} V_{w_{\hat{s}}}^j + V_{w_{\hat{s}}}^{j\,*} V_{\hat{s}}^j & V_{\hat{t}}^{j\,*} + V_{w_{\hat{t}}}^{j\,*} \\ V_{\hat{t}}^j + V_{w_{\hat{t}}}^j & I \end{bmatrix} \geq 0 \tag{5.12}$$

for all $j \in \{1, 2, \ldots, \ell + k\}$ *where* $w_{\hat{s}} = \{w_\sigma, w_s\}$ *and* $w_{\hat{t}} = \{w_\tau, w_t\}$, *if and only if there exist sequences* $w_s, w_t \in \mathbf{W}_s \times \mathbf{W}_t$ *such that*

$$\begin{bmatrix} V_s^{j\,*} V_s^j + V_s^{j\,*} V_{w_s}^j + V_{w_s}^{j\,*} V_s^j & V_t^{j\,*} + V_{w_t}^{j\,*} \\ V_t^j + V_{w_t}^j & I \end{bmatrix} \geq 0 \tag{5.13}$$

for all $j \in \{1, 2, \ldots, k\}$, *and the only* w_τ *satisfying (5.12) is the zero sequence.*

Again, the proof is given in Appendix B.

Remark 5.7 We can see from Theorems 5.5 and 5.6 that there is little to be gained from a simple application of zero padding. In the LTI case we gain nothing at all and in the LTV case a very heavy restriction is placed on the class of allowable noise. ♡

5.2.3 Relinearizing the problem using 'pre-record' sequences

It is possible to circumvent the problems of the previous section by applying relinearization techniques similar to those of Section 5.1.

Remark 5.8 Given measured sequences, $(\tilde{y} \in \mathcal{S}_k^p, \tilde{u} \in \mathcal{S}_k^q)$ and an integer $n > 0$, and noise constraints $\mathbf{W}_{\tilde{u}} \times \mathbf{W}_{\tilde{y}}$, let y, u and $\mathbf{W}_u \times \mathbf{W}_y$ be as given in (5.5), (5.6) and (5.7) on page 73.

Then, given a $p \times q$ LTI system P, a ν-gap radius β, the corresponding central controller M, and sequences $w_{u0} \in \mathcal{S}_{n+k}^q$, $w_{y0} \in \mathcal{S}_{n+k}^p$, there exist a system $\hat{P} = \left[\begin{array}{c|c} \hat{A} & \hat{B} \\ \hline \hat{C} & \hat{D} \end{array}\right] \in \mathcal{B}_\nu^{\mathrm{LTI}}(P, \beta)$, sequences $w_{\tilde{u}}, w_{\tilde{y}} \in \mathbf{W}_{\tilde{u}} \times \mathbf{W}_{\tilde{y}}$ and an initial state x_0 satisfying (5.4) if the conditions for Theorem 5.1 holds. $\hat{P}$ is the same as that satisfying the theorem, $w_{\tilde{u}} = \{w_u\}_{n,\ldots,(n+k-1)}$, $w_{\tilde{y}} = \{w_y\}_{n,\ldots,(n+k-1)}$ and the initial state easily obtained from the state equation:

$$x_{k+1} = \hat{A}x_k + \hat{B}\{w_u\}_k$$

When using $\mathcal{B}_\nu^{\mathrm{LTV}}(P, \beta)$ instead of $\mathcal{B}_\nu^{\mathrm{LTI}}(P, \beta)$, Theorem 5.3 should be used in place of Theorem 5.1. ♡

There is nothing conceptually difficult here: all that has been done is to allow the problem to be relinearized about any suitably-dimensioned sequences.

But what should (w_{u0}, w_{y0}) be? The relinearization is mathematically valid whatever values are chosen, but it is sensible to choose a starting point with some physical significance. When solving noise minimization problems using a constraint

of the form

$$\mathbf{W}_{\tilde{u}} \times \mathbf{W}_{\tilde{y}} := \left\{ (w_{\tilde{u}}, w_{\tilde{y}}) : ||w_{\tilde{u}}||_2^2 + ||w_{\tilde{y}}||_2^2 \leq \gamma^2 \right\} \tag{5.14}$$

a suitable choice of w_{u0}, w_{y0} is that which minimizes γ for the nominal model. To find these, we need expressions for the (stacked) actual signals at the plant input and output for the noise-affected nominal plant.

$$\begin{pmatrix} \hat{U} \\ \hat{Y} \end{pmatrix} := \underbrace{\begin{bmatrix} M \\ N\left(\Pi_{n+k} T_P\right) \end{bmatrix}}_{\Phi} \left(\begin{pmatrix} 0_{nq\times 1} \\ \operatorname{vec} \tilde{u} \end{pmatrix} + \operatorname{vec} w_{u0} \right)$$

where M and N 'select' the parts of the input corresponding the 'real' sampling instants (as opposed to the pre-padding):

$$M := \begin{bmatrix} 0_{kq\times nq} & I_{kq} \end{bmatrix} \qquad\qquad N := \begin{bmatrix} 0_{kp\times np} & I_{kp} \end{bmatrix}$$

Note that $\hat{U}$ and $\hat{Y}$ denote the vectored forms of $\tilde{u}+w_{\tilde{u}}$ and $\tilde{y}+w_{\tilde{y}}$. Though our w_{u0} and w_{y0} exist during the pre-record phase, their norm at this point is not considered important.

The norm we wish to minimize is $\gamma = ||\epsilon||_2$, with ϵ given by

$$\epsilon = \begin{pmatrix} \operatorname{vec} w_{\tilde{u}} \\ \operatorname{vec} w_{\tilde{y}} \end{pmatrix} = \begin{pmatrix} \hat{U} \\ \hat{Y} \end{pmatrix} - \begin{pmatrix} \operatorname{vec} \tilde{u} \\ \operatorname{vec} \tilde{y} \end{pmatrix} = \Phi \operatorname{vec} w_{u0} - z$$

where $z = \begin{pmatrix} \operatorname{vec} \tilde{u} \\ \operatorname{vec} \tilde{y} \end{pmatrix} - \Phi \begin{pmatrix} 0_{nq\times 1} \\ \operatorname{vec} \tilde{u} \end{pmatrix}$. We now have a simple linear least-squares problem, and can write down the solution with no further effort:

Remark 5.9 The (w_{u0}, w_{y0}) corresponding to the $(w_{\tilde{u}}, w_{\tilde{y}})$ minimizing γ in (5.14) with the nominal plant are given by

$$\operatorname{vec} w_{u0} = \Phi^{\dagger} z$$

and

$$\operatorname{vec} w_{y0} = -\begin{pmatrix} 0_{np\times 1} \\ \operatorname{vec} \tilde{y} \end{pmatrix} + \Pi_{n+k}\, T_P \left(\begin{pmatrix} 0_{nq\times 1} \\ \operatorname{vec} \tilde{u} \end{pmatrix} + \operatorname{vec} w_{u0} \right)$$

♡

The expression for w_{y0} is obtained by rearranging (5.4).

5.2.4 Numerical example

Synthetic data were obtained by finding first 94 elements of the response of the discrete time system

$$P_{\text{true}}(z) = \frac{0.02247z + 0.02093}{z^2 - 1.764z + 0.8075}$$

to the chirp signal $u_{\text{true}}(k) = \sin \frac{\pi}{30}\,(k + 0.025k^2)$. The first 14 samples of the data record were discarded, giving the validation data $(\tilde{u}, \tilde{y})$ shown in Figure 5.4(a).

Assuming a nominal model

$$P = \frac{0.01867z + 0.01746}{z^2 - 1.783z + 0.8187}$$

and taking $n = 2$, w_{u0} and w_{y0} were found using Remark 5.9 (Figure 5.4(b)).

Remark 5.8 then was used to find the sequences giving the smallest value of $\gamma = \{||w_{\tilde{u}}||_2^2 + ||w_{\tilde{y}}||_2^2\}^{1/2}$ consistent with a system $\hat{P} \in \mathcal{B}_\nu^{\text{LTI}}(P, 0.12)$. The minimum was found to be zero, corresponding to zero noise sequences (Figure 5.4(c)). Since there was no noise on the original data, and $\delta_\nu(P_{\text{true}}, P) = 0.12$, these results are as expected.

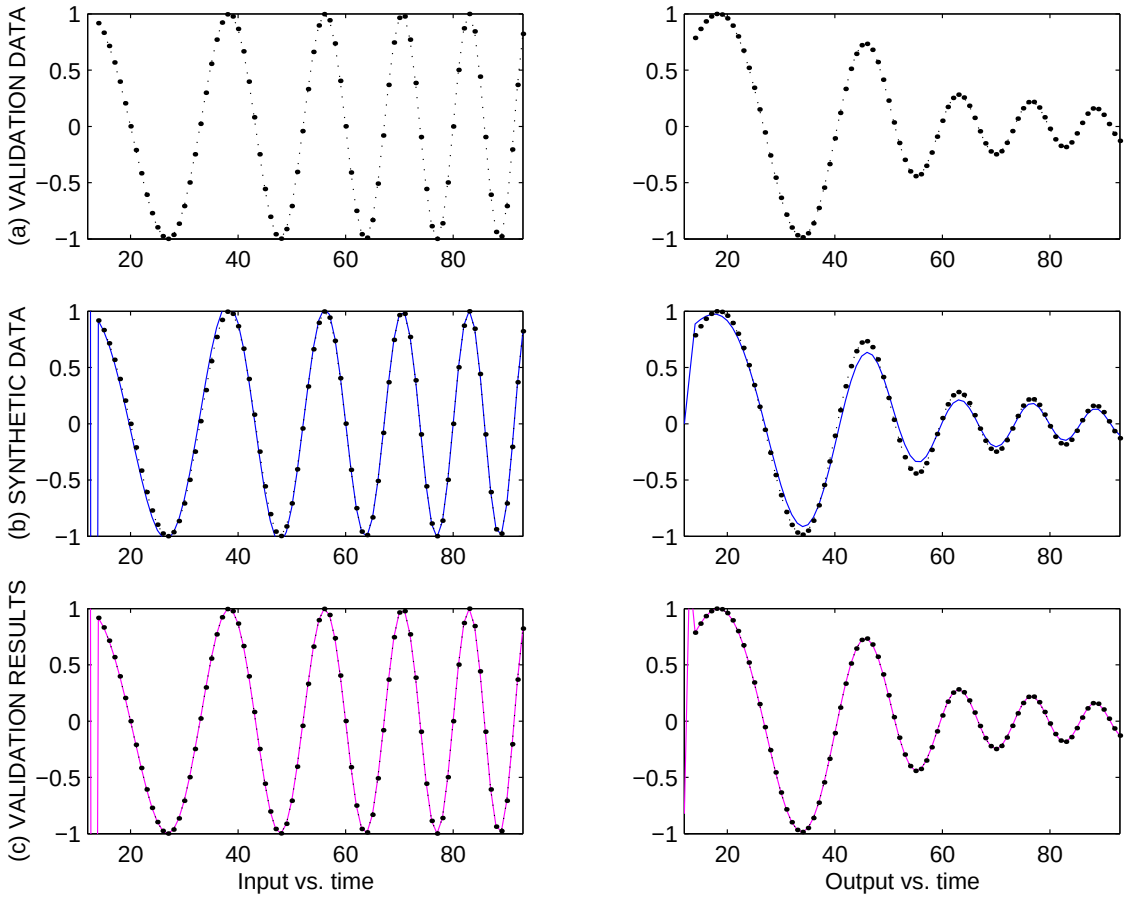

Figure 5.4: Numerical example. The top plots (a) show the initial data sequences. The middle plots (b) show the data including nominal pre-record and noise sequences. The bottom plots (c) show the final sequences from validation, which coincide exactly with the initial data sequences.

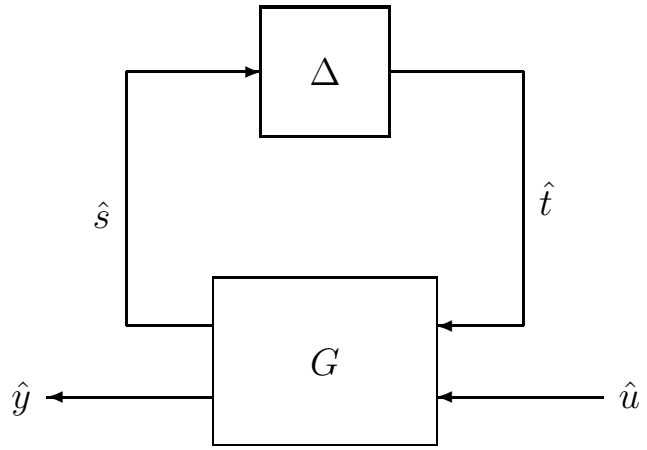

Figure 5.5: LFT model structure.

5.3 Constructing LTI interpolants

Much published literature (e.g. [Dav96, SV01, CG00]) considers the existence of interpolant systems, but there is little about their construction. In this section we consider the case where we have already determined feasible noise sequences and the existence of system within some LTI model set, and we wish to construct an interpolant system to map the relevant inputs to the relevant outputs.

Consider the LFT structure of Figure 5.5. The signals $\hat{u}$, $\hat{y}$, $\hat{s}$, and $\hat{t}$ are known. (Perhaps strictly speaking they are 'possible' since they may have been formed by correcting the measured signals with feasible noise sequences.) Our model set is of the form

$$\mathcal{P}(G,\gamma) := \{P : P = \mathcal{F}_u(G,\Delta), \Delta \in \mathcal{RH}_\infty, ||\Delta||_\infty \leq \gamma\}$$

This is more general than a ν-gap problem, where $G = M^{-1}$, $\gamma = 1$ and $\begin{pmatrix} \hat{s} \\ \hat{t} \end{pmatrix} = (\mathrm{ch}\,(M))^{-1} = \begin{pmatrix} \hat{u} \\ \hat{y} \end{pmatrix}$

We now consider the construction of an interpolant system:

Theorem 5.10 *Let G be a $(p+n) \times (q+m)$ linear time invariant system. Given*

$\mathcal{P}(G,\gamma)$ and signals $\hat{u} \in \mathcal{S}_k^n, \hat{y} \in \mathcal{S}_k^m$, $\hat{s} \in \mathcal{S}_k^q, \hat{t} \in \mathcal{S}_k^p$ such that

$$T_{\hat{t}}^* T_{\hat{t}} \leq \gamma^2 T_{\hat{s}}^* T_{\hat{s}}$$

is satisfied and

$$\begin{pmatrix} \hat{s} \\ \hat{y} \end{pmatrix} = G \begin{pmatrix} \hat{t} \\ \hat{u} \end{pmatrix} \tag{5.15}$$

then there exists a $(n \times m)$ system $\hat{P} \in \mathcal{P}(G,\gamma)$ such that $\hat{y} = \hat{P}\hat{u}$, and a realization is

$$P_1 = \mathcal{F}_u(G, \Delta)$$

where Δ is the interpolant mapping $\hat{s}$ to $\hat{t}$ constructed using Corollary 2.14 on page 24.

Outline of proof. The existence of a system $\Delta \in \mathcal{RH}_\infty$ satisfying $||\Delta||_\infty \leq \gamma$ and mapping $\hat{s}$ to $\hat{t}$ is clear from Theorem 2.10 and its realization is given by Corollary 2.14. It is clear from the definition of $\mathcal{P}$ that $P_1 \in \mathcal{P}(G,\gamma)$. It is clear from (5.15) that (u, y) P_1 should map $\hat{u}$ to $\hat{y}$. □

Remark 5.11 From Remark 2.13, it is clear that P_1 will contain p unobservable modes which may be easily eliminated using balanced truncation. This may be done directly on P_1, or simply eliminated from Δ before its substitution in the linear fractional transformation. ♡

5.3.1 All degree-constrained interpolants

Similarly, the techniques for constructing degree-constrained interpolants in Section 2.6.5 may be applied within the context of an LFT model set. The method employed to construct the perturbation block is different, but by choice of the σ polynomial the poles and zeros of the perturbation block may be moved around.

Figure 5.6 shows the results of a simple example in which the synthetic data

shown in Figure 5.6(a) were compared to the model

$$P = \frac{0.2091z^2 + 0.4183z + 0.2091}{z^2 - 1.402z + 0.5888}$$

with unit sampling period.

The validation record has length 7. It was assumed that the signals were unaffected by noise, and thus any modelling error could be accounted for by model perturbation. An attempt was made to construct three sixth-order interpolants within a ν-gap radius 0.3660 of P.[2] These consisted of a 'central' solution, where the roots of $\sigma(\lambda)$ are at the origin, a second interpolant with the roots of $\sigma(\lambda)$ close to the points $0.9e^{\pm j}$, i.e. very near the unit circle, and a third interpolant with the roots of $\sigma(\lambda)$ close to the points $0.1e^{\pm j}$.

The frequency responses are shown in Figure 5.6(b): the solutions with $\sigma(\lambda)$'s roots close to the origin are relatively smooth; when the roots are close to the unit circle, the interpolant is much less smooth. The impulse responses (Figure 5.6(c)) are identical for the first 7 samples, but differ afterwards. This is entirely as expected.

Unfortunately, the algorithms used are not sufficiently robust to be able to consider much greater record lengths. It would be interesting to see how the observed behaviour transfers to longer record lengths and whether distance from the origin of the roots of $\sigma(\lambda)$ is the only factor at play here.

5.3.2 Other methods of interpolant construction

Among the other methods explored including the construction of FIR filters to interpolate the data. This was straightforward to do with single-input perturbation blocks (where the initial impulse response is uniquely determined by the data), though the $\mathcal{H}_\infty$ norm of the system was often increased by truncation. Methods of extending the filters using Nehari's Theorem were investigated. The lemma below provides a method of extending an FIR response in such a way that the $\mathcal{H}_\infty$-norm

[2]The smallest ν-gap radius consistent with this data and P is 0.1746.

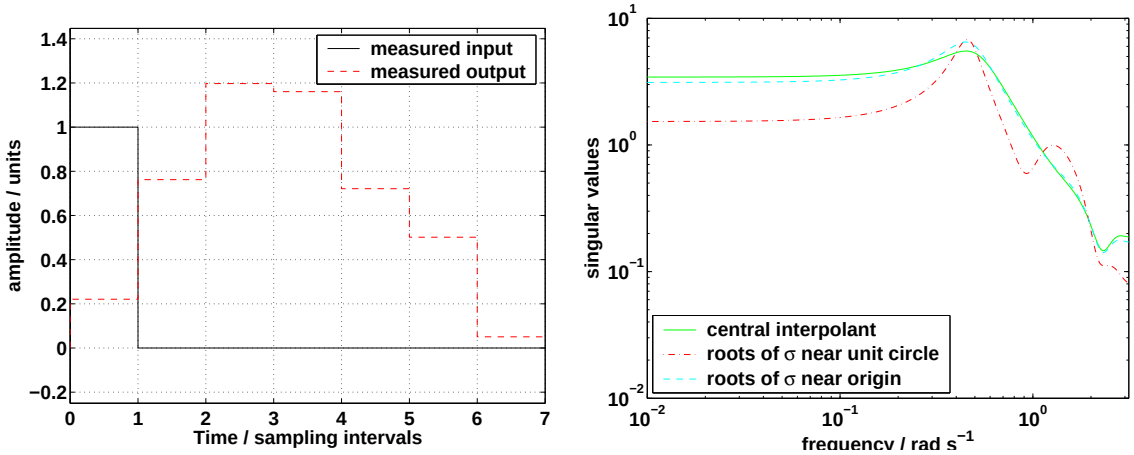

(a) Validation data

(b) Frequency responses

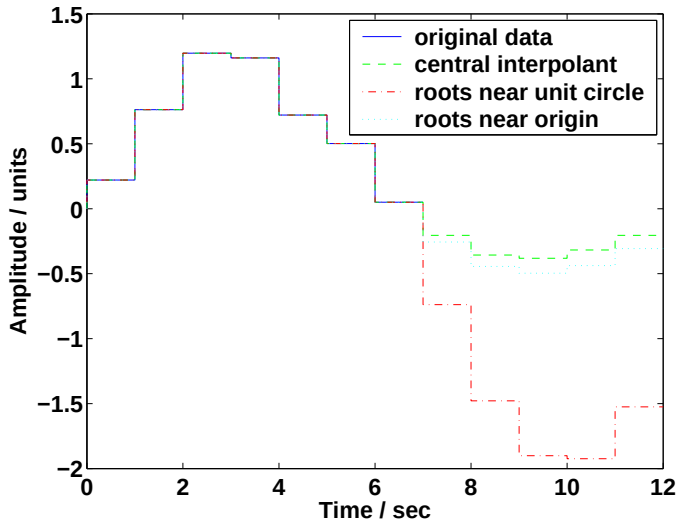

(c) Impulse responses

Figure 5.6: Construction of interpolants using degree-constrained interpolants. See the explanatory text on page 80.

is minimized. The system's initial response is shifted and 'flipped round' and the antistable system constructed via Nehari's Method is then shifted and 'flipped back' to give an infinite norm-reducing 'tail' to the impulse response.

Lemma 5.12 *Let z^{-1} denote the unit delay operator. Given some $\hat{\Delta}$ whose impulse response is zero after ℓ steps, let $\gamma(Q) = \|\hat{\Delta} + z^{-\ell}Q\|_\infty$ and let $\hat{\nabla} = z^{-\ell}\,\hat{\Delta}^\sim$. Then*

$$\gamma_{\min} := \min_{Q \in \mathcal{H}_\infty} \gamma(Q) = \|\Gamma_{\hat{\nabla}}\| \tag{5.16}$$

Proof. Note that $\left\|\hat{\Delta} + z^{-\ell}Q\right\|_\infty = \left\|z^{\ell}\hat{\Delta} + Q\right\|_\infty = \left\|z^{-\ell}\hat{\Delta}^\sim + Q^\sim\right\|_\infty$. Thus (5.16) can be re-written

$$\gamma_{\min} = \min_{Q^\sim \in \mathcal{H}_\infty^-} \|\hat{\nabla} + Q^\sim\|_\infty$$

This may be solved by Nehari's theorem (see [ZDG95], p. 205), giving the stated minimum. □

This method was found to work effectively for the extension of low-order systems, but less so with high-order systems. In a 'toy' example, a nth order system G_{fir} was constructed with a random FIR response g_k, where $g_0, g_1, \ldots g_n$ were normally distributed and $g_{n+1}, \ldots$ were zero. Lemma 5.12 was applied to construct a system $\hat{G}_{\text{iir}}$ with response $\hat{g}_k$ satisfying $\hat{g}_i = g_i \ \forall i = 0, 1, \ldots, n$ such that the minimum value of $\|G_{\text{iir}}\|_\infty$ was achieved. With one particular random seed, it was noted that for values of n up to 75, a solution could be constructed but for higher orders the algorithm ran into numerical problems.[3] The pattern was observed to apply generally. Real-world validation data is likely to be significantly longer than this, limiting the method's usefulness in this context.

When dealing with multiple-input perturbation blocks, following an identification method in [Dat00] it was found to be possible to construct FIR interpolants using the well-known discrete-time Bounded Real Lemma, which states that $\left\|\left[\begin{array}{c|c} A & B \\ \hline C & D \end{array}\right]\right\|_\infty \leq$

[3]The MATLAB function used called 'hankmr' from the *μ-Analysis and Synthesis Toolbox*.

λ if and only if

$$\begin{bmatrix} A^*XA - X & A^*XB & \lambda^{-1}C^* \\ B^*XA & B^*XB - I & \lambda^{-1}D^* \\ \lambda^{-1}C & \lambda^{-1}D & -I \end{bmatrix} \leq 0$$

for some $X \geq 0$, but the computation of such an X required a huge number of decision variables of the order of the square of the data record length. Again, such systems often failed to achieve the minimum possible $\mathcal{H}_\infty$-norm. Extending the length of the FIR filter beyond that of the data record was possible, but very computationally expensive. Nehari Methods were also possible, but numerical instabilities remained a significant problem.

These methods did, however, allow the use of low-order systems in conjunction with the relaxation of noise constraints on the output of the perturbation block, and there could be applications in the visualization of 'simple' interpolants.

Chapter 6

Invalidation using the $\mathcal{S}$-procedure

The conventional necessary and sufficient conditions for invalidation introduced in Theorem 2.10 and Theorem 2.11 are non-convex and not readily soluble. The conventional approximations, where small quadratic terms are neglected, give necessary conditions for invalidation. An alternative approach advocated in [SDM00] is to apply the $\mathcal{S}$-procedure (Proposition 2.5).

[SDM00] looks at a formulation of an LFT model invalidation problem based on a parameterization of all unknown inputs to a central LFT block whether these are from the exogenous noise or from 'Δ blocks' representing model perturbations; this parameterization is used to express bounds on the ℓ_2 norm of the exogenous noise and the $i2$ norms of any Δ blocks. The key result is a convex sufficient condition for invalidation of an LFT model set with multiple LTV perturbation blocks. It is also claimed that, when there is only a single perturbation blocks, the condition is also necessary. (The parameterization and the condition will be described in the body of the chapter.)

In the following pages, we shall

1. Identify a problem with the claimed necessary and sufficient condition for single-Δ LTV invalidation in [SDM00], which we believe to be sufficient but not necessary.

2. Adapt the parameterization of [SDM00] to produce necessary and sufficient

conditions for 'noncausal' invalidation and a tighter sufficient condition for 'LTV' invalidation.

3. Provide a numerical example.

4. Adapt the method to allow a non-zero initial state in conjunction with an output offset (for use in Chapter 7).

The starting points for this work—in particular the use of the S-procedure and the parameterization framework—are to be found in [SDM00], whose inspiration is gratefully acknowledged.

6.1 Model structure and parameterization

The model set we shall consider (paraphrased from [SDM00]) has the form:

$$\begin{bmatrix} s \\ y \end{bmatrix} = \begin{bmatrix} P_{11} & P_{12} & P_{13} \\ P_{21} & P_{22} & P_{23} \end{bmatrix} \begin{bmatrix} t \\ w \\ u \end{bmatrix}$$

where u and y are the usual measured signals, w is an unknown exogenous noise signal, s is the unknown input to the uncertainty block Δ, and t is the unknown output from Δ. For clarity, the structure is shown in Figure 6.1. The blocks P_{ij} represent LTI systems: the non-LTI structure (if any) is represented solely by Δ.

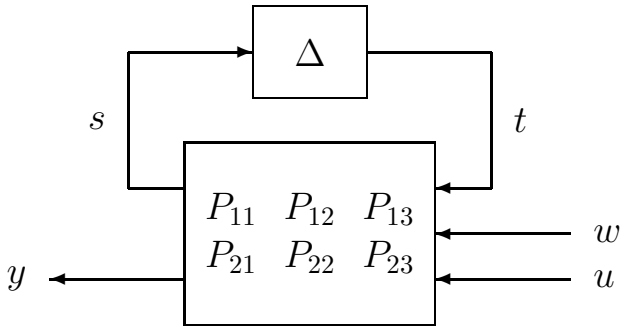

Figure 6.1: A generic LFT model structure

6.1.1 Relation to the ν-gap invalidation model structure

The general LFT parameterization described above encompasses a broader class of model structures than that generally used for the ν-gap type problem. If we are using a model set such as $\mathcal{B}_\nu^{\mathrm{LTI}}(P, \beta)$ then the parameterization of a 'ball' in the ν-gap (described in Section 3.2.3) gives

$$\begin{pmatrix} s \\ y + w_y \end{pmatrix} = \begin{bmatrix} G_{11} & G_{12} \\ G_{21} & G_{22} \end{bmatrix} \begin{pmatrix} t \\ u + w_u \end{pmatrix}$$

or, equivalently

$$\begin{pmatrix} s \\ y \end{pmatrix} = \begin{bmatrix} G_{11} & [G_{12}\ 0] & G_{12} \\ G_{21} & [G_{22}\ -I] & G_{22} \end{bmatrix} \begin{pmatrix} t \\ \begin{bmatrix} w_u \\ w_y \end{bmatrix} \\ u \end{pmatrix}$$

The standard ν-gap problems may thus be formulated in the more general framework using $P_{11} = G_{11}$, $P_{12} = [G_{12}\ 0]$, $P_{13} = G_{12}$, $P_{21} = G_{21}$, $P_{22} = [G_{22}\ -I]$, $P_{23} = G_{22}$, and $w = \begin{bmatrix} w_u \\ w_y \end{bmatrix}$.

6.1.2 Parameterization of all interpolant signals

Following [SDM00] we note that the nominal noise-free model is $y_{\text{nom}} = P_{23}u$, and that y_{nom} is unlikely to match y in practice, and any discrepancy must thus be accounted for by

$$y - P_{23}u = \begin{bmatrix} P_{21} & P_{22} \end{bmatrix} \begin{bmatrix} t \\ w \end{bmatrix} \tag{6.1}$$

All (t, w) satisfying (6.1) may be parameterized

$$\begin{aligned} \begin{bmatrix} t \\ w \end{bmatrix} &= \begin{bmatrix} t_0 \\ w_0 \end{bmatrix} + R\zeta \\ &= x_0 + R\zeta \\ &= x(\zeta) \end{aligned}$$

where (t_0, w_0) is a particular solution of (6.1) and $R\zeta$ spans the input null space of $[P_{21}\ P_{22}]$. (With finite data sets and the corresponding lower-block Toeplitz matrices, these are easily calculated using standard linear algebra techniques.)

6.1.3 Parameterization of the noise constraint

The usual bound on the exogenous noise norm $\|w\|_2 \leq \gamma_w$ is parameterized by writing w as follows:[1]

$$\begin{aligned} w &= \begin{bmatrix} 0_{nv} & I_{nw} \end{bmatrix} x(\zeta) \\ &= \begin{bmatrix} 0_{nv} & I_{nw} \end{bmatrix} (x_0 + R\zeta) \end{aligned}$$

All noise sequences violating the bound will satisfy

$$x(\zeta)^* \begin{bmatrix} 0_{nv} & 0 \\ 0 & I_{nv} \end{bmatrix} x(\zeta) - \gamma_w^2 > 0$$

which can be re-written as

$$F_0(\gamma_w, \zeta) = \zeta^* A_0 \zeta + 2b_0^* \zeta + c_0(\gamma_w) > 0$$

where,

$$A_0 = R^* \begin{bmatrix} 0_{nv} & 0 \\ 0 & I_{nw} \end{bmatrix} R$$

$$b_0 = R^* \begin{bmatrix} 0_{nv} & 0 \\ 0 & I_{nw} \end{bmatrix} x_0$$

and

$$c_0(\gamma_w) = x_0^* \begin{bmatrix} 0_{nv} & 0 \\ 0 & I_{nw} \end{bmatrix} x_0 - \gamma_w^2$$

(Note that we have used 'γ_w' rather than the 'γ' of [SDM00]. In that work, the same bound was applied to both $\|w\|_2$ and $\|\Delta\|_\infty$. There is no reason why these have to

[1]The subscript notation used here matches that of [SDM00], which wisely chose ease of reading over strict notational accuracy. For 'nw' read 'the number of data points in this truncation multiplied by the dimension of w' and so on.

be the same, and we shall consider separate bounds applied to each. Our $||\Delta||_\infty$ will be bounded by some γ_Δ. This enables us to more-readily consider trade-offs between noise and perturbation size. This makes no great difference to the problem—it is equivalent to re-scaling P_{ij}—but means that by fixing γ_Δ, optimization problems may be readily formulated as convex LMIs in γ_w.)

6.1.4 Parameterization of the perturbation block constraints

Defining N_N such that

$$t = [I_{nv}, 0_{nw}]x = N_N x$$

gives expressions for the input and output of the perturbation block:

$$t = N_N(x_0 + R\zeta)$$
$$s = [P_{11}\ P_{12}](x_0 + R\zeta) + P_{13}u$$

When dealing with LTV perturbations, the following projections are also helpful:

$$\Pi_k N_N : x \to \Pi_k t$$
$$\Pi_k M_N : s \to \Pi_k s$$

Recall that for there to exist an LTV system Δ satisfying $||\Delta||_\infty \leq \gamma_\Delta$ and $t = \Delta s$, it is necessary and sufficient that $\|\Pi_k t\|_2^2 \leq \gamma_\Delta^2 \|\Pi_k s\|_2^2$ for all $k = 1, 2, \ldots, N$. The energy bound at any given truncation k—referred to in [SDM00] as the 'LTV extension condition'—can be expressed as a quadratic inequality:

$$F_k(\gamma_\Delta, \zeta) = \zeta^* A_k(\gamma_\Delta)\zeta + 2b_k^*(\gamma_\Delta)\zeta + c_k(\gamma_\Delta) \geq 0 \tag{6.2}$$

where

$$
\begin{aligned}
A_k(\gamma_\Delta) &= \gamma_\Delta^2 R^* \begin{bmatrix} P_{11}^* \\ P_{12}^* \end{bmatrix} (\Pi_k M_N)^* \Pi_k M_N [P_{11}\ P_{12}] R - R^* (\Pi_k N_N)^* (\Pi_k N_N) R \\
b_k(\gamma_\Delta) &= \gamma_\Delta^2 R^* \begin{bmatrix} P_{11}^* \\ P_{12}^* \end{bmatrix} (\Pi_k M_N)^* (\Pi_k M_N) P_{13} u - R^* (\Pi_k N_N)^* \Pi_k N_N x_0 \\
&\quad + \gamma_\Delta^2 R^* \begin{bmatrix} P_{11}^* \\ P_{12}^* \end{bmatrix} (\Pi_k M_N)^* (\Pi_k M_N) [P_{11}\ P_{12}] x_0 \\
c_k(\gamma_\Delta) &= \gamma_\Delta^2 u^* P_{13}^* (\Pi_k M_N)^* \Pi_k M_N P_{13} u - x_0^* (\Pi_k N_N)^* (\Pi_k N_N) x_0 \\
&\quad + \gamma_\Delta^2 x_0^* \begin{bmatrix} P_{11}^* \\ P_{12}^* \end{bmatrix} (\Pi_k M_N)^* (\Pi_k M_N) [P_{11}\ P_{12}] x_0 \\
&\quad + 2\gamma_\Delta^2 x_0 \begin{bmatrix} P_{11}^* \\ P_{12}^* \end{bmatrix} (\Pi_k M_N)^* \Pi_k M_N P_{13} u
\end{aligned} \tag{6.3}
$$

6.2 Invalidation with a noncausal Δ

One of the most significant constraints usually present in our mathematical models is causality: a causal system maps inputs in the past to outputs in the future.

It this section, we break from this slightly and consider a mathematically simpler problem: we will allow our perturbation Δ to have a possibly non-causal structure. Essentially, we are looking for an linear operator that satisfies $t = \Delta s$ and $||\Delta||_\infty \leq \gamma_\Delta$, but that is not constrained to be lower block-triangular.

The condition for the existence of such a Δ is given by Corollary C.2 on page 168: it is necessary and sufficient that $\|s\|_2 \leq \gamma_\Delta \|t\|_2$, i.e. $F_N(\gamma_\Delta) \geq 0$ for data of length N.

Theorem 6.1 (noncausal uncertainty, necessary and sufficient) *Given* $\gamma_\Delta, \gamma_w > 0$*, the LFT perturbation model satisfying* $\|\Delta\|_\infty \leq \gamma_\Delta$ *and* $\|w\|_2 \leq \gamma_w$*, is invalidated by the measured data* ($y \in \mathcal{S}_N^p, u \in \mathcal{S}_N^q$) *if and only if for all* ζ *satisfying* $F_N(\gamma_\Delta, \zeta) \geq 0$*;*

$$F_0(\gamma_w, \zeta) \geq 0$$

Proof. For there to exist an admissible noncausal Δ, by Corollary C.2, $F_k(\gamma_w, \zeta) \geq 0$ for some ζ. However, if for all such ζ the exogenous noise constraint is violated—i.e. $F_0(\gamma_w, \zeta) \geq 0$—then there is no ζ, and thus no (Δ, w), consistent with the model. □

Following the example of [SDM00], this can be converted into a convex (LMI) problem via the S-procedure (Proposition 2.5, p. 16).

Corollary 6.2 *Given γ_Δ, $\gamma_w > 0$, the LFT perturbation model satisfying $\|\Delta\|_\infty \leq \gamma_\Delta$ and $\|w\|_2 \leq \gamma_w$, is invalidated by the measured data ($y \in \mathcal{S}_N^p, u \in \mathcal{S}_N^q$) if and only there exists $\tau \geq 0$ such that*

$$\begin{bmatrix} A_0 - \tau A_N(\gamma_\Delta) & b_0 - \tau b_N(\gamma_\Delta) \\ b_0^* - \tau b_N^*(\gamma_\Delta) & c_0(\gamma_w) - \tau c_N(\gamma_\Delta) \end{bmatrix} \geq 0$$

Proof. By the $\mathcal{S}$-procedure (Proposition 2.5, p. 16), there exists $\tau \geq 0$ such that for all ζ,

$$F_0(\gamma_w, \zeta) - \tau F_N(\gamma_\Delta, \zeta) \geq 0 \tag{6.4}$$

if and only if for all ζ satisfying the perturbation block constraint $F_N(\gamma_\Delta, \zeta) \geq 0$,

$$F_0(\gamma_w, \zeta) \geq 0$$

thus violating the exogenous noise constraint. Following a method of [BEGFB94], we can re-write (6.4) as

$$\begin{bmatrix} \zeta^* & 1 \end{bmatrix} \begin{bmatrix} A_0 - \tau A_N(\gamma_\Delta) & b_0 - \tau b_N(\gamma_\Delta) \\ b_0^* - \tau b_N^*(\gamma_\Delta) & c_0(\gamma_w) - \tau c_N(\gamma_\Delta) \end{bmatrix} \begin{bmatrix} \zeta \\ 1 \end{bmatrix} \geq 0$$

Clearly this quadratic inequality holds for all ζ if and only if the interior matrix is positive semi-definite. □

6.3 Invalidation with a linear time-varying Δ

We now consider the more general case in which Δ is norm-bounded as before, but constrained to be causal. There are two lower bounds here.

6.3.1 A sufficient condition following the pattern of [SDM00]

The following condition is novel compared to [SDM00] in that it does not claim necessity.

Theorem 6.3 (LTV invalidation, first sufficient condition) *Given $\gamma_\Delta, \gamma_w > 0$ the LFT perturbation model satisfying $\|\Delta\|_\infty \leq \gamma_\Delta$ and $\|w\|_2 \leq \gamma_w$ is invalidated by the measured data ($\hat{y} \in \mathcal{S}_L^p, \hat{u} \in \mathcal{S}_L^q$) if for any $N \in \{1, 2, \ldots, L\}$, the analogous non-causal model of Theorem 6.1 is invalidated by $y = \Pi_N \hat{y}$ and $u = \Pi_N \hat{u}$.*

Proof. Essentially what we are saying here is that if there exists any N such that the noncausal model is invalid, then there are no (t, w) that will satisfy $\|w\|_2 \leq \gamma_w$ and satisfy

$$\|\Pi_N t\|_2 \leq \gamma_\Delta \|\Pi_N s\|_2$$

from which it is quite clear that the standard LTV interpolation constraint (Theorem 2.11) will not be satisfied. □

The theorem is not *necessary* because it *might* be possible to find N (t, w) pairs, each of which satisfies the LTV extension condition at a particular N as well as the exogenous noise constraint, but this does not show that there is a *single* (t, w) pair simultaneously satisfying the LTV extension condition for *all* N.

Each separate test is a convex LMI; it is possible to implement them all simultaneously in an optimization problem, giving a lower bound on the smallest γ_w consistent with the model.

Remark 6.4 Given $\gamma_\Delta, \gamma_w > 0$, the conditions of Theorem 6.3 are failed if and only if for each $N \in \{1, 2, \ldots, L\}$ there exist separate (w_N, s_N, z_N) which do not simultaneously satisfy $\|\Pi_N w_N\|_2 \leq \gamma_w$ and $\|\Pi_N t_N\|_2 \leq \gamma_\Delta \|\Pi_N s_N\|_2$. ♡

6.3.2 A second sufficient condition

A logical alternative to Theorem 6.3 is to apply the LTV extension constraint at all truncations simultaneously. This also results in a sufficient condition:

Theorem 6.5 (Second sufficient condition for LTV invalidation) *Given $\gamma_\Delta, \gamma_w > 0$, the LFT perturbation model with Δ satisfying $\|\Delta\|_\infty \leq \gamma_\Delta$ and $\|w\|_2 \leq \gamma_w$ is invalid with respect to the data (y, u) if there exist $\tau_\ell \geq 0$, $\ell = 1, \ldots, N$ such that for all ζ*

$$F_0(\gamma_w, \zeta) - \sum_{\ell=1}^{N} \tau_\ell F_\ell(\gamma_\Delta, \zeta) \geq 0 \tag{6.5}$$

Outline of proof. This follows the same line as the proof of Theorem 6.1. We now include the *whole* LTV perturbation block constraint. The model is invalidated if whenever the perturbation block constraint is satisfied, i.e. $F_\ell(\gamma_\Delta, \zeta) \geq 0$, $\ell = 1, \ldots, N$, the exogenous noise constraint is violated:

$$F_0(\gamma_w, \zeta) \geq 0$$

By the $\mathcal{S}$-procedure (Proposition 2.5, p. 16) this gives (6.5). □

The condition is not necessary because the $\mathcal{S}$-procedure is not lossless in this case.

Corollary 6.6 *Given $\gamma_\Delta, \gamma_w > 0$, the LFT perturbation model satisfying $\|\Delta\|_\infty \leq \gamma_\Delta$ and $\|w\|_2 \leq \gamma_w$ is invalid with respect to the data (y, u) if there exist $\tau_\ell \geq 0$, $\ell = 1, \ldots, N$ such that for all ζ*

$$Q := \begin{bmatrix} A_0 - \sum_{\ell=1}^{N} \tau_\ell A_\ell(\gamma_\Delta) & b_0 - \sum_{\ell=1}^{N} \tau_\ell b_\ell(\gamma_\Delta) \\ b_0^* - \sum_{\ell=1}^{N} \tau_\ell b_\ell^*(\gamma_\Delta) & c_0(\gamma_w) - \sum_{\ell=1}^{N} \tau_\ell c_\ell(\gamma_\Delta) \end{bmatrix} \geq 0 \tag{6.6}$$

Outline of proof. The proof is no different to that of Theorem 6.1. □

Note that the Corollary 6.6 is an LMI in γ_w and $\tau_1, \tau_2, \ldots, \tau_\ell$, again lending itself to ready computation of a lower bound on the smallest admissible γ_w.

6.4 A disagreement with a claim in [SDM00]

The following claim is made in Section 4.4 of [SDM00]. (It has been simplified a little here as we are considering but one perturbation block.)

> **Proposition 6.7** *Given $\gamma_\Delta = \gamma_w > 0$, the LFT perturbation model satisfying $\|\Delta\|_\infty \leq \gamma_\Delta$ and $\|w\|_2 \leq \gamma_w$" is invalidated by the measured datum $(\hat{y} \in \mathcal{S}_L^p, \hat{u} \in \mathcal{S}_L^q)$ (of length L) if and only if there exists a truncation $N \in \{1, 2, \ldots, L\}$ with corresponding truncated datum $(y, u) := (\Pi_N \hat{y}, \Pi_N \hat{u})$ such that for all ζ satisfying $F_N(\gamma_\Delta, \zeta) \geq 0$,*
>
> $$F_0(\gamma_w, \zeta) \geq 0$$

There is an obvious problem here: this is exactly the same as the lower bound proposed in Theorem 6.3. The authors of [SDM00] have neglected the fact that the LTV extension condition is applied to *separate* sequences at each truncation.

Sufficiency is easy enough to show. If the exogenous noise constraint and the LTV extension condition for *any* truncation cannot be simultaneously satisfied, the model is clearly invalid:

$$\begin{aligned}
&\exists N : \forall \zeta \left((F_0(\gamma_w, \zeta) \geq 0) \vee (F_N(\gamma_\Delta, \zeta) < 0) \right) \\
&\quad \rightarrow \exists N : \forall \Delta \forall w \left((||\Pi_N w||_2 > \gamma_w) \vee (||\Pi_N t||_2 > \gamma_\Delta ||\Pi_N s||_2) \right) \\
&\quad\quad \rightarrow \forall \Delta \forall w \left((||w||_2 > \gamma_w) \vee (\exists N : (||\Pi_N t||_2 > \gamma_\Delta ||\Pi_N s||_2) \right)
\end{aligned}$$

But the necessity? Consider the negation of the above:

$$\begin{aligned}
&\forall N \, \exists \zeta : ((F_0(\gamma_w, \zeta) < 0) \wedge (F_N(\gamma_\Delta, \zeta) \geq 0) \\
&\quad \rightarrow \forall N \, \exists \Delta \exists w : ((||\Pi_k w||_2 \leq \gamma_w) \wedge (||\Pi_N t||_2 \leq \gamma_\Delta ||\Pi_N s||_2))
\end{aligned}$$

which is not the same as

$$\exists\Delta\exists w : ((||w||_2 \leq \gamma_w) \wedge \forall N \, (||\Pi_N t||_2 \leq \gamma_\Delta ||\Pi_N s||_2))$$

So, if for each truncation, we can find ζ satisfying the noise constraint and the perturbation block constraint, we can find separate (Δ, w) pairs for each truncation satisfying the exogenous noise constraint and the N-th truncation of the perturbation block constraint. However, this does *not* imply that there is a single (Δ, w) pair simultaneously satisfying the exogenous noise constraint and the noise constraint at *all* truncations of the perturbation block constraint.

The non-implication in the last line was ignored in Proposition 6.7, hence the claim of necessity is false.

A numerical counter-example is given in Section 6.6.

A further typographical correction

The expression for $c_i(\gamma)$ in [SDM00] is given as

$$\begin{aligned} c_i(\gamma) = \gamma^2 u^* P_{13}^* M_1^* M_1 P_{13} u - x_0^* N_1^* N_1 x_0 \\ + \gamma^2 x_0^* \begin{bmatrix} P_{11}^* \\ P_{12}^* \end{bmatrix} M_1^* M_1 [P_{11} \; P_{12}] x_0 \end{aligned} \tag{6.7}$$

This appears to be a typographical error: the term $2\gamma^2 x_0 \begin{bmatrix} P_{11}^* \\ P_{12}^* \end{bmatrix} M_1^* M_1 P_{13} u$ is missing.

6.5 Relating the bounds

Given our LFT model structure and $\gamma_\Delta \geq 0$,

- Let $\gamma_w^{\mathrm{NC}}(u,y)$ be the largest value of γ_w for which the data (u,y) invalidates the model structure w.r.t. non-causal perturbations using Theorem 6.1.
- Let $\gamma_w^{\mathrm{LTV,lb1}}(u,y)$ be the largest value of γ_w for which the data (u,y) invalidates the model structure w.r.t. LTV perturbations using Theorem 6.3.
- Let $\gamma_w^{\mathrm{LTV,lb2}}(u,y)$ be the largest value of γ_w for which the data (u,y) invalidates the model structure w.r.t. LTV perturbations using Theorem 6.5

Theorem 6.8 *Given $u \in \mathcal{S}_L^q$, $y \in \mathcal{S}_L^p$,*

$$\gamma_w^{\mathrm{NC}}(u,y) \leq \gamma_w^{\mathrm{LTV,lb1}}(u,y) \leq \gamma_w^{\mathrm{LTV,lb2}}(u,y)$$

Proof. First, let us show that $\gamma_w^{\mathrm{NC}}(u,y) \leq \gamma_w^{\mathrm{LTV,lb1}}(u,y)$. This is clear from Theorems 6.1 and 6.3:

$$\begin{aligned}\gamma_w^{\mathrm{LTV,\,lb1}}(u,y) &= \max_{N=1,\ldots,L} \gamma_w^{\mathrm{NC}}(\Pi_N u, \Pi_N y) \\ &\geq \gamma_w^{\mathrm{NC}}(u,y)\end{aligned}$$

Showing that $\gamma_w^{\mathrm{LTV,lb1}}(u,y) \leq \gamma_w^{\mathrm{LTV,lb2}}(u,y)$ is less simple: we need to show that if (u,y) invalidate the model by Theorem 6.3, then they will also invalidate it by Theorem 6.5. Looking at Theorem 6.3's definition, we see that the model is invalidated if

$$\exists N : \forall\Delta\forall w \left((||\Pi_N w||_2 > \gamma_w) \vee (||\Pi_N t||_2 > \gamma_\Delta ||\Pi_N s||_2)\right)$$

Now $||\Pi_k w > \gamma_w||_2 \rightarrow ||w||_2 > \gamma_w$, so this implies

$$\exists N : \forall\Delta\forall w \left((||w||_2 > \gamma_w) \vee (||\Pi_N t||_2 > \gamma_\Delta ||\Pi_N s||_2)\right)$$

By the $\mathcal{S}$-procedure (Proposition 2.5), this, in the notation of Theorem 6.5, implies that $\exists \tau_N$ such that for all ζ

$$F_0(\gamma_w, \zeta) - \tau_N F_N(\gamma_\Delta, \zeta) \geq 0$$

Denote this value of τ_N by $\tau_\prime$.

This implies that $\exists \tau_i \in \{1, 2, \ldots, L\}$ such that for all ζ

$$F_0(\gamma_w, \zeta) - \sum_{i=1}^{L} \tau_i F_i(\gamma_\Delta, \zeta) \geq 0$$

Such τ_i are of course given by $\tau_i = \begin{cases} \tau\prime, & i = N \\ 0, & \text{otherwise} \end{cases}$. This is the condition of Theorem 6.5, showing sufficiency as desired. □

6.6 Numerical example

To illustrate the preceding sections, consider a system model

$$\begin{bmatrix} s \\ y \end{bmatrix} = \underbrace{\begin{bmatrix} 0 & 0 & 1 \\ P & 1 & P \end{bmatrix}}_{G} \begin{bmatrix} t \\ w \\ u \end{bmatrix}$$

where (y, u) are the usual measured data, w is an unknown exogenous noise signal, s and t are the input to and output from a single perturbation block Δ and

$$P(z) = \frac{0.008264z^2 + 0.01653z + 0.008264}{z^2 - 1.636z + 0.6694}$$

A block diagram for this system is shown in Figure 6.2(a). An important property of this system is that the input to Δ is known exactly, and thus the LTV model non-invalidation problem is convex and easily solved.

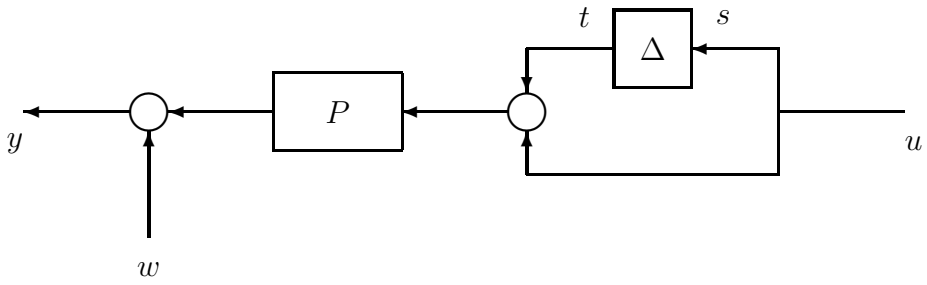

(a) block diagram of system model

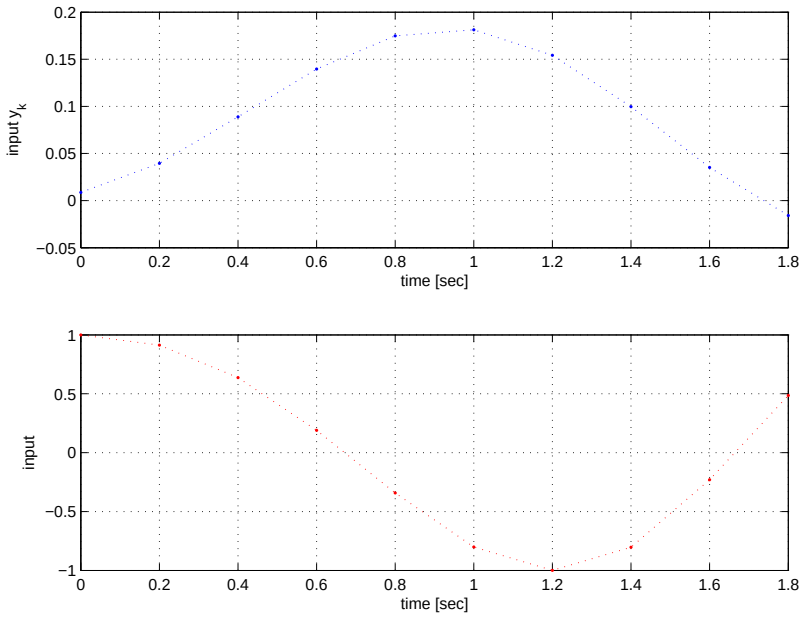

(b) output-input data used in invalidation

Figure 6.2: Numerical example: block diagram and invalidation data

Remark 6.9 Given a $p \times q$ linear time-invariant system P, $\gamma_\Delta > 0$, $u \in \mathcal{S}_k^q$, $y \in \mathcal{S}_k^p$, the smallest value of $\gamma_w := ||w||_2$ consistent with the model of Figure 6.2(a) with LTV uncertainty satisfying $||\Delta||_\infty \leq \gamma_\Delta$ is given by

$$\gamma_w^{\text{LTV}} := \min_{t \in \theta} ||y - P(u+t)||_2$$

where $\theta := \{\tau : ||\Pi_j \tau||_2 \leq \gamma_\Delta ||\Pi_j u||_2 \, \forall j = 1, \ldots, k\}$. This is easily calculated by minimizing γ_w subject to the LMI constraints

$$\begin{bmatrix} \gamma_\Delta^2 ||\Pi_j u||_2 & (\text{vec}\, \Pi_j t)^* \\ \text{vec}\, \Pi_j t & I \end{bmatrix} \geq 0$$

for all $j \in \{1, \ldots, k\}$ and

$$\begin{bmatrix} \gamma_w^2 & (\text{vec}\, w)^* \\ \text{vec}\, w & I \end{bmatrix} \geq 0$$

where $\text{vec}\, w = \text{vec}\, y - T_P \text{vec}\, u - T_P \text{vec}\, t$, and t and γ_w are the decision variables. ♡

Outline of proof. This follows from a simple application of Theorem 2.11. Because the input to the perturbation block is known, the result is a convex problem. □

We can employ a similar technique to calculate $\gamma_w^{\text{LTV,lb1}}$ without using the $\mathcal{S}$-procedure.

Remark 6.10 Given a $p \times q$ linear time-invariant system P, $\gamma > 0$, $u \in \mathcal{S}_k^q$, $y \in \mathcal{S}_k^p$ the smallest value of $\gamma_w := ||w||_2$ consistent with Theorem 6.3 and Proposition 6.7 is given by

$$\hat{\gamma}_w^{\text{LTV,lb1}} := \min_{(t_1, \ldots, t_k) \in \Theta} \left(\max_{j=1,\ldots,k} ||\Pi_j (y - P(u + t_j))||_2 \right)$$

where $\hat{\Theta} := \{(\tau_1, \ldots, \tau_k) : ||\Pi_j \tau_j||_2 \leq \gamma_\Delta ||\Pi_j u||_2 \, \forall j = 1, \ldots, k\}$. Again, this is easily calculated through an LMI minimization. ♡

Outline of proof. This follows naturally from the detail of Theorem 6.3. The condition for the existence of an noncausal perturbation block (Theorem C.1) is readily formulated in a similar way to the LTV condition of Remark 6.9. This is simply applied to each possible truncation, and the 'worst-case' value taken. Again, the known input is essential for convexity. □

The model structure was compared to the sampled data sequences shown in Figure 6.2(b).[2] Four quantities were calculated for a range of γ_Δ: $\gamma_w^{\mathrm{LTV}}(u,y)$, $\gamma_w^{\mathrm{LTV,lb2}}(u,y)$, $\gamma_w^{\mathrm{LTV,lb1}}(u,y)$ and $\hat{\gamma}_w^{\mathrm{LTV,lb1}}(u,y)$.

The results are shown in Figure 6.3. It can be seen that:

- $\gamma_w^{\mathrm{LTV,lb1}}(u,y)$ and $\hat{\gamma}_w^{\mathrm{LTV,lb1}}(u,y)$ are coincident, and smaller than $\gamma_w^{\mathrm{LTV,lb2}}(u,y)$ and $\hat{\gamma}_w^{\mathrm{LTV}}(u,y)$. Both the these facts are as expected: the value obtained using Proposition 6.7 from [SDM00] is equal to our first lower bound, and our improved bound is greater than these. The latter point confirms our claim that Proposition 6.7 is false.

- $\gamma_w^{\mathrm{LTV,lb2}}(u,y)$ is significantly closer to the 'true' value γ_w^{LTV}. In this case, the two actually coincide. Though we always expect $\gamma_w^{\mathrm{LTV,lb2}}(u,y)$ to exceed $\gamma_w^{\mathrm{LTV,lb1}}(u,y)$, it is unlikely that $\gamma_w^{\mathrm{LTV,lb2}}(u,y)$ and γ_w^{LTV} will always coincide. It is possible that the coincidence in this example is a result of the convexity of the problem.

Most problems will not have convex solutions, but we now have a method of applying the $\mathcal{S}$-procedure to find a lower bound on the level of LTV uncertainty present. This nicely complements the methods of previous chapters, which use quadratic approximations to produce upper bounds.

[2]The input sequence is $u_k = \cos\left(2kT + \frac{1}{2}k^2T^2\right)$ where $T = 0.2$ sec. The output y_k is the response of $\mathcal{F}_u(1,G) = \frac{0.008678z^2+0.01736z+0.008678}{z^2-1.636z+0.6694}$ to u_k.

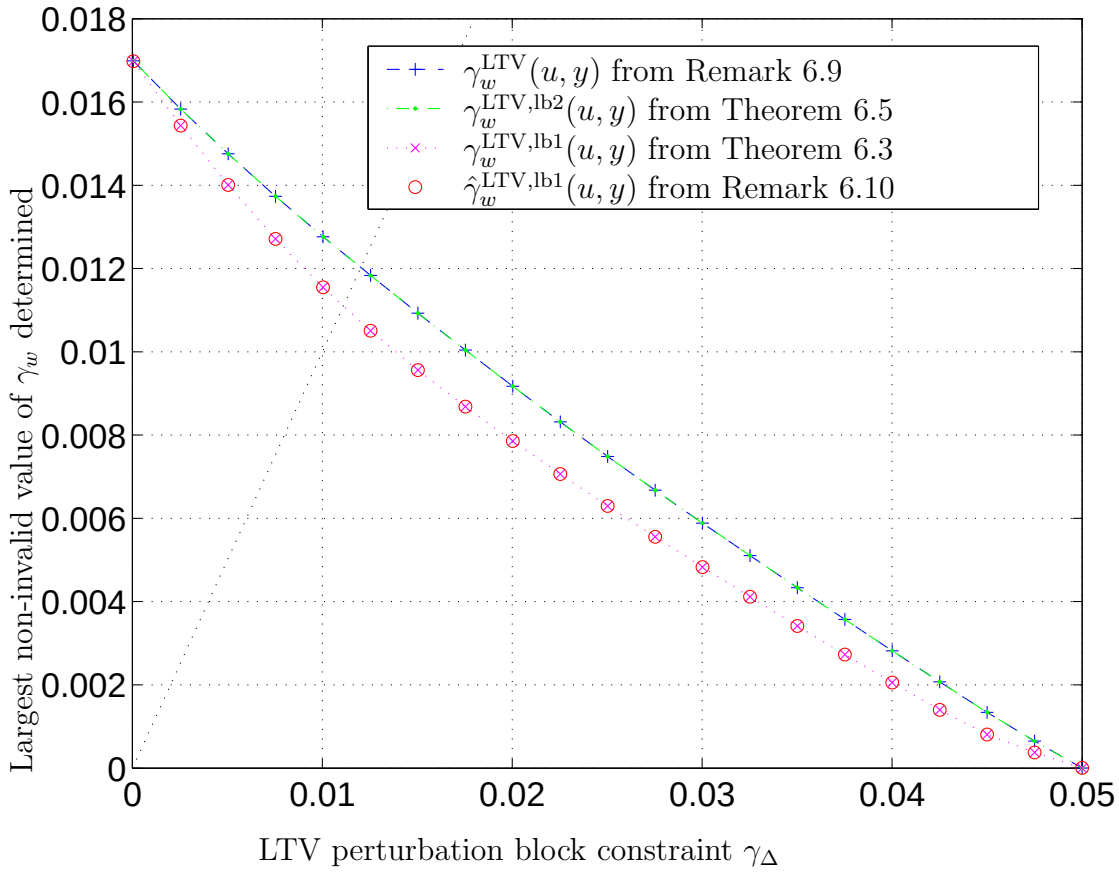

Figure 6.3: Numerical example. $\gamma_w^{\mathrm{LTV,lb1}}(u,y) = \hat{\gamma}_w^{\mathrm{LTV,lb1}}(u,y)$ as expected, since both are intended to be the same quantity. In this case the lower bound $\gamma_w^{\mathrm{LTV,lb2}}(u,y)$ is equal to the exact value $\gamma_w^{\mathrm{LTV}}(u,y)$. See the text of Section 6.6 for a more detailed discussion.

6.7 Adaption for an initial state and an output offset

In real-world applications, it is unlikely that a system will be perfectly at rest at the start of an experiment and offsets and/or trends may be present in the data. As an example, and for application to the VAAC data in Chapter 7, this section sets out a method of compensating for a constant output offset and a short pre-record input sequence. A single uncertainty block is used.

The main variables we shall use are:

$u \in \mathcal{S}_k^q$, $y \in \mathcal{S}_k^p$	input-output data from experiment	(known)
k_p	length of the pre-record to be used	(chosen)
$u_p \in \mathcal{S}_{k_p}^q$, $y_p \in \mathcal{S}_{k_p}^p$	pre-record input-output data	(unknown)
$w_p \in \mathcal{S}_{k_p}^r$	noise sequence during the pre-record section	(unknown)
$w \in \mathcal{S}_k^r$	noise sequence during experimental record	(unknown)
$y_o \in \mathbb{R}^p$	output offset	(unknown)

We shall also use two variables whose values are dependent on others: the uncertainty signals $t \in \mathcal{S}_{k+k_p}^\tau$, $s \in \mathcal{S}_{k+k_p}^\sigma$.

The complete LFT structure is shown in Figure 6.4.

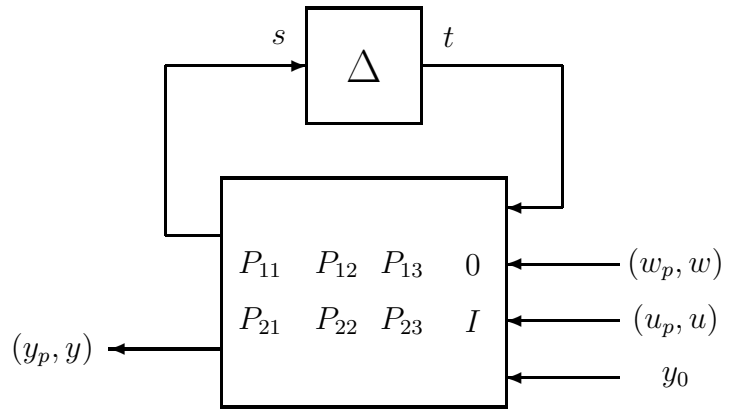

Figure 6.4: LFT structure for invalidation with offset and initializing sequences

Remark 6.11 Given $\gamma_w, \gamma_\Delta > 0$ the LFT model structure of Figure 6.4, where Δ is an unstructured perturbation satisfying $\|\Delta\|_\infty \leq \gamma_\Delta$ and $\|w\| \leq \gamma_w$, is invalidated for the data (u, y) if and only if there exist no w_p, u_p, y_0, s, t satisfying

$$\|w\|_2 \leq \gamma_w \tag{6.8}$$

$$\|t\|_2 \leq \gamma_\Delta \|s\|_2 \tag{6.9}$$

and

$$\begin{bmatrix} \operatorname{vec} s \\ \operatorname{vec} y \end{bmatrix} = \begin{bmatrix} Q_{11} & Q_{12} & Q_{1p} & Q_{13} & Q_{1o} \\ Q_{21} & Q_{22} & Q_{2p} & Q_{23} & Q_{2o} \end{bmatrix} \begin{bmatrix} \operatorname{vec} t \\ \begin{bmatrix} \operatorname{vec} w_p \\ \operatorname{vec} w \end{bmatrix} \\ \operatorname{vec} u_p \\ \operatorname{vec} u \\ \operatorname{vec} y_o \end{bmatrix} \tag{6.10}$$

where

$$Q_{11} := \Pi_{(k+k_\mathrm{p})} T_{P_{11}}, \quad Q_{12} := \Pi_{(k+k_\mathrm{p})} T_{P_{12}},$$

$$Q_{1\mathrm{p}} := \left(\Pi_{(k+k_\mathrm{p})} T_{P_{13}}\right) \begin{bmatrix} I_{qk_\mathrm{p}} \\ 0_{qk \times qk_\mathrm{p}} \end{bmatrix}, \quad Q_{13} := \left(\Pi_{(k+k_\mathrm{p})} T_{P_{13}}\right) \begin{bmatrix} 0_{qk_\mathrm{p} \times qk} \\ I_{qk} \end{bmatrix},$$

$$Q_{1\mathrm{o}} := 0_{\sigma(k+k_\mathrm{p}) \times p},$$

and

$$Q_{21} := \begin{bmatrix} 0_{pk \times pk_\mathrm{p}} & I_{pk} \end{bmatrix} \Pi_{(k+k_\mathrm{p})} T_{P_{21}}, \quad Q_{22} := \begin{bmatrix} 0_{pk \times pk_\mathrm{p}} & I_{pk} \end{bmatrix} \Pi_{(k+k_\mathrm{p})} T_{P_{22}},$$

$$Q_{2\mathrm{p}} := \begin{bmatrix} 0_{pk \times pk_\mathrm{p}} & I_{pk} \end{bmatrix} \left(\Pi_{(k+k_\mathrm{p})} T_{P_{23}}\right) \begin{bmatrix} I_{qk_\mathrm{p}} \\ 0_{qk \times qk_\mathrm{p}} \end{bmatrix}$$

$$Q_{23} := \begin{bmatrix} 0_{pk \times pk_\mathrm{p}} & I_{pk} \end{bmatrix} \left(\Pi_{(k+k_\mathrm{p})} T_{P_{12}}\right) \begin{bmatrix} 0_{qk_\mathrm{p} \times qk} \\ I_{qk} \end{bmatrix}$$

$$Q_{2\mathrm{o}} = -\left.\begin{bmatrix} I_p \\ I_p \\ \vdots \\ I_p \end{bmatrix}\right\} pk$$

♡

Outline of proof. Follows through a simple application of Corollary C.2 to the uncertainty block. □

The parameterization of the problem follows the same line as that of Section 6.1.2:

Pre-parameterization of all values satisfying the interpolation condition

The overall input-output equation which must be satisfied is

$$\operatorname{vec} y - Q_{23}\operatorname{vec} u = \underbrace{\begin{bmatrix} Q_{21} & Q_{22} & Q_{2\mathrm{p}} & Q_{2\mathrm{o}} \end{bmatrix}}_{=:Q_{2\bullet}} \underbrace{\begin{bmatrix} \operatorname{vec} t \\ \begin{bmatrix} \operatorname{vec} w_{\mathrm{p}} \\ \operatorname{vec} w \end{bmatrix} \\ \operatorname{vec} u_{\mathrm{p}} \\ \operatorname{vec} y_{\mathrm{o}} \end{bmatrix}}_{x} \tag{6.11}$$

Note that $Q_{2\bullet} \in \mathbb{R}^{kp\times(k+k_p)(r+\tau)+k_pq+p}$ and $x \in \mathbb{R}^{(k+k_p)(r+\tau)+k_pq+p}$. There is a solution to the equation when $Q_{2\bullet}$ has full row rank. When this is the case, a particular solution may be found from

$$x_0 = Q_{2\bullet}^{\dagger}\left[\operatorname{vec} y - Q_{23}\operatorname{vec} u\right]$$

and the general solution from

$$x = x_0 + R\zeta$$

where R spans $\operatorname{null}(Q_{2\bullet})$ and ζ is a compatibly-dimensioned vector of real numbers.

Reparameterization of the exogenous noise constraint

The exogenous noise constraint $\|w\|_2 < \gamma_w$ is identical to $\|\operatorname{vec} w\|_2 < \gamma_w$. Using (6.11), $\operatorname{vec} w$ may be expressed in terms of x:

$$\begin{aligned}\operatorname{vec} w &= \underbrace{\begin{bmatrix} 0_{rk\times[\tau(k+k_p)+rk_p]} & I_{rk} & 0_{rk\times(qk_p+p)} \end{bmatrix}}_{=:Q_w} x \\ &= Q_w(x_0 + R\zeta)\end{aligned}$$

Thus we can write

$$\begin{aligned}\gamma_w^2 &> (\zeta^* R^* + x_0^*)\, Q_w^* Q_w\, (R\zeta + x_0) \\ 0 &> \zeta^* R^* Q_w^* Q_w R\zeta + 2x_0^* Q_w^* Q_w R\zeta + x_0^* Q_w^* Q_w x_0 - \gamma_w^2\end{aligned}$$

which is true if and only if

$$0 > \begin{bmatrix} \zeta^* & 1 \end{bmatrix} \begin{bmatrix} A_0 & b_0 \\ b_0^* & c_0(\gamma_w) \end{bmatrix} \begin{bmatrix} \zeta \\ 1 \end{bmatrix}$$

where

$$A_0 = R^* Q_w^* Q_w R, \quad b_0 = R^* Q_w^* Q_w x_0, \quad c_0(\gamma_w) = x_0^* Q_w^* Q_w x_0 - \gamma_w^2$$

Reparameterization of the perturbation block constraint

To reparameterize the unstructured norm-bounded perturbation block constraint $\|t\|_2 \leq \gamma_\Delta \|s\|_2$, expressions for s and t are needed, and may be obtained from (6.10) and (6.11)

$$\operatorname{vec} s = \underbrace{\begin{bmatrix} Q_{11} & Q_{12} & Q_{1\mathrm{p}} & Q_{1\mathrm{o}} \end{bmatrix}}_{Q_{1\bullet}} (x_0 + R\zeta) + Q_{13} \operatorname{vec} u \tag{6.12}$$

$$\operatorname{vec} t = \underbrace{\begin{bmatrix} I_{\tau(k+k_p)} & 0_{\tau(k+k_p)\times[(k+k_p)r+qk_p+p]} \end{bmatrix}}_{=:N} (x_0 + R\zeta) \tag{6.13}$$

The constraint thus becomes:

$$\underbrace{(x_0^* + \zeta^* R^*) N^* N (x_0 + R\zeta)}_{\|t\|_2^2} \leq \underbrace{\gamma_\Delta^2 \left(\left[x_0^* + \zeta^* R^* \right] Q_{1\bullet}^* + \begin{bmatrix} \operatorname{vec} u \end{bmatrix}^* Q_{13}^* \right) \left(Q_{1\bullet} \left[x_0 + R\zeta \right] + Q_{13} \operatorname{vec} u \right)}_{\|s\|_2^2}$$

Looking at the left-hand side:

$$\text{l.h.s.} = \zeta^* (R^* N^* N R)\, \zeta + 2\, (x_0^* N^* N R)\, \zeta + x_0^* N^* N x_0$$

Looking at the right-hand side:

$$\begin{aligned} \text{r.h.s.} &= \gamma_\Delta^2 \left(\zeta^* R^* Q_{1\bullet}^* + \begin{bmatrix} x_0 \\ \operatorname{vec} u \end{bmatrix}^* \begin{bmatrix} Q_{1\bullet}^* \\ Q_{13}^* \end{bmatrix} \right) \left(Q_{1\bullet} R\zeta + \begin{bmatrix} Q_{1\bullet}^* \\ Q_{13}^* \end{bmatrix}^* \begin{bmatrix} x_0 \\ \operatorname{vec} u \end{bmatrix} \right) \\ &= \zeta^* \left(\gamma_\Delta^2 R^* Q_{1\bullet}^* Q_{1\bullet} R \right) + 2 \left(\gamma_\Delta^2 \begin{bmatrix} x_0 \\ \operatorname{vec} u \end{bmatrix}^* \begin{bmatrix} Q_{1\bullet}^* \\ Q_{13}^* \end{bmatrix} Q_{1\bullet} R \right) \zeta \\ &\quad + \gamma_\Delta^2 \begin{bmatrix} x_0 \\ \operatorname{vec} u \end{bmatrix}^* \begin{bmatrix} Q_{1\bullet}^* \\ Q_{13}^* \end{bmatrix} \begin{bmatrix} Q_{1\bullet}^* \\ Q_{13}^* \end{bmatrix}^* \begin{bmatrix} x_0 \\ \operatorname{vec} u \end{bmatrix} \end{aligned}$$

Rearranging the expression, we see that we need

$$\gamma_\Delta^2 \|s\|_2^2 - \|t\|_2^2 \geq 0$$

i.e.

$$\zeta^* A_1 \zeta + 2b_1\zeta + c_1 \geq 0 \iff \begin{bmatrix} \zeta^* & 1 \end{bmatrix} \begin{bmatrix} A_1(\gamma_\Delta) & b_1(\gamma_\Delta) \\ b_1^*(\gamma_\Delta) & c_1(\gamma_\Delta) \end{bmatrix} \begin{bmatrix} \zeta \\ 1 \end{bmatrix} \geq 0$$

where

$$\begin{aligned} A_1 &= R^* \left(\gamma_\Delta^2 Q_{1\bullet}^* Q_{1\bullet} - N^* N\right) R \\ b_1 &= \gamma_\Delta^2 \left(x_0^* Q_{1\bullet}^* + [\operatorname{vec} u]^* Q_{13}^*\right) Q_{1\bullet} R \\ c_1 &= \gamma_\Delta^2 \begin{pmatrix} x_0^* & \begin{bmatrix} \operatorname{vec} u \end{bmatrix}^* \end{pmatrix} \begin{bmatrix} Q_{1\bullet}^* Q_{1\bullet} & Q_{1\bullet}^* Q_{13} \\ Q_{13}^* Q_{1\bullet} & Q_{13}^* Q_{13} \end{bmatrix} \begin{pmatrix} x_0 \\ \operatorname{vec} u \end{pmatrix} \end{aligned}$$

6.7.1 Invalidation condition

Remark 6.12 (Noncausal Δ) Given $\gamma_w, \gamma_\Delta > 0$, the LFT structure of Figure 6.4 with an unstructured Δ satisfying $\|\Delta\|_\infty \leq \gamma_\Delta$ and w satisfying $\|w\|_2 \leq \gamma_w$ is invalidated if and only if the following equivalent conditions are met:

(i) There exist no w_p, u_p, y_0, s, t simultaneously satisfying (6.8), (6.9) and (6.10).

(ii) For all ζ satisfying $F_1(\gamma_\Delta, \zeta) \geq 0$,

$$F_0(\gamma_w, \zeta) \geq 0$$

(iii) There exists no $\tau_1 \geq 0$ such that

$$F_0(\gamma_w, \zeta) - \tau_1 F_1(\gamma_\Delta, \zeta) \geq 0$$

(iv) There exists no $\tau_1 \geq 0$ such that

$$\begin{bmatrix} A_0 - \tau_1 A_1(\gamma_\Delta) & b_0 - \tau_1 b_1(\gamma_\Delta) \\ b_0^* - \tau_1 b_1^*(\gamma_\Delta) & c_0(\gamma_w) - \tau_1 c_1(\gamma_\Delta) \end{bmatrix} \geq 0$$

♡

Proof (sketch). (i) follows from remark. (ii) follows from (i) via the parameterizations discussed in the preceding sections. (iii) follows from (ii) via the S-procedure. Finally (iv) follows from (iii) following the method of [BEGFB94]. □

Remark 6.13 Near-identical techniques can be employed to calculate (a) the first and (b) the second lower bounds. This is omitted for the sake of brevity and to avoid repetition. ♡

6.8 Concluding notes

At is logical to ask whether allowing non-causal Δ blocks is useful; we know that in the real world, no such systems exist. (Yet there are situations where an element of non-causal behaviour can be a reasonable approximation, e.g. human-in-the-loop control.) More importantly, the associated mathematical problem is very straightforward being convex and containing only one decision variable; its ease of solution is likely to prove its most useful aspect.

Chapter 7

An Application in Flight Control

7.1 The VAAC Harrier

The British Aerospace Harrier entered service with the RAF in 1969, earning its 'jump jet' nickname from its famous vertical take-off and landing capability. The aircraft's engines are equipped with nozzles that may be directed partially or wholly downwards: the jargon describing this is 'vectored thrust'. The VAAC acronym is a contraction of 'vectored-thrust aircraft advanced flight control'; it is used both to describe a programme of research conducted by the vehicle's owner QinetiQ ('the VAAC programme') and to describe the specially-equipped 'VAAC Harrier' used as a test bed for this programme.[1]

7.1.1 Aircraft description

The technical specifications of the VAAC Harrier are given in brief in [GAR01], from which Figure 7.1 is taken. The VAAC Harrier is a two-seater version, adapted to incorporate a full-authority flight control system for the rear pilot. The control surfaces are connected to the flight control system with optical fibres, an arrangement

[1]QinetiQ p.l.c. was formed when the H.M. Government's research agency DERA was split into two and partially privatized. (QinetiQ is now privately owned, with the smaller DSTL retained in public ownership.) The group operating the VAAC programme is based at Bedford at what was once the Royal Aircraft Establishment, though the VAAC Harrier itself operates from Boscombe Down.

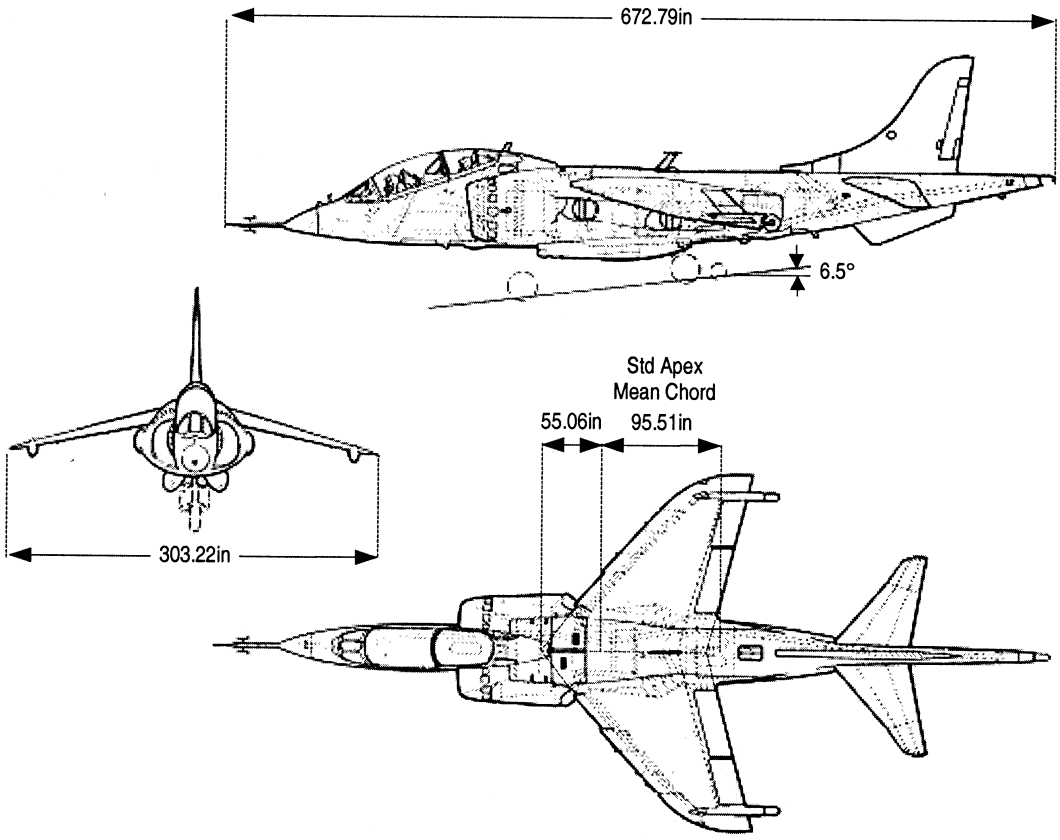

Figure 7.1: Basic dimensions of the VAAC Harrier [GAR01]

described by the aviation industry as 'fly-by-light'. The front pilot is equipped with conventional mechanically-linked controls, and the flight control system is overridden automatically whenever these are used. This is used for take-off and landing, and may also be used to end a flight test in the event of something going wrong.

7.1.2 The Harrier Wide-Envelope Model

The longitudinal dynamics of the Harrier are believed to be well-approximated by linear models. The Harrier Wide-Envelope Model or 'HWEM' is a Simulink model of the Harrier whose applications include real-time use in QinetiQ's large motion simulator. It is supplied with British Aerospace's 'CL002' control law; both are detailed in the literature [GAR01]. A particular characteristic of the HWEM not present in earlier models is that it is implemented wholly as a Simulink block diagram. There are no external S-functions, and no dependence on C or FORTRAN. The model depends on workspace constants; MATLAB script files are provided to initialize and trim such values, and to generate linear models of the plant and the controller.

The accompanying control law, 'CL002', was developed by QinetiQ's predecessors in conjunction with British Aerospace and is described briefly in [Dic00]. We will be considering longitudinal motion only. The HWEM's Simulink block diagram for the relevant parts of the controller is shown in Figure 7.2, and its function described in Table 7.1.[2] The longitudinal control law also compensates for the effects of flap position, nozzle position and bank angle. It is gain-scheduled, and scripts for trimming the controller are provided.

[2]Those with access to the HWEM will be able to examine this more closely by inspecting the Simulink model`wemsim05ca.mdl`.

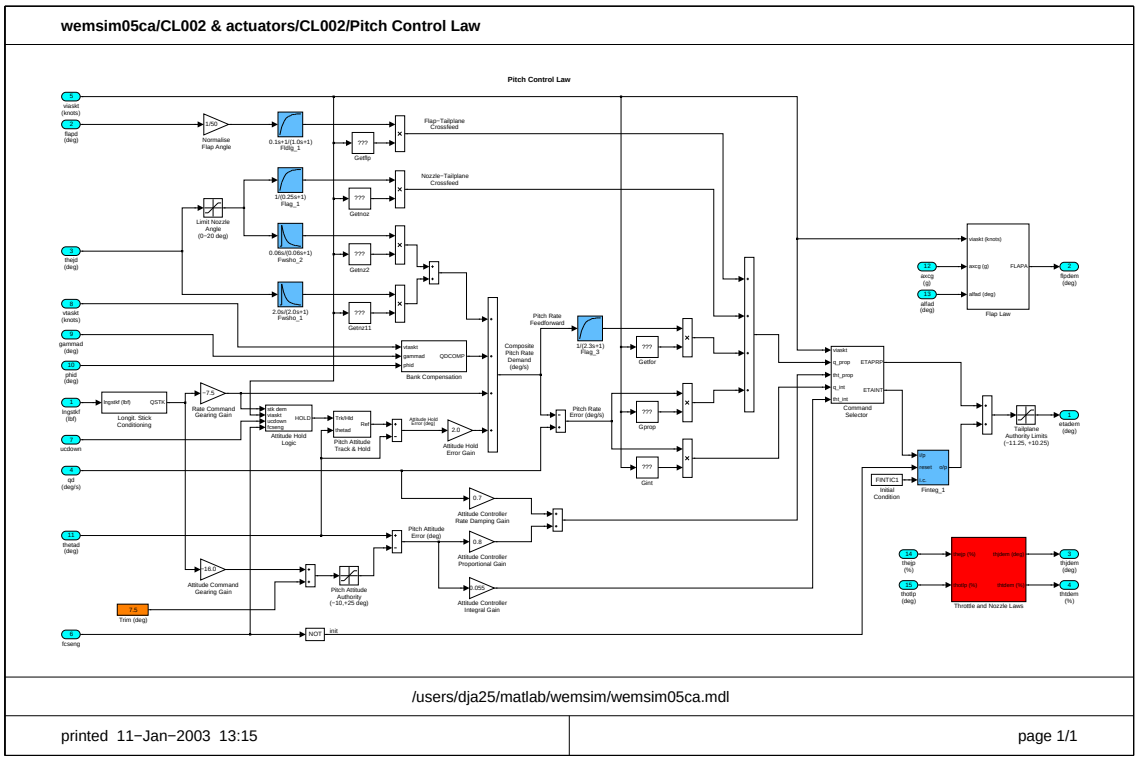

Figure 7.2: Longitudinal Control Law from CL002

Indicated air speed	CL002 functionality
$<$ 50 knots	Controls pitch attitude.
$>$ 60 knots	Controls pitch rate. If undercarriage down, pitch hold function also engaged.
50–60 knots	Provides a blend of the functions described above.

Table 7.1: Summary of CL002 longitudinal action

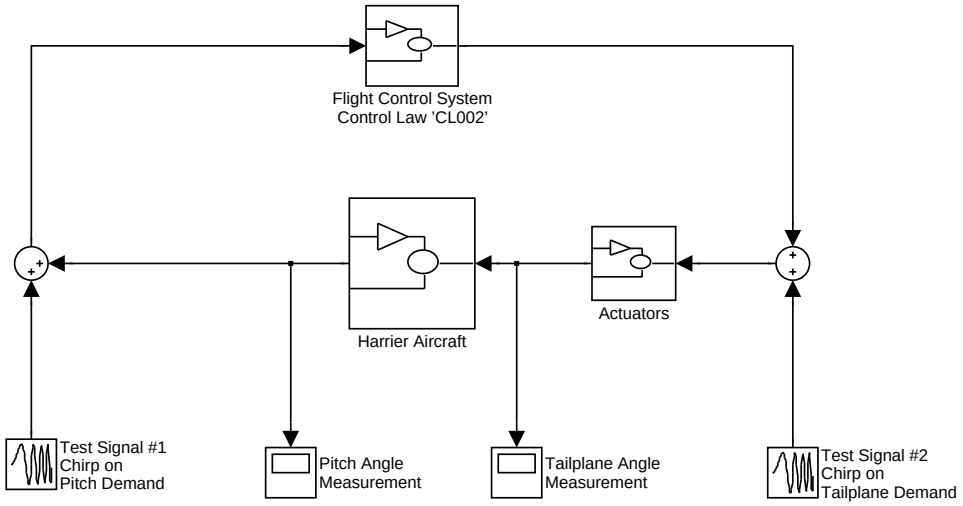

Figure 7.3: A simplified flight test schematic showing signal injection points and signal measurement points. Sensor models, present in HWEM, are omitted for clarity.

7.2 Flight Test 1858

Flight Test 1858 took place at Boscombe Down in December 2001 under the supervision of QinetiQ.[3] The flight had two objectives: firstly, to test work by Mathworks on an 'in flight stability metric', a continuation of work in [Dav96]; and, secondly, to collect data for use in validation. We only consider the latter here.

7.2.1 Experimental procedure

In both experiments, the aircraft was set-up in straight-and-level flight with an indicated air speed of about 210 knots, an attitude of about 3.5 degrees and an altitude of about 3 000 feet. Weather at ground level was not extreme. Then, a 'chirp' signal was injected as shown in Figure 7.3: in the first test, hereafter referred to as 'Test Point 1', the chirp entered the loop at the 'pitch demand'; at the second, 'Test Point 2', the point of entry was the 'tailplane demand'.

[3]Acknowledgements made in particular to Glenn D'Mello for his help in this.

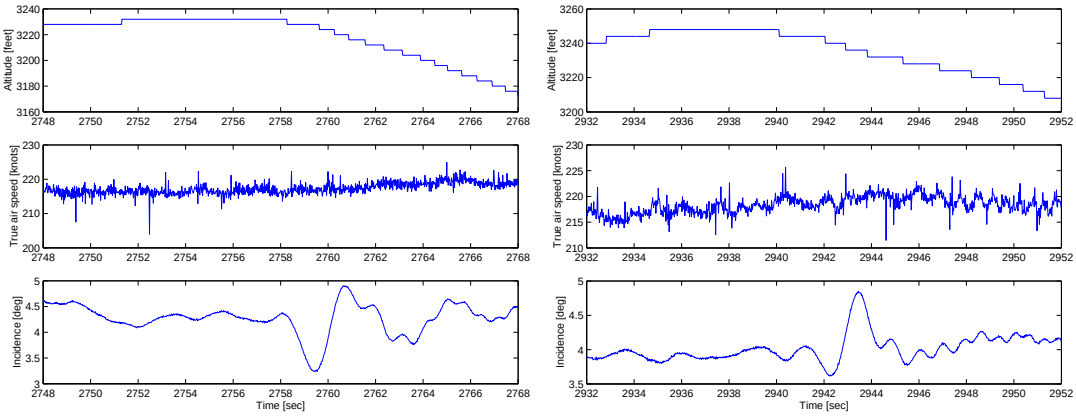

(a) Test Point 1

(b) Test Point 2

Figure 7.4: Time histories showing altitude, true air speed and incidence at each test point

7.2.2 Data extraction and time histories

The measured data were logged by the VAAC Harrier's on-board computer and delivered 'raw', with the Simulink model used to decode the measurements in-flight. An adapted version of this was used to 'decalibrate' the logged signals. Time histories for the trim variables are given in Figure 7.4, and mean values are given in Table 7.2.

	Test Point 1	Test Point 2
Altitude	3.32×10^3 ft	3.34×10^3 ft
True air speed	217 knots	218 knots
Incidence	4.3 deg	4.0 deg

Table 7.2: Mean values of trim variables from Figure 7.4

The data were down-sampled to give 180 data-point records.[4] The new inter-sample period was chosen as 0.05 sec to allow as much as possible of the ten-second chirp to be recorded. The down-sampled signals are shown in Figure 7.5.

[4]This results in 360+ decision variables. More are theoretically possible, but our computers' memory was insufficient: the 'yalmip' software used took up several hundred megabytes of memory, and increasing the record length to 190, for example, consistently caused crashes.

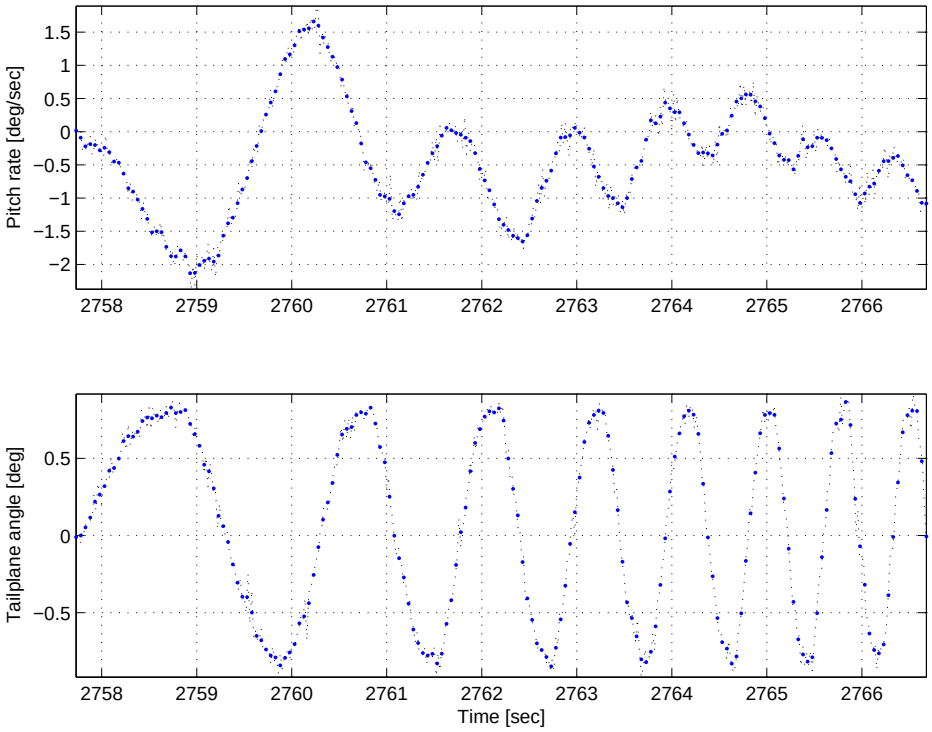

(a) Test Point 1

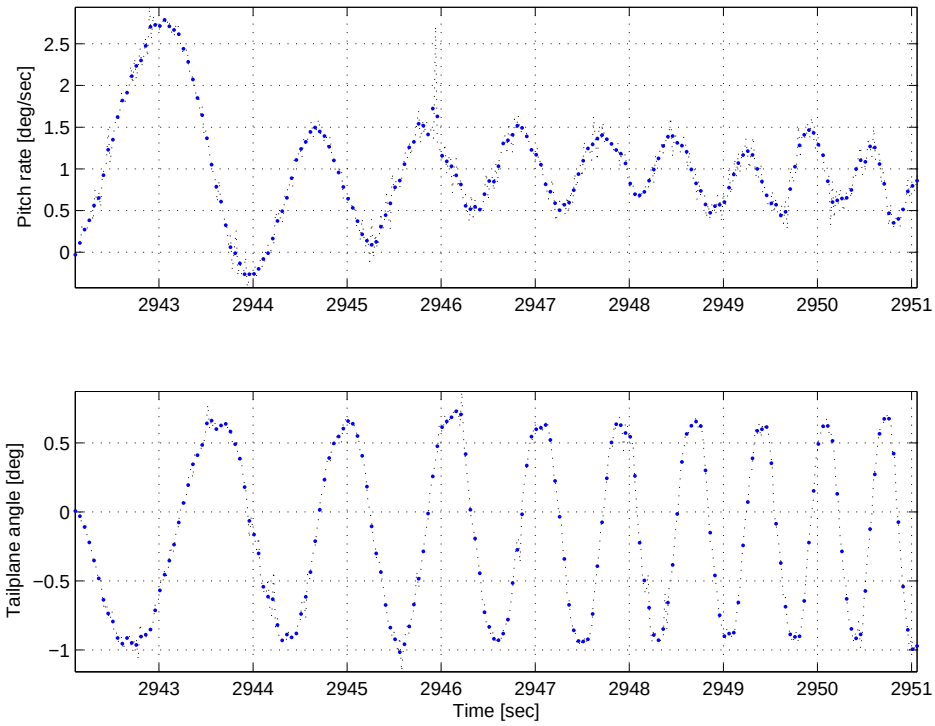

(b) Test Point 2

Figure 7.5: Down-sampled signals

7.2.3 Modelling the plant and controller

Linear continuous-time plant models were extracted by trimming the HWEM to the required operating point and using QinetiQ-supplied linearization scripts to determine the plant model.[5] A similar procedure (detailed in the appendices on page 177) was used to find the corresponding controller models. Numerical values are presented on page 178.

7.3 Model analysis using near-optimal weighting

Having computed a nominal $[P, C]$ at each test point, the magnitude of the optimal input-output weighting $W_{\mathrm{i}}^{\circ}, W_{\mathrm{o}}^{\circ}$ described in Section 3.3 was calculated for the frequency range 10^{-2} to 10^{1} rad/sec.[6] Note that because we are dealing with a single channel, that from tailplane angle to pitch, we need only one dynamic weight, so we shall consider only W_{i}°. Though there is no theoretical difficulty in producing a real-rational transfer function to fit $|W_{\mathrm{i}}^{\circ}(j\omega)|$ exactly, this could produce a very high-order system. Instead, weights close in magnitude to the optimal were constructed. The weights $W_{\mathrm{i}}(j\omega)$ used for each test point are shown in Figure 7.6.[7] These weights were visually fitted to the data, with integral action used to provide the low frequency response, and a compatible phase response was generated.[8]

[5] More details on the trimming procedure are given on page 174.

[6] The MATLAB function used to do this is included in the appendices, starting on page 184.

[7] Numeric values are given on page 186.

[8] The MATLAB functions `fitmag` and `genphase` from the μ-synthesis and analysis toolbox were used.

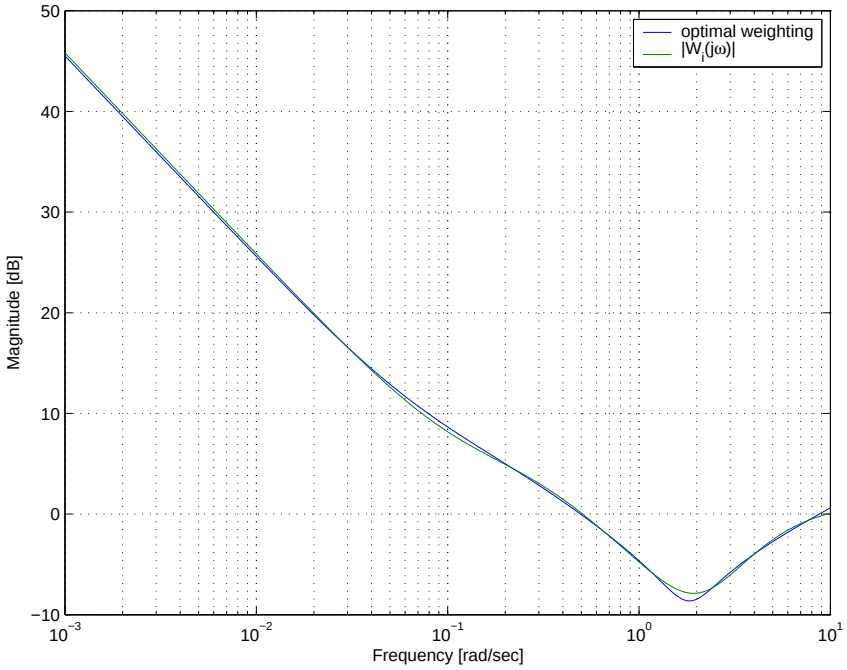

(a) Test Point 1

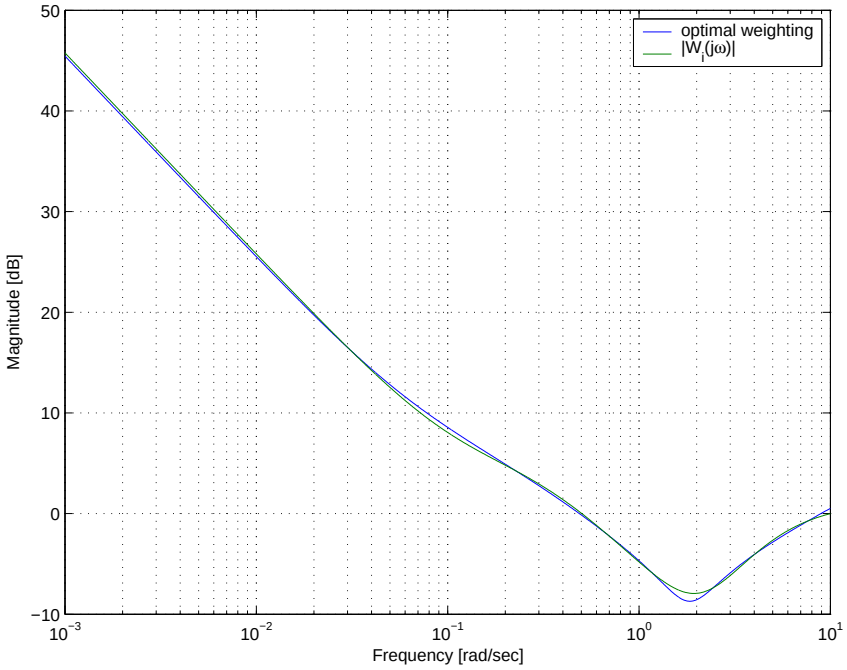

(b) Test Point 2

Figure 7.6: Optimal weighting (blue) and near-optimal weights $W_{\mathrm{i}}(j\omega)$ used for validation (green)

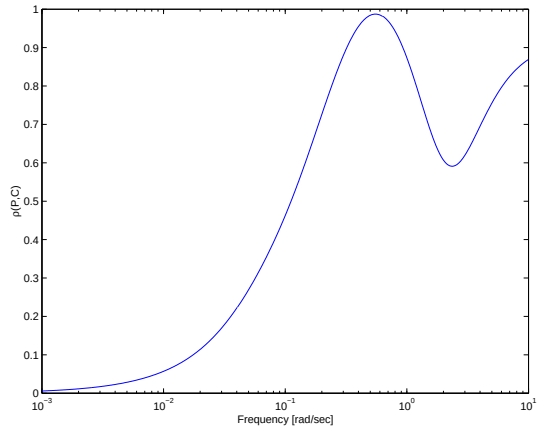

(a) TP1: $\rho(P(j\omega), C(j\omega))$

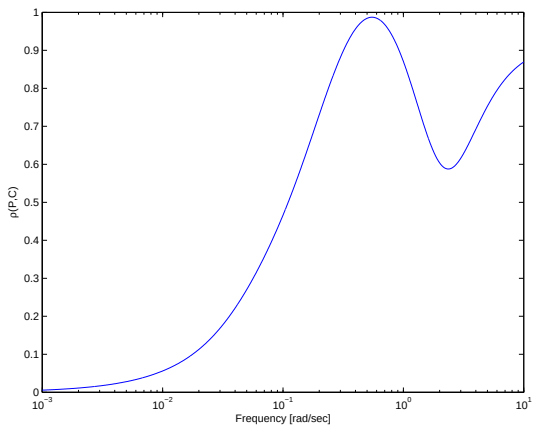

(b) TP2: $\rho(P(j\omega), C(j\omega))$

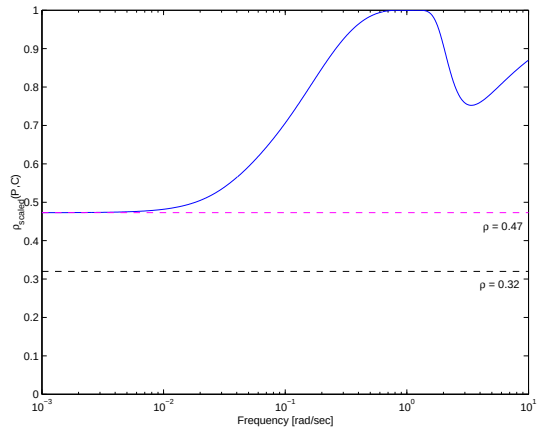

(c) TP1: $\rho_{\text{scaled}}(P(j\omega), C(j\omega))$

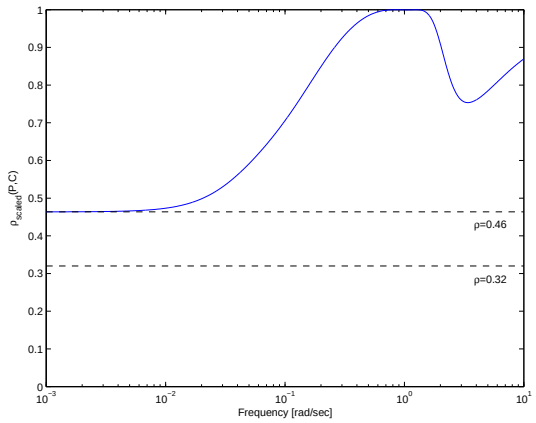

(d) TP2: $\rho_{\text{scaled}}(P(j\omega), C(j\omega))$

Figure 7.7: Frequency-wise robust stability margins with and without weighting. The left plots are for Test Point 1, the right plots for Test point 2.

7.3.1 Effects on the frequency-wise robust stability margin

The effect of the weighting on the frequency-wise robust stability margin is illustrated by Figure 7.7 on page 122. Note that the system is marginally stable: a closed-loop pole at the origin is considered acceptable in many flight applications. Thus $b_{P,C} = 0$. However, with weighting this problem is circumvented: $b_{\text{scaled}}(P, C) = 0.47$ for Test Point 1, and 0.46 for Test Point 2.

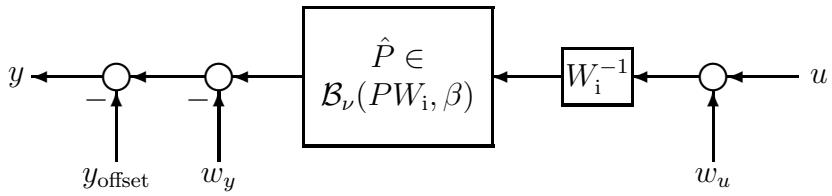

Figure 7.8: Block diagram for model validation. (u, y) are the down-sampled validation data; the plant P and weight W_i are sampled at the same rate. $\hat{P}$, w_u, w_y, and y_offset are unknowns to be determined. If consistent values exist, our model is considered not invalidated.

7.3.2 Validation procedure

The models and weighting were sampled with a period $T_\mathrm{s} = 0.05$ seconds to match the down-sampled data.[9] The effect on the weighted singular values of the plant is shown in Figure 7.9 (page 124). Note that the shape of the plots and the crossover frequencies are not greatly affected by this. The scheme initially adopted for validation is shown in Figure 7.8 on page 123.

A condition for LTI non-invalidation follows:

Proposition 7.1 (LTI suff. condition for non-invalidation) *Given a nominal plant $P(z)$, input weight $W_\mathrm{i}(z)$ and validation data $(u \in \mathcal{S}_k^q, y \in \mathcal{S}_k^p)$, all sampled with the same period, $\gamma > 0$ and a ν-gap radius β, let M be the central controller satisfying*

$$b\left(PW_\mathrm{i}, C\right) > \beta \;\forall\; C \in \left\{\hat{C} : \hat{C} = \mathcal{F}_\ell(M, Q), Q \in \mathcal{RH}_\infty, \|Q\|_\infty < 1\right\}$$

Given any sequences $w_{u0} \in \mathcal{S}_k^q, w_{y0} \in \mathcal{S}_k^p$, let

$$\begin{pmatrix} s \\ t \end{pmatrix} = \mathrm{ch}\left(M\right)^{-1} \begin{bmatrix} W_\mathrm{i}^{-1} & 0 \\ 0 & I \end{bmatrix} \begin{pmatrix} u + w_{u0} \\ y + w_{y0} \end{pmatrix}$$

Then there exists a system $\hat{P}(z) \in \mathcal{B}_\nu^{\mathrm{LTI}}\left(PW_\mathrm{i}, \beta\right)$, $w_u \in \mathcal{S}_k^q$, $w_y \in \mathcal{S}_k^p$, $y_\mathrm{offset} \in \mathbb{R}^p$

[9] MATLAB's default 'sample-and-hold' method was used.

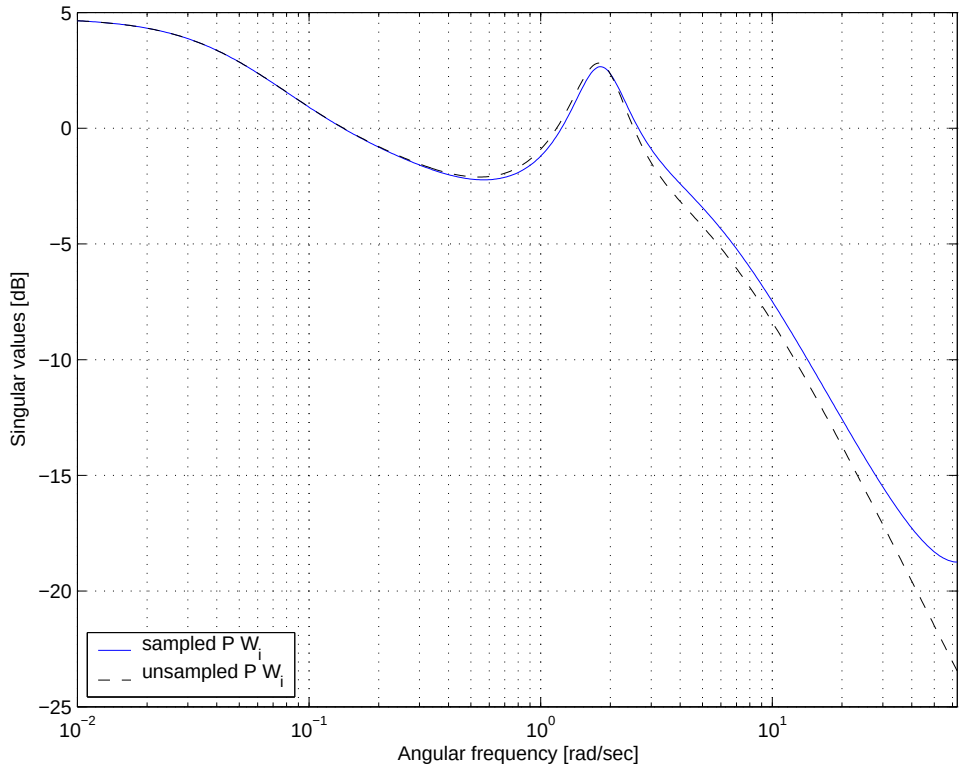

(a) Test Point 1

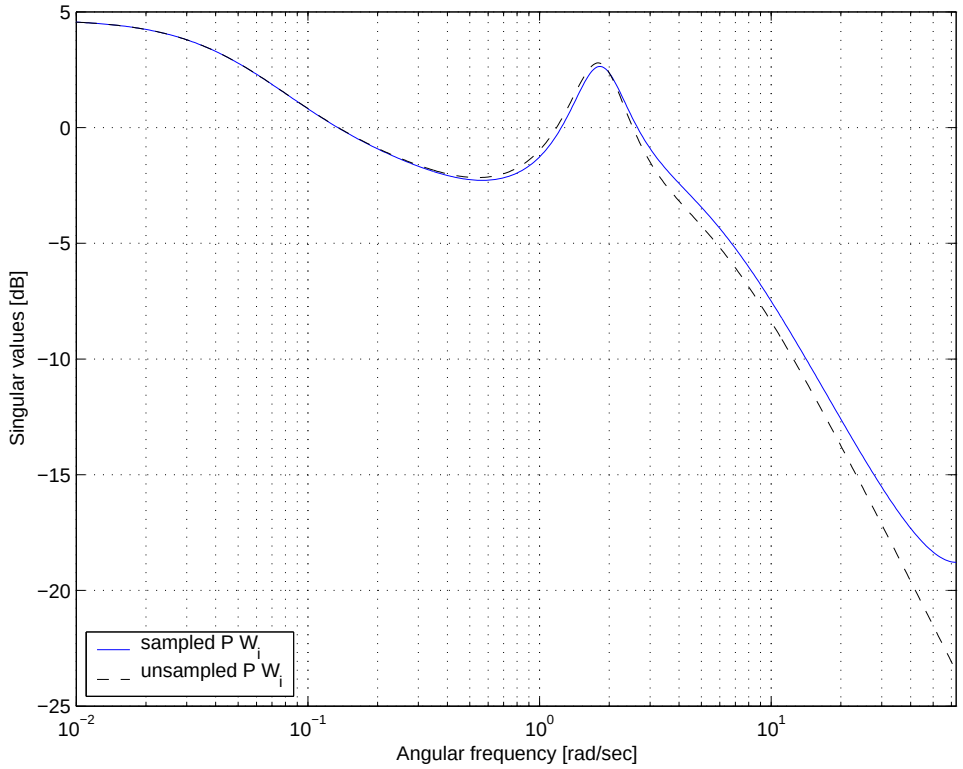

(b) Test Point 2

Figure 7.9: Frequency responses of PW_{i} after sampling with $T_{\mathrm{s}} = 0.05$ sec

such that

$$y + w_y + y_{\text{offset}} = \hat{P} W_{\text{i}}^{-1}(u + w_u)$$

and

$$||w_u||_2^2 + ||w_y||_2^2 \leq \gamma^2 \tag{7.1}$$

if there exist $w_s \in \mathcal{S}_k^q$, $w_t \in \mathcal{S}_k^p$ *and* $y_{\text{offset}} \in \mathbb{R}^p$ *simultaneously satisfying*

$$\begin{bmatrix} T_s^* T_s + T_{w_s}^* T_s + T_s^* T_{w_s} & T_t^* + T_{w_t}^* \\ T_t + T_{w_t} & I \end{bmatrix} \geq 0$$

and

$$\begin{bmatrix} \gamma^2 & \operatorname{vec} \xi^* \\ \operatorname{vec} \xi & I \end{bmatrix} \geq 0 \tag{7.2}$$

where

$$\xi = \begin{bmatrix} W_{\text{i}} & 0 \\ 0 & I \end{bmatrix} \operatorname{ch}(M) \begin{pmatrix} w_s \\ w_t \end{pmatrix} + \begin{pmatrix} w_{u0} \\ w_{y0} \end{pmatrix} - \begin{pmatrix} 0 \\ y_{\text{offset}} \end{pmatrix} \tag{7.3}$$

When these exist, realizations of w_u *and* w_y *are given by* $\begin{pmatrix} w_u \\ w_y \end{pmatrix} = \xi$.

Proof. This follows naturally from Theorem 5.1. Since we are considering a weighted ν-gap radius, we take as the total input to the weighted plant $\hat{u} = W_{\text{i}}^{-1}(u + w_u)$ and the total output $\hat{y} = y + w_y + y_{\text{offset}}$. This gives the following input/output for the perturbation block.

$$\begin{aligned} \begin{pmatrix} \hat{s} \\ \hat{t} \end{pmatrix} &= \operatorname{ch}(M)^{-1} \begin{bmatrix} W_{\text{i}}^{-1} & 0 \\ 0 & I \end{bmatrix} \begin{pmatrix} u + w_u \\ y + w_y + y_{\text{offset}} \end{pmatrix} \\ &= \underbrace{\operatorname{ch}(M)^{-1} \begin{bmatrix} W_{\text{i}}^{-1} & 0 \\ 0 & I \end{bmatrix} \begin{pmatrix} u + w_{u0} \\ y + w_{y0} \end{pmatrix}}_{(s,t)} + \underbrace{\operatorname{ch}(M)^{-1} \begin{bmatrix} W_{\text{i}}^{-1} & 0 \\ 0 & I \end{bmatrix} \begin{pmatrix} w_u - w_{u0} \\ w_y - w_{y0} + y_{\text{offset}} \end{pmatrix}}_{(w_s, w_t)} \end{aligned}$$

From this it is clear that

$$\begin{pmatrix} w_u - w_{u0} \\ w_y - w_{y0} + y_{\text{offset}} \end{pmatrix} = \begin{bmatrix} W_{\text{i}} & 0 \\ 0 & I \end{bmatrix} \text{ch}\,(M) \begin{pmatrix} w_s \\ w_t \end{pmatrix}$$

which gives (7.3).

Writing $\xi = \begin{pmatrix} w_u \\ w_y \end{pmatrix}$, the noise bound (7.1) may equally well be expressed as $\text{vec}\,\xi^* \text{vec}\,\xi \leq \gamma^2$, which, by the Schur complement (2.9) gives (7.2). □

Remark 7.2 Having obtained w_u, w_y and y_{offset}, a realization of $\hat{P}$ can be constructed by applying Theorem 5.10 to $\hat{u}$ and $\hat{y}$. ♡

Remark 7.3 The ideas of Remark 5.8 can be applied here too, in order to accommodate a non-zero initial state. Repeating the mathematics here would be tedious and not contribute greatly to the discussion. ♡

The analogous result for $\mathcal{B}_\nu^{\text{LTV}}(PW_{\text{i}}, \beta)$ (Proposition D.1) is presented in the appendices on page 186. The necessary and sufficient condition for $\mathcal{B}_\nu^{\text{NC}}(PW_{\text{i}}, \beta)$ is simply obtained from Remark 6.12. A starting point for the LTI and LTV (in)validation procedures was found by solving a least-squares noise-minimization problem for the nominal model.

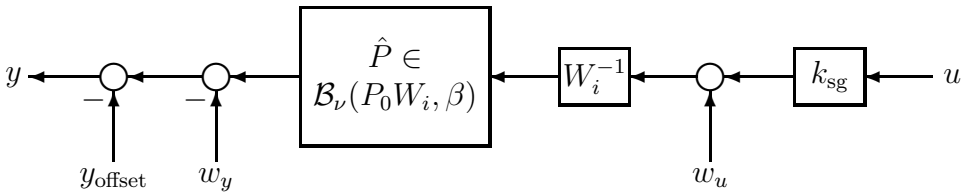

Figure 7.10: Block diagram: weighted model validation with input scaling

7.3.3 Initial results and re-scaling

When processing the initial results, it was noticed that the 'best' models seemed to produce signals with smaller amplitude than the sampled data. It was hypothesized that there was a gain scaling error, perhaps in one or more of the decalibration constants. To accommodate this, the model of Figure 7.10 was proposed. A scalar 'sensor gain' k_{sg} was included on the input signal, applying only to the measured signal itself.

The effects of varying k_{sg} are shown in Figure 7.11.

Remark 7.4 From this point forward, it will be assumed that all the input data has been scaled by $k_{\text{sg}} = 1.8$. ♡

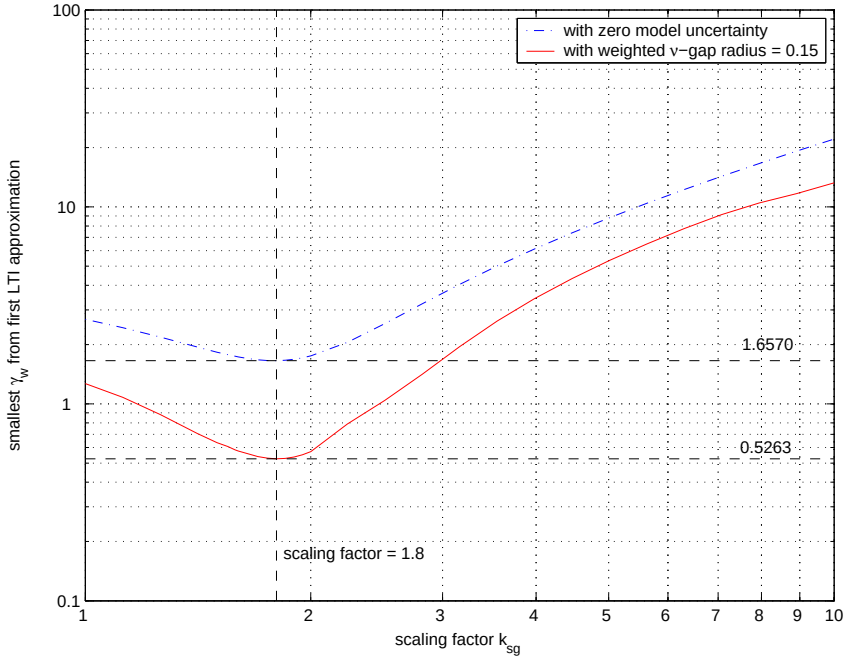

(a) noise minimization with fixed ν-gap radius

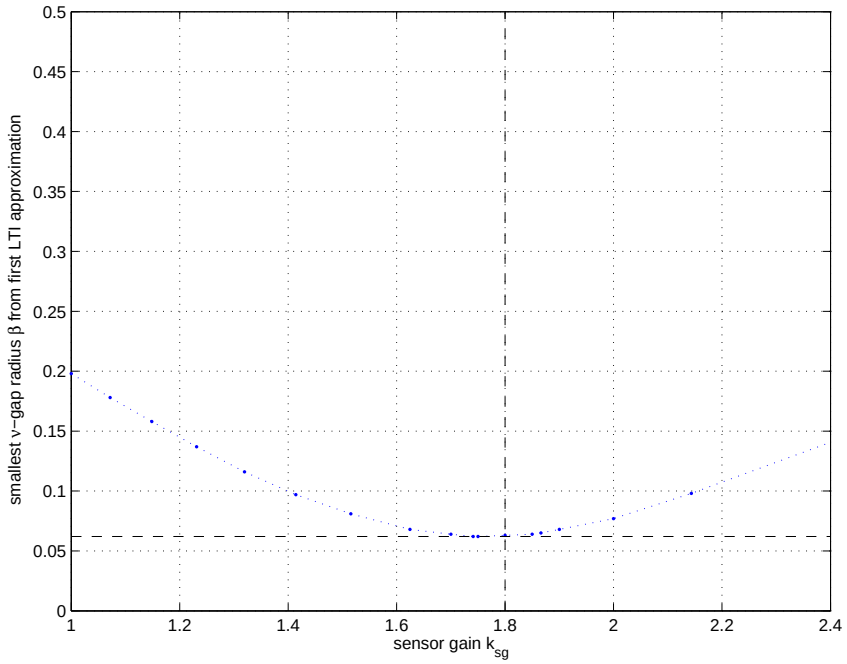

(b) ν-gap minimization with fixed noise bound

Figure 7.11: The effects of varying k_{sg}. Both plots show the results for the first approximation of the full LTI non-invalidation problem, considering both a noise minimization problem and an uncertainty minimization problem. In both cases, the optimal k_{sg} is approximately 1.8.

7.3.4 Computation and results

The most practical way to analyse the results is to compute the smallest noise norm γ that can be determined for any given value of β. This is, at least under approximation, easily formulated as an LMI objective minimization problem.[10]

The algorithms used to compute the results for Test Point 1 and Test Point 2 were slightly different: the method adopted for Test Point 2 was slightly more refined, with greater scope for repeatability. In both cases, the optimization processes ran on several machines over several weeks. During the computations for Test Point 2, computation of one iteration for sixty β points took between 24 and 48 hours, running on 12 processors.

Algorithm for Test Point 1

- The first few upper bounds on $\gamma(\beta)$ for the first approximation were calculated using a least-squares solution for the nominal model as a starting point (w_{u0}, w_{y0}) in Propositions 7.1 and D.1.
- As the computations finished, the corresponding values of (w_u, w_y) were stored, and used as starting points for subsequent computations.
- The upper bounds were refined by repeated applications of Propositions 7.1 and D.1. In each case, the (w_u, w_y) from the previous iteration was used to provide the starting point (w_{u0}, w_{y0}) for the next. This was stopped either at the tenth iteration, or after the value had converged such that the improvement on the previous iteration was less than 0.1%.

Only the results of the final iteration were recorded.

[10] When trying to minimize the smallest compatible ν-gap radius as a function of γ, it is necessary to use a bisection method since the ν-gap parameterization differs for every value of β considered. A separate feasibility problem must be considered at every iteration of the bisection algorithm. This is of course very slow.

Algorithm for Test Point 2

The algorithm for Test Point 2 was simpler, and more easily repeatable:

- The first iteration was carried out using a least-squares solution for the nominal model for all values of β.
- Nine subsequent iterations were carried out. After each iteration, monotonicity was enforced since this makes logical sense.

The results for *all* iterations were recorded.

For both test points, the validation process was carried out in two ways:

(i) with no pre-record sequence, assuming the system was initially in equilibrium;

(ii) with pre-record sequence of length $n = 2$, allowing for an initial state.[11]

[11] Numerical problems were encountered with $n = 3$ and greater. Time did not permit exploration of the cause.

Final results: Test Point 1

The validation results assuming a zero initial state are shown in Figure 7.12(a). The results with a non-zero initial state are shown in Figure 7.12(b). A number of points are worth noting:

1. The values shown for LTI and LTV uncertainties are *upper bounds* on their true minima, produced by successive relinearizations about the local minima in the approximate non-invalidation problems.

2. It is clear that the structure of the model perturbation is very important: the results for LTI uncertainty are far more conservative than those for LTV and noncausal uncertainty.

3. Allowing for an initial state (using pre-data sequences) has a big effect, particularly in the LTV and noncausal cases; for a given level of uncertainty, much less noise is required to account for the remaining discrepancy between model and data when a non-zero initial state is allowed.

4. In the non-zero initial state case, the LTV and noncausal lines appear to be coincident. This is not true for the zero initial state case. This will be discussed further in Section 7.3.6.

(The graphs shown represent spline fits to the points numerically analysed. The 'raw' numerical results are shown in page 187 in the appendices.)

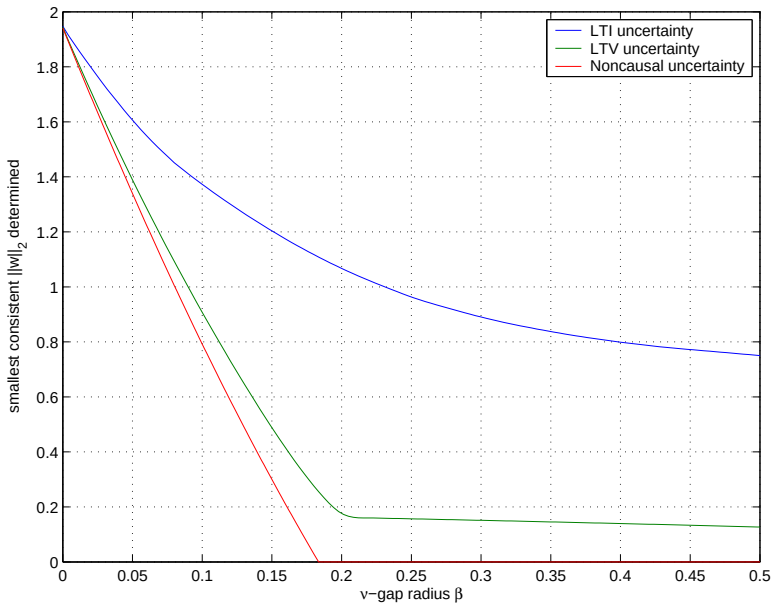

(a) β vs. $||w||_2$ trade-off with initial state fixed to zero

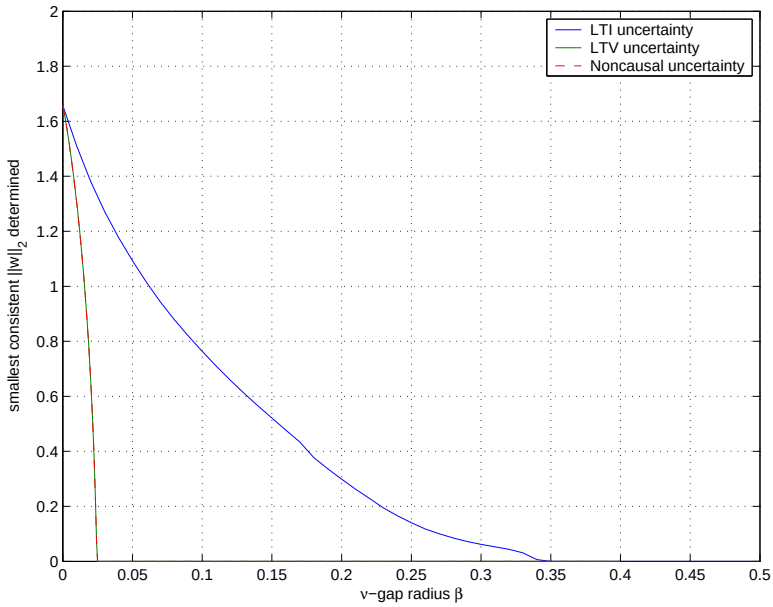

(b) β vs. $||w||_2$ trade-off with initial state free

Figure 7.12: (Test Point 1) These graphs show the trade-off between ν-gap radius β and the smallest $||w||_2$ required to account for modelling discrepancy, both for zero initial state (Figure 7.12(a)) and for a 'free' initial state generated using pre-input sequences (Figure 7.12(b)).

Final results: Test Point 2

The validation results for Test Point 2 are shown in Figure 7.13. Although there is difference in the detail, very much the same observations can be made here as for Test Point 1.

It can be seen that the noise-norm values obtained for Test Point 2 are slightly greater than those obtained for Test Point 1. This suggests that the second experiment was more informative than the first. If it were not for the approximation inherent in the constraints, we could categorically state that smallest γ-values consistent with each ν-gap radius *for all data* was at least as small as the values from Test Point 2. (Even with the approximation, it remains likely that Test Point 2 is giving us something closer to the truth.)

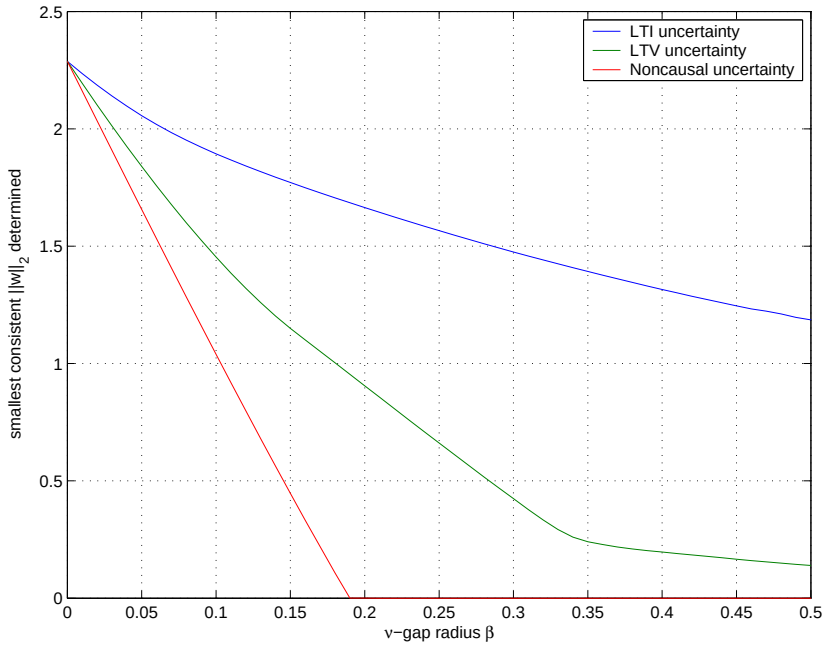

(a) no allowance for non-zero initial state

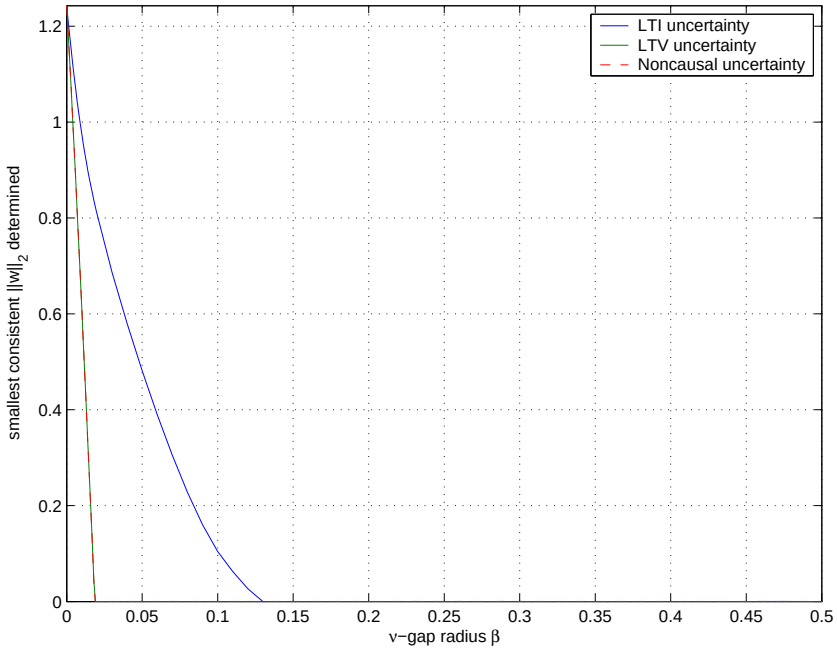

(b) allowing for non-zero initial state with $n = 2$

Figure 7.13: Validation results for Test Point 2: these curves illustrate the trade-offs between noise and weighted ν-gap radius in accounting for discrepancy between noise and data.

7.3.5 The effects of relinearization

The algorithm used to analyse Test Point 2 was implemented such that the result at each iteration was recorded. This enables a clear picture of the effects of relinearization to be seen. The LTI, $x_0 = 0$ case is illustrated by Figure 7.14. Relinearization brings a clear improvement for large ν-gap radii, though little improvement occurs for small radii. Most of the refinement takes place at the second stage of relinearization. The curves produced at the ninth and tenth stages are near-coincident.

Similar observations can be made for the other Test Point 2 data.

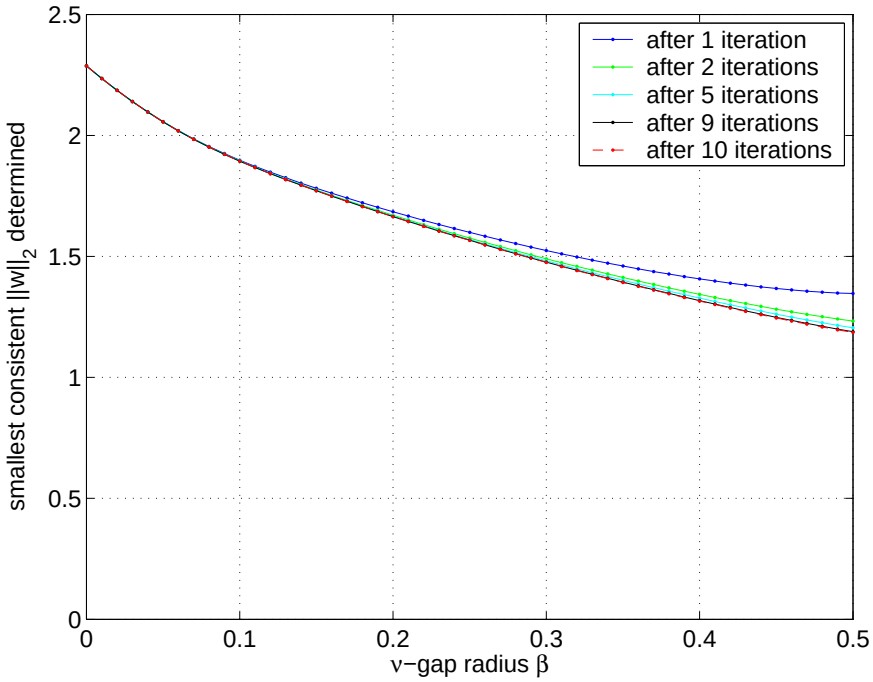

(a) The smallest consistent $||w||_2$-values determined for a given β at the jth iteration. The curves for $j = 9$ and $j = 10$ are very close.

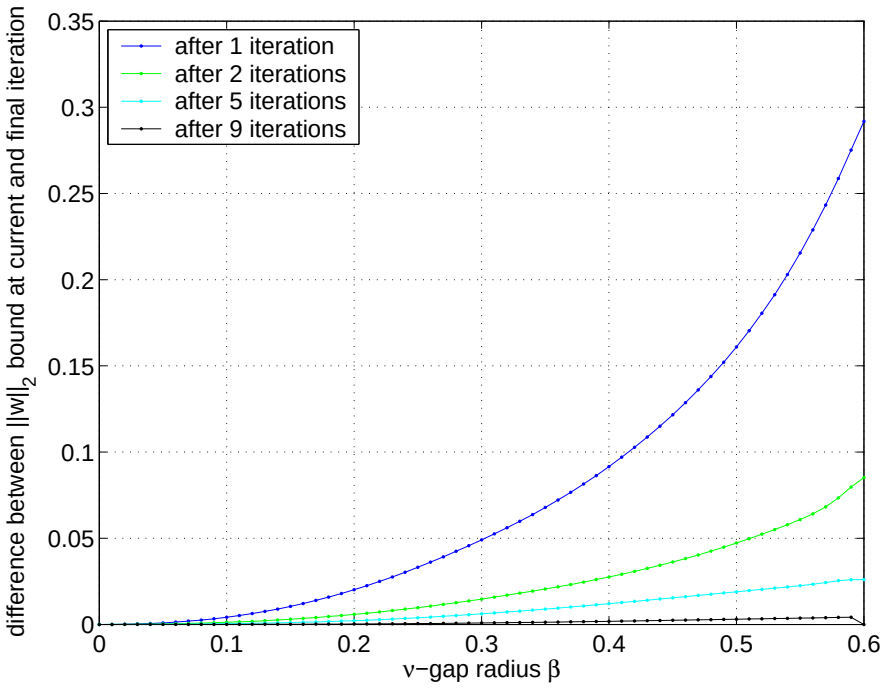

(b) The difference between the values obtained and the j-th iteration and the tenth. The values for $j = 9$ and j=10 are well within 1% of each other.

Figure 7.14: The effects of successive relinearization, demonstrated using the LTI, zero initial state data. Similar phenomena can be observed for the LTV data. Note that convergence is more rapid for small ν-gap radii

7.3.6 Noncausality versus causality

It will be noted that for both test points, the trade-off curves for noncausal and LTV perturbation structures appear very close together. In the calculations for Test Point 1, particular care was taken to include a high density of β-values in the region of interest.[12] The results are shown in Figure 7.15.

This is as expected, since the value for the LTV γ, itself an upper bound, is always greater than the corresponding noncausal value. The difference appears to increase with β, just as the more-obvious difference between the LTI and LTV curves does.

What we can see, however, is that in the case where the initial state is not fixed at zero, the effect of causality is minimal. Time-invariance remains important, however.

[12]The same analysis was not repeated for Test Point 2, owing to the high computational expense. However, the lines appear coincident.

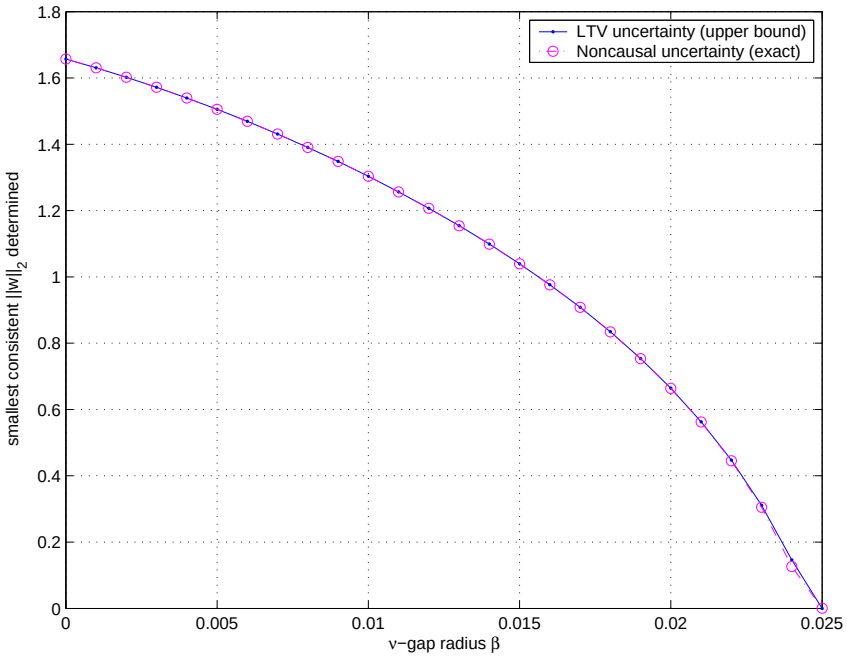

(a) Smallest γ-values for LTV and noncausal perturbation structures

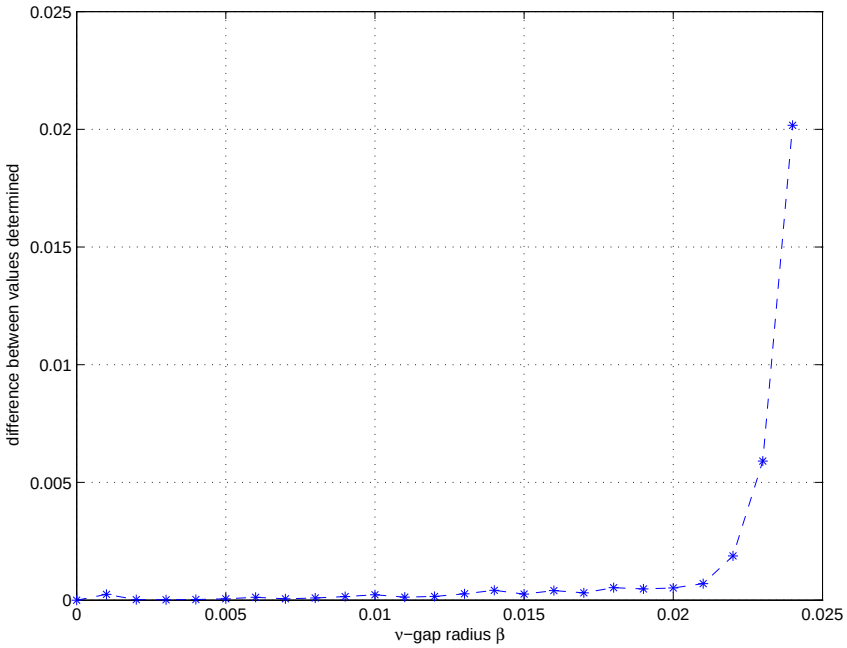

(b) Difference between LTV and noncausal values

Figure 7.15: The difference between smallest γ-values obtained with LTV and noncausal structures. At first, there is little to distinguish the curves. When the difference is plotted, it becomes clear that the LTV-value is always greater than the noncausal value, and the difference becomes greater as β increases.

.

7.3.7 Lower bounds for LTV uncertainty

The $\mathcal{S}$-procedure based techniques of Chapter 6 were applied to the Test Point 2 data, assuming a ν-gap radius $\beta = 0.07$ a zero initial state. (The zero initial state was chosen so that there would be discernable difference between LTV and noncausal values. The values are too close to see any difference when the initial state is free.) The results are given in Table 7.3.

Description	Reference	Value
LTV uncertainty, upper bound	Prop. D.1	1.68
LTV uncertainty, first lower bound	Remark 6.13(a)	1.41
LTV uncertainty, second lower bound	Remark 6.13(b)	1.62
Noncausal uncertainty	Remark 6.12	1.41

Table 7.3: Comparison of lower bounds at $\beta = 0.07$ (Test Point 2, zero initial state)

The first lower bound, effectively formed by applying the noncausal invalidation criterion to all truncations and taking the 'worst' result is, to the given accuracy, no different from the value that would obtained from the final truncation. (Figure D.7 on page 189 of the appendices illustrates this in more depth.) The value obtained using the *second* lower bound is considerably higher. At 1.62, it is relatively close to the upper bound of 1.68; the 'unknown' space in-between is less than 4% of either value.

7.4 A simplified proportional-integral weighting strategy

The near-optimal weighting strategy, though no doubt of interest, does not have obvious real-world significance. In the aviation industry, low-frequency unstable eigenvalues are often tolerated [Cor02] and some recent work [Hal02] has considered the application of relaxed stability criteria to multi-loop design. It can be seen that a major effect of the optimal and near-optimal weighting strategies of Figure 7.6 is to introduce integral actions at low frequencies, thus allowing for the presence of a closed loop pole at the origin. It was hypothesised that the use of proportional-integral weight

$$W_{\mathrm{PI}}(s) = K_{\mathrm{P}} + \frac{1}{sT_{\mathrm{I}}}$$

would provide similar benefits, yet be simpler and more intuitive than the optimal weighting strategy.

The near-optimal weight used in the analysis of Test Point 2 is well-approximated at low and high frequencies by

$$W_{\mathrm{PI}}(s) = 1.14 + \frac{0.1942}{s}$$

The frequency response of both the weights and the plants are shown in Figure 7.16, and the effect on the frequency-wise robust stability margin in Figure 7.17. The big difference in the frequency responses close to cross-over is clearly reflected in the frequency-wise robust stability margin, but not enough to affect the smallest value:

$$\sup_{\omega} \rho\left(PW_{\mathrm{PI}}, W_{\mathrm{PI}}^{-1}C\right)(j\omega) = \sup_{\omega} \rho\left(PW_{\mathrm{i}}, W_{\mathrm{i}}^{-1}C\right)(j\omega) \approx 0.46$$

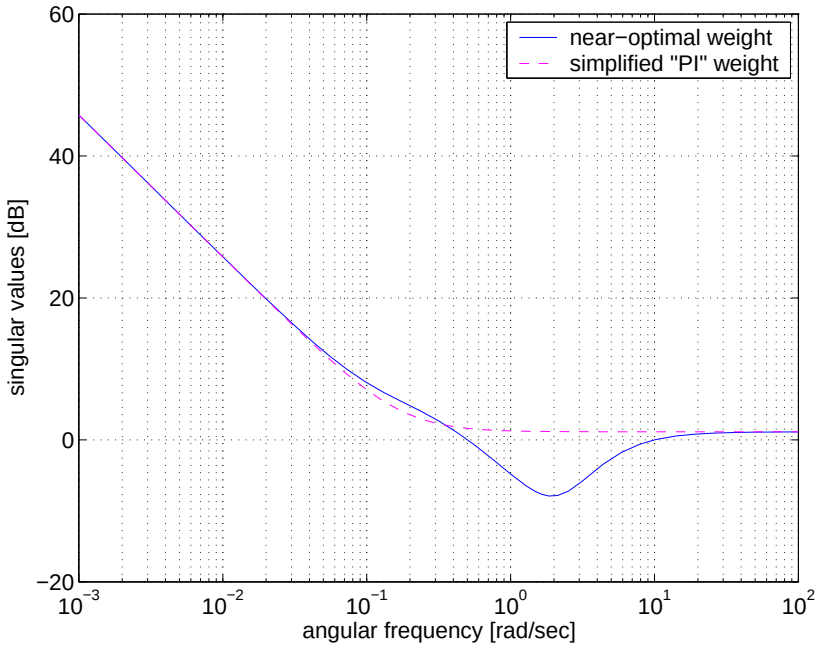

(a) frequency response of weight

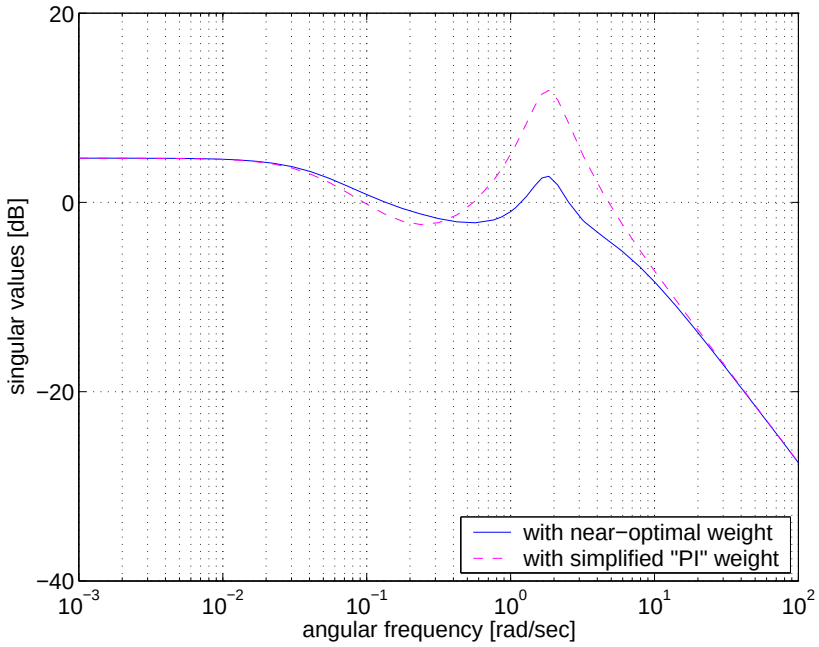

(b) frequency response of weighted plant

Figure 7.16: Comparing the near-optimal weighting strategy to the proportional-integral one. There is very little difference at high and low frequencies, but this is certainly not true close to crossover

Uncertainty type / initial state		$W_{\mathrm{i}}(j\omega)$	$W_{\mathrm{PI}}(j\omega)$
LTI uncertainty,	$x_0 = 0$	1.98	1.95
LTV uncertainty,	$x_0 = 0$	1.68	1.63
Noncausal uncertainty,	$x_0 = 0$	1.41	1.33
LTI uncertainty,	$x_0 \neq 0$	0.31	0.24
LTV uncertainty,	$x_0 \neq 0$	0.00	0.00
Noncausal uncertainty,	$x_0 \neq 0$	0.00	0.00

Table 7.4: Comparing the weighting strategies. This table shows the smallest values of $||w||_2$ determined at $\beta = 0.07$ using the 'near-optimal' weight $W_{\mathrm{i}}(j\omega)$ and the proportional-integral weight $W_{\mathrm{PI}}(j\omega)$. The PI weights give slightly smaller but similar values.

This weighting was used to re-validate the Test Point 2 data with $\beta = 0.07$. The results are shown in Table 7.4, with the zero initial-state LTI and LTV cases illustrated by Figure 7.18.

The values are slightly lower than those obtained with the 'near-optimal' weights, but similar. Note that the first weights' optimality was in terms of the frequency-wise ν-gap radius, not $b(P, C)$ itself: the proportional-integral weights are equally optimal in that sense. It is no great surprise that the values we find should be slightly higher or (as in this case) lower than those found before, but the fact that two 'sensible' weighting strategies give similar results increases confidence in both approaches.

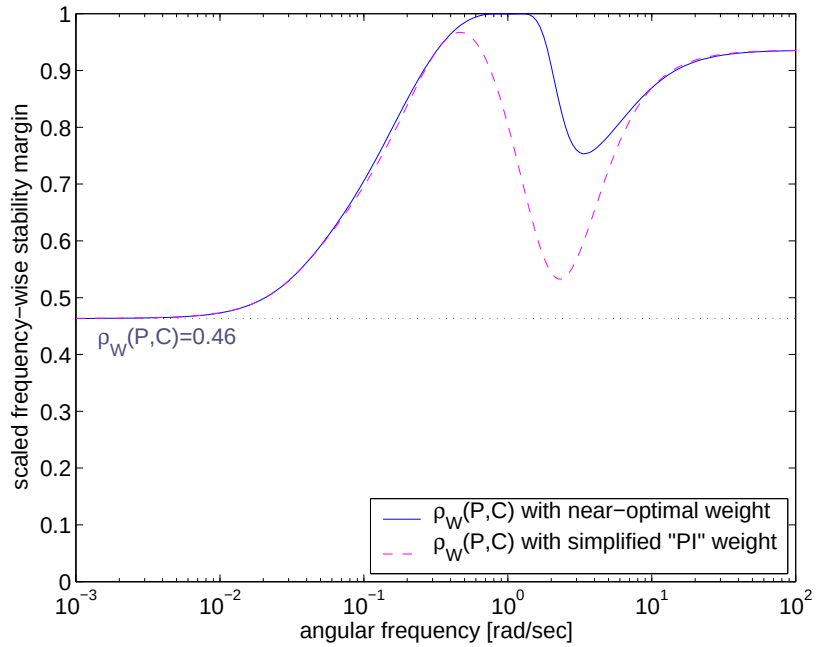

Figure 7.17: Comparing the near-optimal weighting strategy to the proportional-integral one. The smallest frequency-wise robust stability margin is unchanged, though the difference between this and values close to crossover is much smaller.

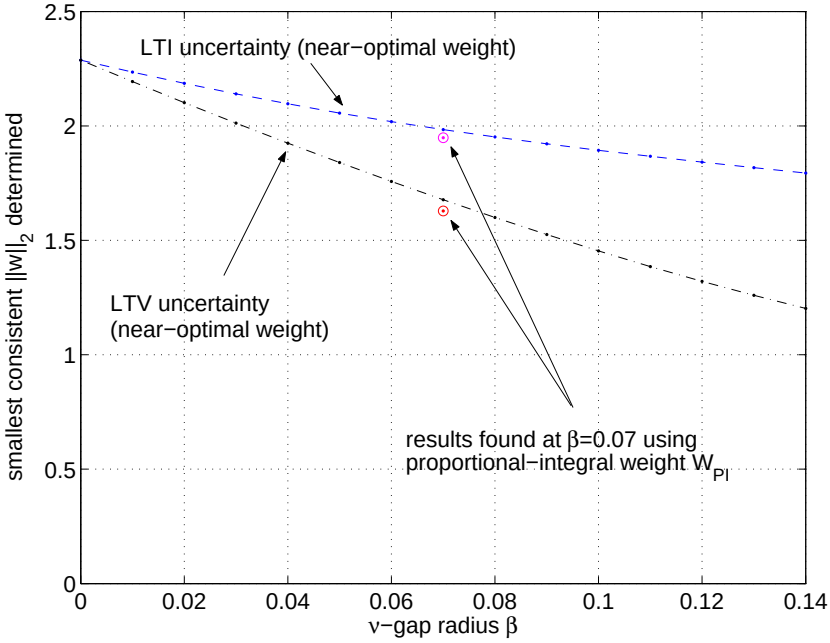

Figure 7.18: Effects of proportional integral weighting at $\beta = 0.07$, illustrated using the LTI/LTV cases with no initial state.

7.5 Construction of interpolants

The noise sequences found during the validation process can be used to find plausible plant input-output pairs $(\hat{u}, \hat{y})$ which can be used in Theorem 5.10 to construct interpolants. Figure 7.19 shows an example: the interpolant matches the down-sampled data perfectly. The nominal model, however, does not. Examples of a weighted frequency response and the frequency-wise ν-gap between a constructed interpolant and the (sampled) nominal plant are shown in Figure 7.20. Notice that the frequency-responses are not at all smooth: this is a natural consequence of the interpolation methods employed. The raggedness is more pronounced for the higher of the two ν-gap radii considered, a fact that is not particularly surprising given that more discrepancy must be accounted for in the model.

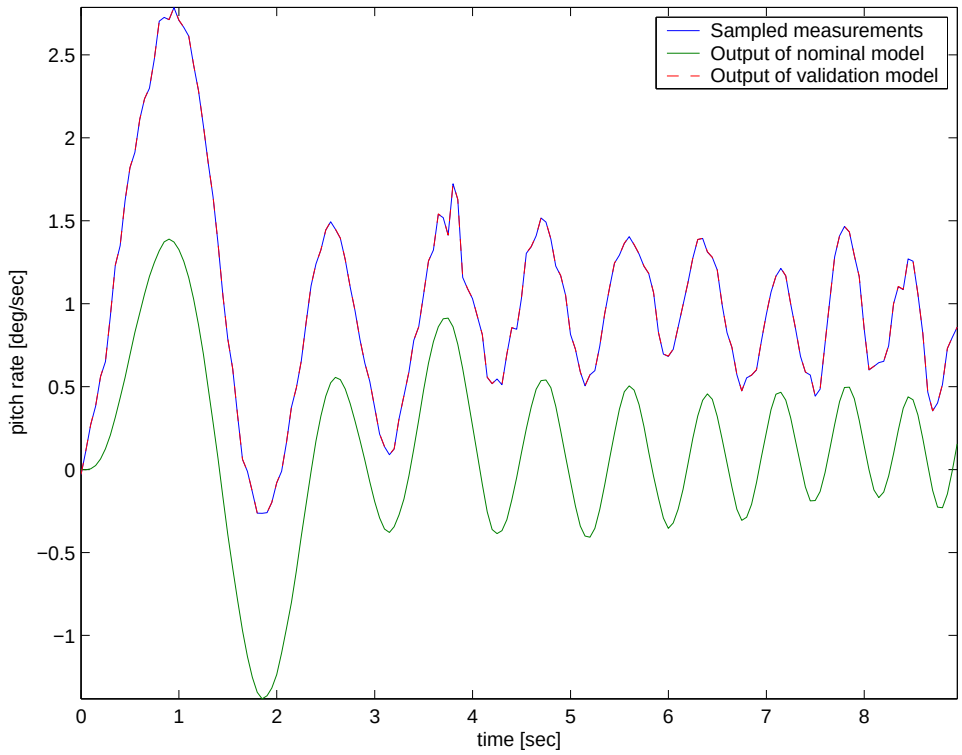

Figure 7.19: Time domain results (LTI, initial state non-zero, $\beta = 0.01$): the solid blue line shows the down-sampled output measurement; the solid green line is the output of nominal P; the dashed red line is the noise-adjusted output of $\hat{P}W_{\mathrm{i}}^{-1}$ from validation.

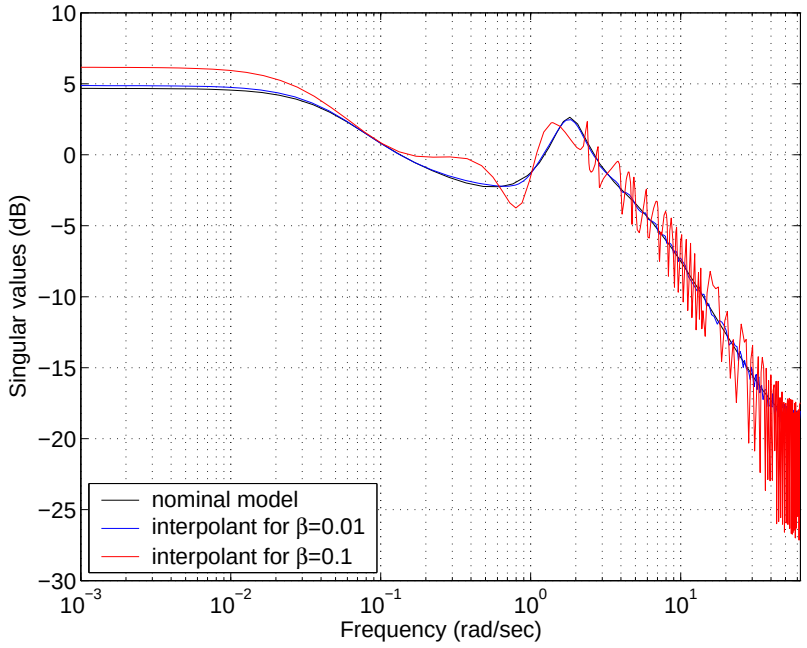

(a) Weighted frequency response

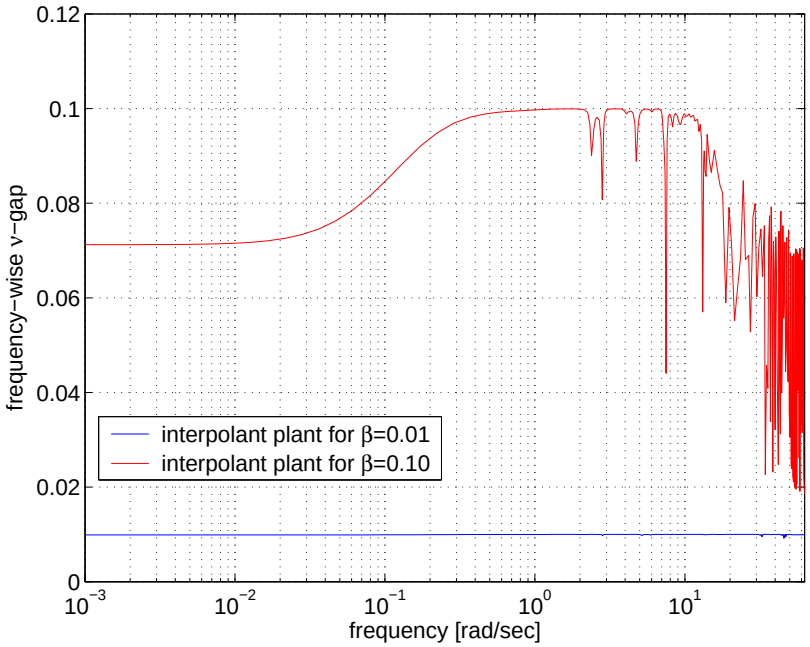

(b) Weighted frequency-wise ν-gap

Figure 7.20: Visualising interpolant plants. These diagrams show the weighted frequency responses of LTI interpolants constructed to match the Test Point 2/non-zero initial state data with $\beta = 0.01$ and $\beta = 0.1$. Notice the 'raggedness' of the frequency responses, which is more pronounced for the higher ν-gap radius.

Final comments

In this chapter, we have succesfully demonstrated the application of the model (in)validation techniques introduced in Chapters 5 and 6 to a real-world example. It is worth noting the following:

1. Some of the trade-off curves show that a model set with a ν-gap radius above some value of β is sufficient to account for all the discrepancy between nominal model and observed behaviour. (An example is Figure 7.12(b), where LTI model set with $\beta > 0.35$ is consistent with the data without any noise.) This does **not** mean that a controller designed for this value of β is *guaranteed* to work up to specification; all the (in)validation test has done is to show that such a mode set *could* account for all the discrepancy in the finite time section concerned, increasing our confidence in the model.

2. There may well be nominal plants (and associated controllers) achieving 'better' trade-off curves. In the example of Figure 7.12(b), it would be possible to construct a system that would account for the observed data perfectly. It does not follow that this would be a better model; it would need to perform this well when considered over *all* possible data records, not just a single observed case.

3. The full trade-off curves for PI weighting (section 7.4) have not been computed.

Further conclusions are given in the following chapter.

Chapter 8

Conclusions

Most of the original work in this thesis is in Chapters 5, 6 and 7. Conclusions drawn are listed separately for each chapter.

Chapter 5: Extensions to model validation theory

This chapter considered the ν-gap LTI/LTV non-invalidation problems, developing a method of improvement by relinearization which could be applied to non-zero initial states. Methods of constructing interpolants were also discussed. The following conclusions were drawn:

- It is often possible to improve on the first approximation of LTI/LTV non-invalidation conditions by successively relinearizing about the 'best' solution found using the approximations. This is useful, both in providing 'better' solutions and—in cases where the relinearization does not result in a great improvement—increases confidence that the approximations are useful. It is not possible to state categorically that this method will always result in the true global minimum for the unapproximated non-convex constraints. In the numerical example, the fact that the 'brute force' optimisation routine was unable to improve on the value from successive relinearizations strongly suggests that we are finding local minima for the non-convex constraints.

- It is possible to account for a non-zero initial state by 'pre-padding' the input/output data. Perturbation block constraints should be applied across the extended record, but noise constraints should only be applied across the 'real time' part. When the problem is approximated, linearization should *not* take place about 'zero' pre-record values; a least-squares solution based on minimizing the ℓ_2-norm of the noise sequences using the nominal model was found to be effective in a numerical example.

- The noise-corrected data from non-invalidation tests can be used to construct interpolant systems of comparable order to the record length.

Chapter 6: Invalidation using the $\mathcal{S}$-procedure

An alternative approach to LFT invalidation problems using the $\mathcal{S}$-procedure was considered. A problem was identified with a claimed necessary and sufficient condition for LTV invalidation from [SDM00], which we show to be sufficient but not necessary. The techniques were adapted to produce necessary and sufficient conditions for invalidation with a noncausal perturbation structure and a tighter sufficient condition for LTV invalidation. This was illustrated using a numerical example, also serving as a counter-example to the claim of [SDM00]. The techniques are adapted for application to a system with an output offset and potentially non-zero initial state. The following conclusions were drawn:

- The claimed necessary and sufficient condition of LTV invalidation proposed in [SDM00] is only sufficient. A tighter sufficient condition has been found. This is useful, since we now have upper and lower bounds for LTV (in)validation problems. In a convex numerical example, the new lower bound of the smallest noise ℓ_2 norm consistent with any given perturbation size was seen to be very close to the true value from convex optimization. Model (in)validation problems are not generally convex, though: LTI/LTV ν-gap type problems are not obviously so.

- A necessary and sufficient condition for invalidation using noncausal perturbations has been derived. This is potentially useful in assessing the effects of causality on a given problem. (It also provides a lower bound for the LTV and LTI cases.) This is very easy to compute, requiring only a simple LMI optimization with few decision variables, but—when considered as a lower bound for the LTV case—it is less tight than the bounds described above.

Chapter 7: An application in flight control

The techniques of Chapters 5 and 6 were applied to experimental flight test data from QinetiQ's VAAC Harrier for two sections of straight-and-level flight data. The following conclusions were drawn:

- The LTI, LTV and noncausal (in)validation techniques of the Chapters 5 and Chapters 6 can be successfully applied to real-world data.

- A system model consisting of a linear model (from the HWEM) in series with a scalar gain and dynamic frequency weighting accounted well for the data when input/output noise and an output offset were allowed. For computational reasons, it was not possible to consider more than 180 data points. It is necessary to compromise between actual-time record length and resolution, and the down-sampling no doubt has a considerable attenuating effect on the influence of high-frequency uncertainty and noise.

- A frequency-wise 'near-optimal stability' weighting strategy was successfully used. The real-world significance of this is unclear, and a much simpler proportional-integral weighting strategy was employed with very similar results. (The second strategy was as optimal as the first in terms of the overall robust stability margin, so this is as would be expected.)

- Of the two data records considered, the second—produced by injecting a chirp signal on the 'tailplane demand' rather than the 'pitch demand'— can be considered the more informative since more noise is required for consistency with any given ν-gap radius.

- When the initial state is fixed at zero, time-invariance and causality both seem to be active constraints.

- When the initial state is allowed to vary, time-invariance remains an active constraint but the significance of causality seems much reduced: the 'noise-against-perturbation' curves for LTV and noncausal uncertainty are effectively coincident.

- The method of successive refinement for LTI/LTV uncertainty appears to work in practice. Most of the improvement takes place between the first and second iterations. The potential for improvement is greater for larger ν-gap radii, and very small when the ν-gap radius is close to zero.

- The estimates of the smallest noise-norm found using the two LTV lower bounds—considered with a zero initial state so as to make the difference clear—suggest that the bound derived from [SDM00] is not particularly useful, since the numerical value given was identical to that found for noncausal uncertainty. The new bound from Chapter 6 was more useful being comparable to but lower than the upper bound computed using the 'traditional' methods of Chapter 5.

- It was possible to find LTI interpolants. The frequency-responses of these were very ragged, particularly for comparatively large ν-gap radii. These interpolated the noise-corrected data perfectly.

- The LMI algorithms used are not yet sufficiently fast for the method to be used to 'real time' flight clearance.

In summary, we have developed new techniques for (in)validation and construction of interpolant systems, and we have applied them to real world data. Our techniques were seen to work within certain limitations, and they could usefully be applied to other real-world feedback-oriented model (in)validation problems.

Bibliography

[BEGFB94] S. Boyd, L. El Ghaoui, E. Feron, and V. Balakrishnan. Linear matrix inequalities in system and control theory. *SIAM*, 1994.

[BN02] Anders Blomqvust and Ryozo Nagamune. Efficient convex optimization for engineering design. In *Proceedings of the 41st IEEE Conference on Decision and Control*, pages 2552–2557, 2002.

[Boy04] Stephen Boyd. EE363 Lecture 14: Linear matrix inequalities and the $\mathcal{S}$-procedure. Available on the Internet at http://www.stanford.edu/class/ee363/, Winter 2003-04.

[BP90] B. Bamieh and J.B. Pearson. A general framework for linear periodic systems with application to $\mathcal{H}_\infty$ sampled-data control. Technical Report 9021, Rice University, 1990.

[BVG94] S. Boyd, L. Vandenberghe, and M. Grant. Efficient convex optimization for engineering design. In *Proceedings IFAC Symposium on Robust Control Design*, pages 14–23, 1994.

[Can01] Michael Cantoni. On model reduction in the ν-gap metric. In *Proceedings of the 40th IEEE Conference on Decision and Control*, 2001.

[CG00] Jie Chen and Guoxiang Gu. *Control-Oriented System Identification: An $\mathcal{H}_\infty$ Approach*. Wiley, 2000.

[Col95] R. P. G. Collinson. *Introduction to Avionics*. Chapman & Hall, 1995.

[Cor02] Federico Corraro. Selected clearance criteria for HIRM+RIDE. In *Advanced Techniques for Clearance of Flight Control Laws*. Springer, 2002.

[CQ04] Li Chai and Li Qiu. Multirate periodic systems and constrained analytic interpolation problems (preprint). *Accepted for the SIAM Journal on Control and Optimization*, 2004.

[CW96] J. Chen and S. Wang. Validation onf linear fractional uncertainty models. *IEEE Transactions of Automatic Control*, 42:1822–1828, 1996.

[Dat00] P. Date. *Identification for Control: Deterministic Algorithms and Error Bounds*. PhD thesis, University of Cambridge, 2000.

[Dav96] R. A. Davis. *Model Validation for Robust Control*. PhD thesis, University of Cambridge, 1996.

[DFT92] John C. Doyle, Bruce A. Francis, and Allen R. Tannenbaum. *Feedback Control Theory*. Macmillan, 1992.

[Dic00] G. Dickman. Wide Envelope Model (WEM) Incorporation of Sensor Models, Uncertainties Model and CL002 Trim Capability. Technical Report BSE-PR-0003, Burnell Systems Engineering Limited, 2000.

[Dym89] Harry Dym. *J contractive matrix functions, reproducing kernel Hilbert spaces and interpolation*. The American Mathematical Society, 1989.

[FF90] Ciprian Foias and Arthur E. Frazho. *The Commutant Lifting Approach to Interpolation Problems*. Birkhäuser, 1990.

[FFGK91] Ciprian Foias, Arthur E. Frazho, I. Gohberg, and M.A. Kaashoek. *Metric Constrained Interpolation, Commutant Lifting and Systems*. Birkhäuser, 1991. (This book seems to be particularly difficult to get hold of and is not available in Cambridge. I was able to borrow a copy from the British Library.).

[GAR01] GARTEUR FM(AG11). The Harrier Wide Envelope Model (HWEM). Technical report, GARTEUR, 2001.

[Geo01] Tryphon T. Georgiou. Analytic interpolation and the degree constraint. *Int. J. Applied Mathematics and Computer Science*, 2001.

[GGLD90] M. Green, K. Glover, D. Limebeer, and J. Doyle. A J-spectral factorization approach to $\mathcal{H}_\infty$ control. *SIAMCTRL*, 28(6):1350–1371, Nov 1990.

[Hal02] Kelvin M. Halsey. *Nested feedback systems: analysis and design within an $\mathcal{H}_\infty$-loopshaping framework*. PhD thesis, University of Cambridge, 2002.

[HGS95] R.A. Hyde, K. Glover, and G.T. Shanks. VSTOL first flight of an $\mathcal{H}_\infty$ control law. *Comput. Control. Eng. J.*, 6(1):11–16, 1995.

[Hyd91] R.A. Hyde. *The application of robust control to VSTOL aircraft*. PhD thesis, University of Cambridge, 1991.

[Hyd00] R.A. Hyde. An $\mathcal{H}_\infty$ loop-shaping design for the VAAC Harrier. In *Flight Control Systems: practical issues in design and implementation*. The Institution of Electrical Engineers, 2000.

[Lju99a] Lennart Ljung. Model validation and model error modeling. Technical report, Department of Electrical Engineering, Linköping University, 1999.

[Lju99b] Lennart Ljung. *System Identification: Theory for the User*. Prentice Hall, 2nd edition, 1999.

[Mat00] The MathWorks, Inc. *MATLAB Optimization Toolbox Users' Guide version 2*. The MathWorks, Inc., 2000.

[MG90] D.C. McFarlane and K. Glover. *Robust controller design using normalized coprime factor plant descriptions*. Springer-Verlag, 1990.

[Pag96] F. Paganini. *Sets and Constraints in the Analysis of Uncertain Systems*. PhD thesis, California Institute of Technology, 1996.

[PKT+92] K. Poola, P. P. Kharonekar, A. Tikku, J. Krause, and K. M. Nagpal. A time-domain approach to model validation. In *Proceedings of the American Control Conference*, pages 313–317, 1992.

[PKT+94] K. Poola, P. P. Kharonekar, A. Tikku, J. Krause, and K. M. Nagpal. A time-domain approach to model validation. *IEEE Transactions on Automatic Control*, 39(5):951–959, May 1994.

[QD92] L. Qiu and E. J. Davison. Feedback stability under simultanous gap metric uncertainties in plant and conroller. In *Systems and Control Letters*, volume 18, pages 9–22, 1992.

[SD96] Roy S. Smith and Dullerud. Continuous-time control model validation using finite experimental data. In *IEEE Transactions on Automatic Control*, volume 41:8, pages 1094–1105, 1996.

[SDM00] Roy S. Smith, Geir Dullerud, and Scott A. Miller. Model validation for nonlinear feedback systems. In *Procedings of CDC 2000*, volume 1, pages 1232–1237, 2000.

[SDwn] Roy Smith and Geir Dullerud. Analysis of continuous-time robust control models using finite sampled, experimental data. Technical Report CCEC-95-0313, Dept of Electrical and Computer Engineering, University of California, Santa Barbara, publication date unknown.

[Ste01] John H. Steele. *Approximation and Validation of Models with Uncertainty: A closed-loop perspective*. PhD thesis, University of Cambridge, 2001.

[SV01] John H. Steele and Glenn Vinnicombe. Closed-loop time-domain model validation in the nu-gap metric. In *Proceedings of the 40th IEEE Conference on Decision and Control*, pages 4332–7, 2001.

[SV02] John Steele and Glenn Vinnicombe. The ν-gap metric and the generalised stability margin. In *Advanced Techniques for Clearance of Flight Control Laws*. Springer, 2002.

[Ver00] Sándor M. Veres. Self-tuning control by model unfalsification (part i). *International Journal of Control*, 73(17):1548–1559, 2000.

[VG94] Glenn Vinnicombe and Keith Glover. Best possible robustness results for $\mathcal{H}_\infty$ controllers, with applications to identification and model validation. Submitted to IEEE Transactions on Automatic Control, 1994.

[Vin01] Glenn Vinnicombe. *Uncertainty and Feedback: $\mathcal{H}_\infty$ loop-shaping and the ν-gap metric*. Imperial College Press, 2001.

[VW00] Sándor M. Veres and Derek S. Wall. *Synergy and Duality of Identification and Control*. Taylor and Francis, 2000.

[Yak77] V. A. Yakubovich. S-procedure in nonlinear control theory. In *Vestnik Leningrad Univ. Math.*, volume 4, pages 73–93, 1977.

[ZDG95] Kemin Zhou, John C. Doyle, and Keith Glover. *Robust and Optimal Control*. Prentice-Hall, 1995.

[Zho98] Kemin Zhou. *Essentials of Robust Control*. Prentice Hall, 1998.

Appendix A

Appendices to Chapter 4

Conditions for non-invalidation/validation in the ν-gap with $w_s = 0$

Proposition A.1 ([SV01]) *Given some nominal model P, noise sets $\mathbf{W}_u$ and $\mathbf{W}_y$ and a ν-gap radius β, there exist noise sequences $\begin{pmatrix} w_u \\ w_y \end{pmatrix} \in \mathbf{W}_u \times \mathbf{W}_y \cap \mathrm{gr}(M_{11})$, and a linear, time-invariant $\hat{P} \in \mathcal{P}_\nu(P, \beta)$ such that $w_y = \hat{P} * (u - w_u) + w_y$ if, but* not *only if, there exist sequences (w_s, w_t) such that $\begin{pmatrix} w_u \\ w_y \end{pmatrix} = \mathrm{ch}(M) * \begin{pmatrix} w_s \\ w_t \end{pmatrix} \in \mathbf{W}_u \times \mathbf{W}_y$ and*

$$0 \leq \begin{bmatrix} T_s^* T_s & T_t^* - T_{w_t}^* \\ T_t - T_{w_t} & I \end{bmatrix} \tag{A.1}$$

Proposition A.2 ([SV01]) *Given some nominal model P, noise sets $\mathbf{W}_u$ and $\mathbf{W}_y$ and a ν-gap radius β, there exist noise sequences $\begin{pmatrix} w_u \\ w_y \end{pmatrix} \in \mathbf{W}_u \times \mathbf{W}_y \cap \mathrm{gr}(M_{11})$, and a linear, time-varying $\hat{P} \in \mathcal{P}_\nu(P, \beta)$ such that $w_y = \hat{P} * (u - w_u) + w_y$ if, but* not *only if, there exist sequences (w_s, w_t) such that $\begin{pmatrix} w_u \\ w_y \end{pmatrix} = \mathrm{ch}(M) * \begin{pmatrix} w_s \\ w_t \end{pmatrix} \in \mathbf{W}_u \times \mathbf{W}_y$*

and

$$0 \leq \begin{bmatrix} (\Pi_k s)^* \Pi_k s - (\Pi_k w_s)^* \Pi_k s - (\Pi_k s)^* \Pi_k w_s & (\Pi_k (t - w_t))^* \\ \Pi_k (t - w_t) & I \end{bmatrix} \tag{A.2}$$

The graph condition follows since with $w_s = 0$, the chain scattering operation gives $w_u = M_{11} M_{21}^{-1} w_t$ and $w_y = M_{21} w_t$. Hence $w_u = M_{11} w_y$.

Theorem A.3 (Necessary and Sufficient Conditions for Invalidation[SV01]) *Given P, $\beta < b_{\text{opt}}(P)$ and data $z := \begin{pmatrix} y \\ u \end{pmatrix}$, if there exists a $\bar{P} \in \mathcal{P}_\nu(P, \beta)$ and a $\bar{w} := \begin{pmatrix} \bar{w}_y \\ \bar{w}_u \end{pmatrix}$ such that $z - \bar{w} \in \text{gr}(\hat{P})$ and $\|\bar{w}\|_2 \leq \alpha$, then there exists a $\hat{P} \in \mathcal{P}_\nu(P, \beta)$ and a $\hat{w} := \begin{pmatrix} \hat{w}_y \\ \hat{w}_u \end{pmatrix} \in \text{igr}(\hat{C})$ such that $z - \hat{w} \in \text{gr}(\hat{P})$ and $\|\hat{w}\|_2 \leq \frac{\alpha}{b_{\hat{P},\hat{C}}}$ for all controllers $\hat{C}$ achieving $b_{P,\hat{C}} > \beta$.*

This sufficient and necessary condition is achieved at a cost of a restriction in the class of possible noise constraints: we must use a two-norm bound on the *combined* input-output noise sets to take advantage of it.

Appendix B

Appendices to Chapter 5

This rather tedious material leads to the proofs of Theorem 5.5 and 5.6 from Chapter 5.

The 'Ruler' Lemmas

Intuition suggests that if a model is not corroborated by the first part of a data sequence, it will not be corroborated by the whole sequence. The following 'ruler' lemmas show that this remains true under the approximations used to form the sufficient non-validation conditions. (The 'ruler' nomenclature draws on the analogy that given k points on a piece of paper, it is impossible to draw a straight line through any subset of them, it will not be possible to draw a straight line through them all.)

Lemma B.1 (LTI 'Ruler' Lemma) *Given sequences* $\sigma \in \mathcal{S}^q_\ell, \tau \in \mathcal{S}^p_\ell, s \in \mathcal{S}^q_k, t \in \mathcal{S}^p_k$, *define*

$$\hat{s} = \{\sigma_0, \sigma_1, \ldots, \sigma_{\ell-1}, s_0, s_1, \ldots, s_{k-1}\} \tag{B.1}$$

$$\hat{t} = \{\tau_0, \tau_1, \ldots, \tau_{\ell-1}, t_0, t_1, \ldots, t_{k-1}\} \tag{B.2}$$

there exist sequences $w_\sigma, w_\tau \in \mathbf{W}_\sigma \times \mathbf{W}_\tau$ *and* $w_s, w_t \in \mathbf{W}_s \times \mathbf{W}_t$ *satisfying the*

sufficient condition for validation

$$\begin{bmatrix} T_{\hat{s}}^* T_{\hat{s}} + T_{\hat{s}}^* T_{w_{\hat{s}}} + T_{w_{\hat{s}}}^* T_{\hat{s}} & \left(T_{\hat{t}} + T_{w_{\hat{t}}}\right)^* \\ T_{\hat{t}} + T_{w_{\hat{t}}} & I_{p(\ell+k)} \end{bmatrix} \geq 0 \tag{B.3}$$

where $w_{\hat{s}} = \{w_\sigma, w_s\}$ *and* $w_{\hat{t}} = \{w_\tau, w_t\}$*, the sequences* w_σ *and* w_τ *will also satisfy*

$$\begin{bmatrix} T_\sigma^* T_\sigma + T_\sigma^* T_{w_\sigma} + T_{w_\sigma}^* T_\sigma & \left(T_\tau + T_{w_\tau}\right)^* \\ T_\tau + T_{w_\tau} & I_{p\ell} \end{bmatrix} \geq 0 \tag{B.4}$$

Proof. For convenience, write $T_{\hat{s}} = \begin{bmatrix} T_\sigma & 0 \\ M_{\hat{s}} & T_\sigma \end{bmatrix}$, $T_{\hat{t}} = \begin{bmatrix} T_\tau & 0 \\ M_{\hat{t}} & T_\tau \end{bmatrix}$, $T_{\hat{ws}} = \begin{bmatrix} T_{w_\sigma} & 0 \\ N_{\hat{s}} & T_{w_\sigma} \end{bmatrix}$ and $T_{\hat{w}_t} = \begin{bmatrix} T_{w_\tau} & 0 \\ N_{\hat{t}} & T_{w_\tau} \end{bmatrix}$. Let $Q_{11} = T_{\hat{s}}^* T_{\hat{s}} + T_{\hat{s}}^* T_{w_{\hat{s}}} + T_{w_{\hat{s}}}^* T_{\hat{s}}$ and $Q_{21} = T_{\hat{t}} + T_{w_{\hat{t}}}$. (B.3) can thus be re-written

$$\begin{bmatrix} Q_{11} & Q_{21}^* \\ Q_{21} & I_{p(\ell+k)} \end{bmatrix} \geq 0$$

Substituting for the lower block Toeplitz matrices gives

$$Q_{11} = \begin{bmatrix} P_{11} + M_{\hat{s}}^* M_{\hat{s}} + M_{\hat{s}}^* N_{\hat{s}} + N_{\hat{s}}^* M_{\hat{s}} & \left(T_\sigma^* M + T_\sigma^* N_{\hat{s}} + T_{w_\sigma}^* M\right)^* \\ T_\sigma^* M + T_\sigma^* N_{\hat{s}} + T_{w_\sigma}^* M & P_{11} \end{bmatrix}$$

where $P_{11} = T_\sigma^* T_\sigma + T_\sigma^* T_{w_\sigma} + T_{w_\sigma}^* T_\sigma$ or, for simplicity,

$$Q_{11} = \begin{bmatrix} A & B^* \\ B & P_{11} \end{bmatrix}$$

similarly,

$$Q_{21} = \begin{bmatrix} P_{21} & 0 \\ C & P_{21} \end{bmatrix}$$

where $P_{21} = T_\sigma + T_{w_\sigma}$ and $C = M_{\hat{t}} + N_{\hat{t}}$. Thus (B.3) can be re-written

$$\begin{bmatrix} A & B^* & P_{21}^* & C^* \\ B & P_{11} & 0 & P_{21}^* \\ P_{21} & 0 & I & 0 \\ C & P_{21} & 0 & I \end{bmatrix} \geq 0$$

Clearly, this is only true if

$$\begin{bmatrix} P_{11} & P_{21}^* \\ P_{21} & I \end{bmatrix} \geq 0$$

This is gives (B.4), as desired. □

Corollary B.2 *Given sequences $s \in \mathcal{S}_k^q, t \in \mathcal{S}_k^p, \sigma \in \mathcal{S}_\ell^q, \tau \in \mathcal{S}_\ell^p$ and $\hat{s}, \hat{t}$ as defined by (B.1) and (B.2), there exist sequences $w_\sigma, w_\tau \in \mathbf{W}_\sigma \times \mathbf{W}_\tau$ and $w_s, w_t \in \mathbf{W}_s \times \mathbf{W}_t$ satisfying (B.3) only if there exist $w'_\sigma, w'_\tau \in \mathbf{W}_\sigma \times \mathbf{W}_\tau$ satisfying (B.4).*

Proof. This follows trivially from Lemma B.1, since any w_σ and w_τ satisfying (B.3) *must* also satisfy (B.4). □

Lemma B.3 (LTV 'Ruler' Lemma) *Given sequences $\sigma \in \mathcal{S}_\ell^q, \tau \in \mathcal{S}_\ell^p, s \in \mathcal{S}_k^q, t \in \mathcal{S}_k^p$, define $\hat{s}$ and $\hat{t}$ as in (B.1) and (B.2). Then there exist sequences $w_\sigma, w_\tau \in \mathbf{W}_\sigma \times \mathbf{W}_\tau$ and $w_s, w_t \in \mathbf{W}_s \times \mathbf{W}_t$ satisfying the LTV sufficient condition for validation*

$$\begin{bmatrix} (\Pi_j \operatorname{vec} \hat{s})^* (\Pi_j \operatorname{vec} \hat{s}) + (\Pi_j \operatorname{vec} \hat{s})^* (\Pi_j \operatorname{vec} w_{\hat{s}}) + (\Pi_j \operatorname{vec} w_{\hat{s}})^* (\Pi_j \operatorname{vec} \hat{s}) & \left(\Pi_j \operatorname{vec} \hat{t} + \Pi_j \operatorname{vec} w_{\hat{t}}\right)^* \\ \Pi_j \operatorname{vec} \hat{t} + \Pi_j \operatorname{vec} w_{\hat{t}} & I_{pj} \end{bmatrix} \geq 0 \quad \text{(B.5)}$$

for all $j \in \{1, 2, \ldots, \ell + k\}$, where $w_{\hat{s}} = \{w_\sigma, w_s\}$ and $w_{\hat{t}} = \{w_\tau, w_t\}$, the sequences w_σ and w_τ will also satisfy

$$\begin{bmatrix} (\Pi_j \operatorname{vec} \sigma)^* (\Pi_j \operatorname{vec} \sigma) + (\Pi_j \operatorname{vec} \sigma)^* (\Pi_j \operatorname{vec} w_\sigma) + (\Pi_j \operatorname{vec} w_\sigma)^* (\Pi_j \operatorname{vec} \sigma) & (\Pi_j \operatorname{vec} \tau + \Pi_j \operatorname{vec} w_\tau)^* \\ \Pi_j \operatorname{vec} \tau + \Pi_j \operatorname{vec} w_\tau & I_{pj} \end{bmatrix} \geq 0 \quad \text{(B.6)}$$

for all $j \in \{1, 2, \ldots, \ell\}$.

Proof. This is much simpler than the LTV case since (B.6) is obvious from (B.5). □

Corollary B.4 *Given sequences $s \in \mathcal{S}_k^q, t \in \mathcal{S}_k^p, \sigma \in \mathcal{S}_\ell^q, \tau \in \mathcal{S}_\ell^p$ and $\hat{s}, \hat{t}$ as defined by (B.1) and (B.2), there exist sequences $w_\sigma, w_\tau \in \mathbf{W}_\sigma \times \mathbf{W}_\tau$ and $w_s, w_t \in \mathbf{W}_s \times \mathbf{W}_t$ satisfying (B.5) only if there exist $w'_\sigma, w'_\tau \in \mathbf{W}_\sigma \times \mathbf{W}_\tau$ satisfying (B.6).*

Proof. This follows trivially from Lemma B.3, since any w_σ and w_τ satisfying (B.5) *must* also satisfy (B.6). □

The Zero Signal Lemmas

The following Lemmas show that given zero sequences, the sufficient validation conditions are only satisfied when w_t is the zero sequence.

Lemma B.5 (LTI Zero Signal Lemma) *Given sequences $s \in \mathcal{S}_k^q, t \in \mathcal{S}_k^p$ such that $s = \{0, 0, \ldots, 0\}$ and $t = \{0, 0, \ldots, 0\}$, the sufficient condition for validation*

$$\begin{bmatrix} T_s^* T_s + T_s^* T_{w_s} + T_{w_s}^* T_s & (T_t + T_{w_t})^* \\ T_t + T_{w_t} & I \end{bmatrix} \geq 0 \tag{B.7}$$

is satisfied if and only if $w_t = \{0, 0, \ldots, 0\}$.

Proof. Substituting $s = t = \{0, 0, \ldots, 0\}$ in (B.7) gives

$$\begin{bmatrix} 0 & T_{w_t}^* \\ T_{w_t} & I \end{bmatrix} \geq 0$$

By the Schur complement, this is positive semidefinite if and only if $-T_{w_t}^* T_{w_t} \geq 0$. It is clear that this is only true if $w_t = \{0, 0, \ldots, 0\}$. □

Lemma B.6 (LTV Zero Signal Lemma) *Given sequences $s \in \mathcal{S}_k^q, t \in \mathcal{S}_k^p$ such*

that $s = \{0, 0, \ldots, 0\}$ *and* $t = \{0, 0, \ldots, 0\}$*, the sufficient condition for validation*

$$\begin{bmatrix} (\Pi_j \operatorname{vec} s)^* + (\Pi_j \operatorname{vec} s) + (\Pi_j \operatorname{vec} w_s)^* + (\Pi_j \operatorname{vec} s) + (\Pi_j \operatorname{vec} s)^* + (\Pi_j \operatorname{vec} w_s) & (\Pi_j \operatorname{vec} t + \Pi_j \operatorname{vec} w_t)^* \\ (\Pi_j \operatorname{vec} t + \Pi_j \operatorname{vec} w_t) & I \end{bmatrix} \geq 0 \quad \text{(B.8)}$$

for all $j \in \{0, 1, \ldots, k\}$ *is satisfied if and only if* $w_t = \{0, 0, \ldots, 0\}$*.*

Proof. Substituting $s = t = \{0, 0, \ldots, 0\}$ in (B.8) gives

$$\begin{bmatrix} 0 & (\Pi_j \operatorname{vec} w_t)^* \\ \Pi_j \operatorname{vec} w_t & I \end{bmatrix} \geq 0$$

for all $j \in \{0, 1, \ldots, k\}$. By the Schur complement, this is positive semidefinite for any j if and only if $-(\Pi_j \operatorname{vec} w_t)^* (\Pi_j \operatorname{vec} w_t) \geq 0$. It is clear that this is only true if w_t is the zero sequence. □

Remark B.7 It is worth noting that w_s is unconstrained by the validation conditions of Lemmas B.5 and B.6. ♡

Final Preliminaries

The following simple lemmas will also be useful they show that a positive semidefinite matrix whose bottom right-hand term is zero must have zero terms on the minor diagonal and show that providing that $x(0) \neq 0$, $T_x^* T_y = 0$ implies that y is a zero sequence.

Lemma B.8 *Given* $M \in \mathbb{C}^{m \times m}$ *and* $N \in \mathbb{C}^{n \times m}$*, if*

$$\begin{bmatrix} M & N^* \\ N & 0 \end{bmatrix} \geq 0 \quad \text{(B.9)}$$

then $M \geq 0$ *and* $N = 0$*.*

Proof. (B.9) is equivalent to stating that for all combinations of $z_1 \in \mathbb{C}^m$ and $z_2 \in \mathbb{C}^n$

$$\begin{bmatrix} z_1^* & z_2^* \end{bmatrix} \begin{bmatrix} M & N^* \\ N & 0 \end{bmatrix} \begin{bmatrix} z_1 \\ z_2 \end{bmatrix} = z_1^* M z_1 + 2\,\mathrm{Re}\,\{z_2^* N z_1\} \geq 0$$

Considering the case when $z_2 = 0$, it is clear that $M \geq 0$. That $N = 0$ may be seen by noting that if $N \neq 0$ the expression can always be made negative by choosing z_1 and z_2 such that $z_2^* N z_1 < 0$ and making z_2 arbitrarily large and of appropriate sign. □

Lemma B.9 *Given $x \in \mathcal{S}_k^p$ and $y \in \mathcal{S}_k^q$, if $T_x^* T_y = 0$, $y_i = 0\ \forall i$ if $x_0 \neq 0$.*

Proof.

$$T_x^* T_y = \begin{bmatrix} \sum_{i=0}^{k-1} x_i^* y_i & \sum_{i=0}^{k-2} x_{i+1}^* y_i & \cdots & x_{k-1}^* y_0 \\ \sum_{i=0}^{k-2} x_i^* y_{i+1} & \sum_{i=0}^{k-2} x_i^* y_i & & x_{k-2}^* y_0 \\ \vdots & & \ddots & \vdots \\ x_0^* y_{k-1} & x_0^* y_{k-2} & \cdots & x_0^* y_0 \end{bmatrix}$$

It is clear from the last row of the matrix that if $x_0 \neq 0$ $T_x^* T_y$ will only be the zero matrix if all $y_i = 0$. □

Proof of Theorem 5.5 (page 73). By Lemma B.1 any w_σ and w_τ satisfying (5.10) will also satisfy

$$\begin{bmatrix} T_\sigma^* T_\sigma + T_\sigma^* T_{w_\sigma} + T_{w_\sigma}^* T_\sigma & T_\tau^* + T_{w_\tau}^* \\ T_\tau + T_{w_\tau} & I \end{bmatrix} = \begin{bmatrix} 0 & T_{w_\tau}^* \\ T_{w_\tau} & I \end{bmatrix} \geq 0$$

By Lemma B.5, this is true if and only if $w_\tau = \{0, 0, \ldots, 0\}$. Write $T_{\hat{s}} = \begin{bmatrix} 0 & 0 \\ T_s & 0 \end{bmatrix}$, $T_{\hat{t}} = \begin{bmatrix} 0 & 0 \\ T_t & 0 \end{bmatrix}$, $T_{w_{\hat{s}}} = \begin{bmatrix} T_{w_\sigma} & 0 \\ T_{w_\sigma} + U_{w_\sigma} & T_{w_\sigma} \end{bmatrix}$ and $T_{w_{\hat{t}}} = \begin{bmatrix} 0 & 0 \\ T_{w_t} & 0 \end{bmatrix}$ where

$$U_{w_\sigma} := \begin{bmatrix} 0 & w_\sigma(\ell-1) & w_\sigma(\ell-2) & \cdots & w_\sigma(1) \\ 0 & 0 & w_\sigma(\ell-1) & \cdots & w_\sigma(2) \\ \vdots & \vdots & \ddots & \ddots & \vdots \\ 0 & 0 & \cdots & 0 & w_\sigma(\ell-1) \\ 0 & 0 & \cdots & 0 & 0 \end{bmatrix}$$

Thus (5.10) is equivalent to

$$\begin{bmatrix} P_{11} + U_{w_\sigma}^* T_s + T_s^* U_\sigma & T_s^* T_{w_\sigma} & 0 & P_{21}^* \\ T_{w_\sigma}^* T_s & 0 & 0 & 0 \\ 0 & 0 & I & 0 \\ P_{21} & 0 & 0 & I \end{bmatrix} \geq 0$$

where $P_{11} = T_s^* T_s + T_{w_s}^* T_s + T_{w_s}^* T_s$ and $P_{21} = T_t + T_{w_t}$. By the Schur complement, this is true if and only if

$$\begin{bmatrix} P_{11} - P_{21}^* P_{21} + U_{w_\sigma}^* T_s + T_s^* U_\sigma & T_s^* T_{w_\sigma} \\ T_{w_\sigma}^* T_s & 0 \end{bmatrix} \geq 0$$

By Lemma B.8, $T_s^* T_{w_\sigma} = 0$. By Lemma B.9 this is true if and only if $w_\sigma = \{0, 0, \ldots, 0\}$. Noting that $U_{w_\sigma} = 0$, the constraint is equivalent to

$$\begin{bmatrix} P_{11} - P_{21}^* P_{21} & 0 \\ 0 & 0 \end{bmatrix} \geq 0$$

this is true if and only if the top left partition is positive semidefinite. By the Schur complement, this is true if and only if

$$\begin{bmatrix} P_{11} & P_{21}^* \\ P_{21} & 0 \end{bmatrix} \geq 0$$

Thus (5.10) and (5.11) are equivalent. □

Proof of Theorem 5.6 (page 74). By Lemma B.3 any w_σ and w_τ satisfying (5.12) will also satisfy

$$\begin{bmatrix} 0 & (\Pi_j \operatorname{vec} w_\tau)^* \\ (\Pi_j \operatorname{vec} w_t) & I \end{bmatrix} \geq 0$$

By Lemma B.6, this is true if and only if w_τ is the zero sequence. Write $\operatorname{vec} \hat{s} = \begin{bmatrix} 0 \\ \operatorname{vec} s \end{bmatrix}$, $\operatorname{vec} \hat{t} = \begin{bmatrix} 0 \\ \operatorname{vec} t \end{bmatrix}$, $\operatorname{vec} \hat{w}_s = \begin{bmatrix} \operatorname{vec} w_\sigma \\ \operatorname{vec} w_s \end{bmatrix}$ and $\operatorname{vec} \hat{w}_t = \begin{bmatrix} 0 \\ \operatorname{vec} w_t \end{bmatrix}$.

Thus when $j > \ell$, (5.12) becomes

$$\begin{bmatrix} P_{11} & 0 & P_{21}^* \\ 0 & I & 0 \\ P_{21} & 0 & I \end{bmatrix} \geq 0$$

for all $j' \in \{1, 2, k\}$, where $P_{11} = (\Pi_{j'} \operatorname{vec} s)^* (\Pi_{j'} \operatorname{vec} s) + (\Pi_{j'} \operatorname{vec} s)^* (\Pi_{j'} \operatorname{vec} w_s) + (\Pi_{j'} \operatorname{vec} w_s)^* (\Pi_{j'} \operatorname{vec} s)$ and $P_{21} = (\Pi_{j'} \operatorname{vec} t) + (\Pi_{j'} \operatorname{vec} w_t)$. By the Schur complement this is true if and only if

$$P_{11} - \begin{bmatrix} 0 & P_{21}^* \end{bmatrix} \begin{bmatrix} I & 0 \\ 0 & I \end{bmatrix} \begin{bmatrix} 0 \\ P_{21} \end{bmatrix} = P_{11} - P_{21}^* P_{21} \geq 0$$

which again by the Schur complement is true if and only if

$$\begin{bmatrix} P_{11} & P_{21}^* \\ P_{21} & I \end{bmatrix} \geq 0$$

Thus (5.12) and (5.13) are equivalent. □

Appendix C

Appendices to Chapter 6

Validation with noncausal perturbation blocks

Theorem C.1 *Given $u \in \mathcal{S}_k^q$, $y \in \mathcal{S}_k^p$, there exists a an infinite contractive matrix $\Delta_{\mathrm{U}\infty}$ such that*

$$\operatorname{vec} y = (\Pi_k \Delta_{\mathrm{U}\infty}) \operatorname{vec} u$$

if and only if

$$\|y\|_2 \leq \|u\|_2$$

Proof. *If.* The solution

$$\Delta_{\mathrm{U}\infty} = \frac{1}{\|u\|_2^2} \begin{bmatrix} \operatorname{vec} y \, (\operatorname{vec} u)^* & \mathbf{0} \\ \mathbf{0} & \mathbf{0} \end{bmatrix}$$

gives $(\Pi_k \Delta_{\mathrm{U}_\infty}) \operatorname{vec} u = \operatorname{vec} y$. It is clear that

$$\Delta_{\mathrm{U}_\infty} = \frac{1}{\|u\|_2^2} \|\operatorname{vec} y \, (\operatorname{vec} u)^*\| \leq \frac{\|u\|_2}{\|y\|_2} \leq 1$$

as required.

Only if. It is clear that

$$\left\| \begin{pmatrix} \operatorname{vec} y \\ \mathbf{r} \end{pmatrix} \right\|_2 \leq \overline{\sigma}(\Delta_{\mathrm{U}\infty}) \left\| \begin{pmatrix} \operatorname{vec} u \\ \mathbf{0} \end{pmatrix} \right\|_2$$

Since $\Delta_{\mathrm{U}\infty}$ is contractive, $\overline{\sigma}(\Delta_{\mathrm{U}\infty}) \leq 1$. Thus,

$$\|\operatorname{vec} y\|_2^2 + \|\operatorname{vec} r\|_2^2 \leq \|\operatorname{vec} u\|_2^2 + \|\mathbf{0}\|_2^2$$

Which gives $\|\operatorname{vec} y\|_2^2 \leq \|\operatorname{vec} u\|_2^2$, i.e. $\|y\|_2 \leq \|u\|_2$ as desired. □

Corollary C.2 *Given $u \in \mathcal{S}_k^q$, $y \in \mathcal{S}_k^p$, and $\gamma \geq 0$ there exists a an infinite matrix $\Delta_{\mathrm{U}\infty}$ with $\|\Delta_{\mathrm{U}\infty}\| \leq \gamma$ such that*

$$\operatorname{vec} y = (\Pi_k \Delta_{\mathrm{U}\infty}) \operatorname{vec} u$$

if and only if

$$\|y\|_2 \leq \gamma \|u\|_2$$

Proof. This follows trivially from Theorem C.1 by substituting $u_1 = \gamma u$.

□

Appendix D

Appendices to Chapter 7

Briefing sheet from Flight 1858

The briefing sheets for Flight 1858 (supplied by QinetiQ) are reproduced on the following pages.

VAAC HARRIER FLIGHT RECORD SHEET

General Information

Flight Id	1857 1858	Date	13-12-01	Cost Code	154 888 - 0001
Flight Task	In-flight Stability inquiries (Yaw) / Data collection for model validation				
Crew (FC)	Parker			Desk Operator 1	D'Mello
Crew (RC)	Lewis			Desk Operator 2	Hayhurst
S/W Config:	427			CLC SW ID	P234M1

Flight Information

	1	2	3	4	5	6	7	8	9
Take Off Time	14:54	15:35							
Land Time									

Switch Positions during Sortie

TP	1	2	3	4	5	6	7	8	9
Telemetry Group									
RSW 2									
RSW 3									

Meteorological Information

QFE	1023 mb	Cloud Cover	1 @ 1,800 ft	
QNH	1038 mb		4 @ 4500 ft	
Wind Dir/Speed	030° / 3 kts		@ ft	
Visibility	18 km.		@ ft	
R/W	05	OAT	+6 °C	
TL		FL	3K ft	

Flight Data

Flight Data Collected	Yes/No		Useful Telephone Numbers	
CLC Data Collected	Yes/No		MET 2131	
Video On	Yes/No		TOWER 2114	
Pic in Pic Mode	HUD / Ckpt / None		HANGAR 3200	

Comments

Nozzle temp over limit - check nozzle servo (Nozzles aft)

Continued Overleaf

1858

Flight No. 1859

18th December, 2001.

Harrier XW175 Briefing Sheet

Objectives: In-flight stability metric (γ_{TV}) / Data collection for model validation.

FCS Configuration: **427** (see 703X)

Briefing:

- The "**INST. MASTER**" switch in the rear cockpit MUST be turned ON after engine start and must be left on for the duration of ALL flights (whether FCS engaged or not).
- Telemetry and continuous voice may be used.
- The VAAC FCS can be engaged during this flight.
- Communications between the aircraft and the ground will be on **VHF 118.75MHz**.
- Telemetry call sign is "*TELEMETRY*".

Limitations:

- **During flight with FCS ON, if the 'FC' / 'RC' port coaming lamps flash (1s period), disengage FCS (if necessary) and turn FCS OFF.**
- The FCS engagement process may only be carried out when VFR.
- FCS-engaged flight may not be conducted when IMC below 1000ft.
- Safety Pilot must select HUD STANDBY mode during FCS reboots.

A	After start up	* **INST. MASTER ON** **TELEMETRY ON** **HEIM ON** **INS ON** **FCS ON**
	INS Alignment	After HDD boots, select **GC ALIGN** HDD 5 field display shows HIGGER GPS status as "a b c d e" Where: **a** = HIGGER figure of merit (**1**, good to 9,bad) **b** = GPS filter type **c** = Actual **Differential** Mode (3 = relative) **d** = Actual Receiver Mode (2 = Nav) **e** = Key In Use (1 = in use) A counter on the HDD will count erratically upwards to show alignment progress. When align is complete HDD will clear align screen. Wait for "***Fuel Wt***" Display (Top)
		☛UTILS ☛COAM (Lamp Test).
	Check HIGGER	☛RSW2 ☛1 (HIGGER status display) Check HDD 5 field display digit "a" is 1 or 2 and digit "e" is 1
B	FCS cockpit check	Perform VAAC FCS cockpit check with DH (flap down). Select **FLAP UP** in rear cockpit.
	Select Control Law	☛MENU ☛SLOT SEL ☛SLOT 7 Confirm software version string shows "***P23GM1***" displayed.

Flight No. 1859

5	210 KIAS 3.5° AOA	☛MENU ☛UTILS ☛RSW3 ☛2	Chirp on pitch demand.
		Trim a/c straight & level	
		☛MODE 6	Set "Trial Running" flag
		Wait >10 sec	
		☛MODE 1	Set "Manoeuvre" flag
		☛MODE7	Start Chirp.
		After 20 secs, when "Pitch F/L" coaming lamp lights continuously -	
		☛MODE7	Stop Chirp.
		Wait >10 sec	
		☛MODE 6	Reset "Trial Running" flag
		☛MODE 1	Reset "Manoeuvre" flag
		Note reading on HUD "Mach No." display.	
6	210 KIAS 3.5° AOA	☛MENU ☛UTILS ☛RSW3 ☛5	Chirp on Tailplane demand.
		Repeat procedure as for TEST POINT 5	
end		Datalogging OFF (☛LOG)	

Flight No. 1859

F	Shutdown	Shut down Head Down Display ☛Exit HDD ☛9 Wait for "Shutdown Complete ..." screen. **RECORD OFF** **FCS OFF** **INS OFF** **HEIM OFF** **IMPORTANT:** Wait at least 10 seconds **TELEMETRY OFF** **INST MASTER OFF**

G W D'Mello
18th December, 2001

Aircraft Captain

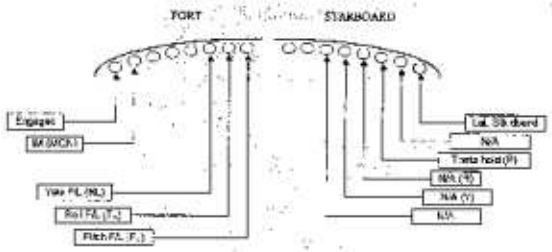

MODES

1	'Manoeuvre' flag
2	Pitch Law bank compensation INHIBIT
3-5	No function
6	'Trial Running' flag
7	Chirp start/stop
8-10	No function

RSW3 =	1	Normal operation
	2	Chirp → Pitch demand
	3	Chirp → Roll demand
	4	Chirp → Yaw demand
	5	Chirp → Tailplane
	6	Chirp → Ailerons
	7	Chirp → Rudder

VGs	30	Chirp START freq (Hz)
	31	Chirp Time to freq F1 (x10sec)
	32	Chirp freq F1 (Hz)
	33	Chirp Ampl (x0.1 or x1)

HWEM: Notes on trimming

The HWEM was trimmed on true air speed speed in knots, `VTKT`, and altitude in feet, `H`, using the values given in Table 7.1. Modified forms of the supplied trimming scripts were used. The nozzle angle `ANOZZ` was set to zero. Following advice from QinetiQ, the weight, `W`, was assumed to be 18 500 lbs.

Trimming away from the conditions supplied in `wemsimics170` was carried out in small increments. It was not possible to simultaneously obtain the exact values of α and V_{T} desired, but it was possible to get a close match (Table D.1).

The open-loop 'trim plots' for Test Points 1 and 2 are shown in Figures D.1 and D.2 respectively. It can be seen that the models are well-trimmed, increasing confidence that the trimming routines have been applied correctly.

	α (Table 7.1)	Achieved `ALFAD`
Test Point 1	4.3 deg	4.1 deg
Test Point 2	4.0 deg	4.0 deg

Table D.1: Angles of incidence achieved in trimming

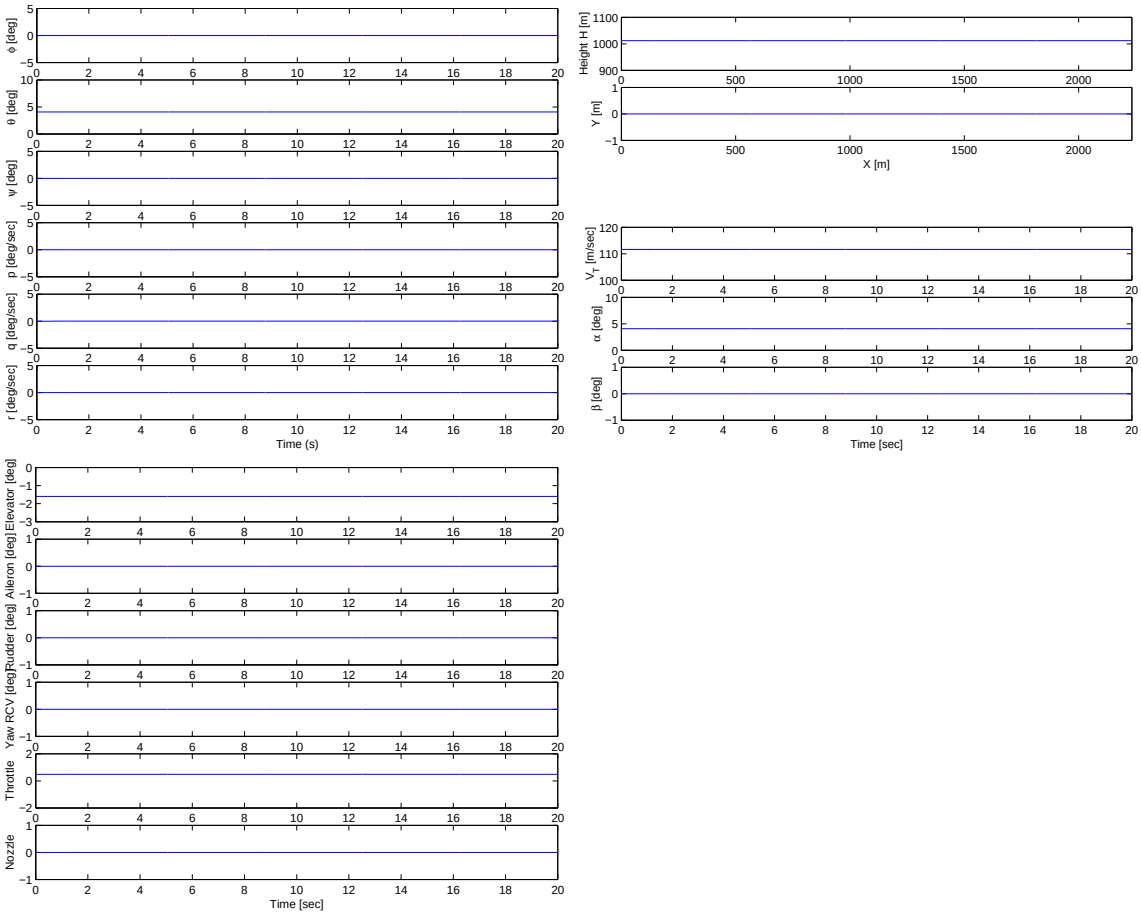

Figure D.1: Open-loop trim plots for HWEM at Test Point 1

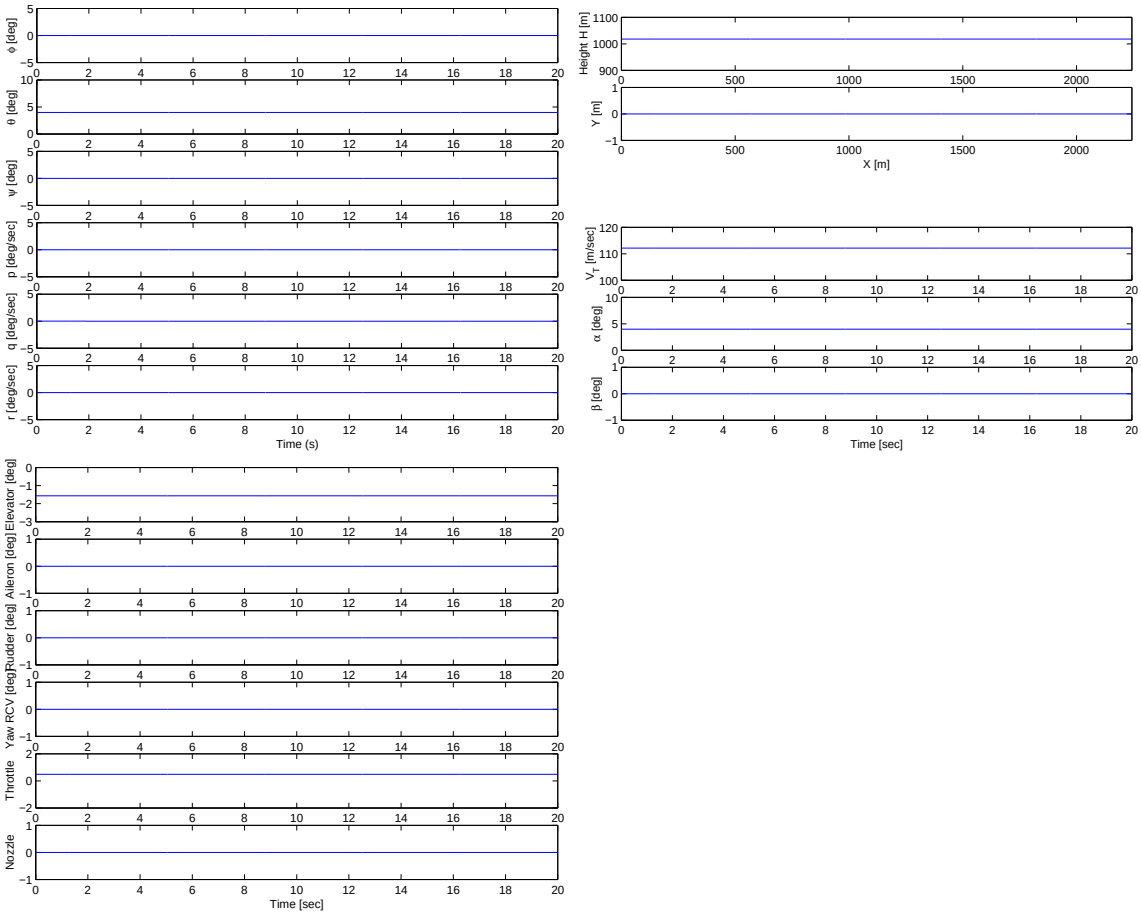

Figure D.2: Open-loop trim plots for HWEM at Test Point 2

Controller linearization

For optimal stability weighting, a linearized version of the longitudinal part of CL002 was required. A simplified block diagram was created, noting the following:

- the pitch-attitude functionality can be eliminated, since the air speed during flight tests was close to 200 knots and the undercarriage was in.
- the flap and nozzle angles were constant. The corresponding cross-feeds have a proportional effect on the output, so they will produce constant offsets in the controller output. This they may also be eliminated.
- The bank angle ϕ was more-or-less zero since the tests took place during straight-and-level flight. The bank angle compensation pitch rate, q_{comp} ([Dic00][page 16]) is given by

$$q_{\text{comp}} = \left(\frac{180}{\pi}\right) \frac{g \cos\gamma}{V_{\text{T}}} \left(\frac{1}{\cos\phi} - \cos\phi\right) = \left(\frac{180}{\pi}\right) \frac{g \cos\gamma}{V_{\text{T}}} \cos\phi \tan\phi$$

  With $\gamma \approx 0$ and $\phi \approx 0$, $\cos\gamma \approx 1$ and $\cos\phi \approx 1$ and $\tan\phi \approx \phi$ and this approximates for small values of ϕ to

$$q_{\text{comp}} \approx \left(\frac{180}{\pi}\right) \frac{g}{V_{\text{T}}} \phi$$

  A small change in ϕ will result in a correspondingly small q_{comp}. However, for the purpose of stability analysis, it will be assumed that $\phi = 0$ and the longitudinal and lateral dynamics are wholly decoupled.

The simplified controller is shown in Figure D.3. Like the HWEM, it is trimmed on altitude and true air speed. This is contains the simplifications above. The original model used indicated air speed as its input, it has been necessary to deduce this from the true air speed and the height. (See page 180.) The look-up tables are defined in WEMSIM's `const002.m` script, and the model is easily linearized using MATLAB's `linmod` command.

Numerical values for plant and controller models

Test Point 1

Plant:

$$\begin{bmatrix} \dot{u} \\ \dot{w} \\ \dot{q} \\ \dot{\theta} \end{bmatrix} = \begin{bmatrix} -0.0327 & 0.0549 & -7.8604 & -9.7819 \\ -0.1570 & -0.4938 & 110.4550 & -0.6967 \\ -0.0106 & -0.0279 & -0.5988 & 0 \\ 0 & 0 & 1 & 0 \end{bmatrix} \begin{bmatrix} u \\ w \\ q \\ \theta \end{bmatrix} + \begin{bmatrix} 0.3538 \\ -4.9712 \\ -3.6716 \\ 0 \end{bmatrix} \eta$$

where u, w, q, θ are the usual longitudinal states and η is the tailplane angle.

Transfer function from tailplane angle to pitch rate:

$$P(s) := \frac{q(s)}{\eta(s)} = \frac{-3.6716s(s+0.4376)(s+0.05219)}{(s+0.062)(s-0.04601)(s^2+1.109s+3.32)}$$

The linearized controller has state-space representation:

$$\left[\begin{array}{c} \dot{x}_1 \\ \hline \dot{x}_2 \\ \hline \eta_{\mathrm{c}} \end{array}\right] = \left[\begin{array}{cc|cc} -0.43478 & 0 & -7.5 & 0 \\ 0 & 0 & 2.3659 & 0.31546 \\ \hline -0.55626 & 1 & 3.2505 & 0.4334 \end{array}\right] \left[\begin{array}{c} x_1 \\ \hline x_2 \\ \hline q_{\mathrm{stk}} \\ \hline q \end{array}\right]$$

where the pitch rate demand q_{stk}, pitch rate q and tailplane angle demand η_{c} are in degrees. Separating this into 'feed-forward' and 'feedback' terms:

$$\bar{\eta}_{\mathrm{c}}(s) = C_{q_{\mathrm{stk}}}(s)\,\bar{q}_{\mathrm{stk}}(s) + C_q(s)\,\bar{q}(s)$$

Gives

$$C_{q_{\rm stk}}(s) = \frac{3.2505(s+2.309)(s+0.1371)}{s(s+0.4348)} = \left[\begin{array}{cc|c} -0.43478 & 0 & -7.5 \\ 0 & 0 & 2.3659 \\ \hline -0.55626 & 1 & 3.2505 \end{array}\right]$$

and

$$C_q(s) = 0.4334 + \frac{0.7279}{s} = \left[\begin{array}{c|c} 0 & 0.31546 \\ \hline 1 & 0.4334 \end{array}\right]$$

Test Point 2

Plant:

$$\begin{bmatrix} \dot{u} \\ \dot{w} \\ \dot{q} \\ \dot{\theta} \end{bmatrix} = \begin{bmatrix} -0.0320 & 0.0542 & -7.7120 & -9.7830 \\ -0.1569 & -0.4955 & 110.9774 & -0.6805 \\ -0.0106 & -0.0280 & -0.6011 & 0 \\ 0 & 0 & 1 & 0 \end{bmatrix} \begin{bmatrix} u \\ w \\ q \\ \theta \end{bmatrix} + \begin{bmatrix} 0.3486 \\ -5.0150 \\ -3.7035 \\ 0 \end{bmatrix} \eta$$

Transfer function from tailplane angle to pitch rate:

$$P_q(s) := \frac{-3.7035s(s+0.4395)(s+0.05106)}{(s+0.06129)(s-0.04592)(s^2+1.113s+3.35)}$$

The linearized controller is

$$\left[\begin{array}{c} \dot{x}_1 \\ \hline \dot{x}_2 \\ \hline \eta_{\rm c} \end{array}\right] = \left[\begin{array}{cc|cc} -0.43478 & 0 & -7.5 & 0 \\ 0 & 0 & 2.321 & 0.30947 \\ \hline -0.55973 & 1 & 3.2116 & 0.42821 \end{array}\right] \left[\begin{array}{c} x_1 \\ \hline x_2 \\ \hline q_{\rm stk} \\ q \end{array}\right]$$

Where the pitch rate demand $q_{\rm stk}$, pitch rate q and tailplane angle $\eta_{\rm c}$ are in degrees.

Separating this into 'feed-forward' and 'feedback' terms:

$$\bar{\eta}_{\rm c}(s) = C_{q_{\rm stk}}(s)\,\bar{q}_{\rm stk}(s) + C_q(s)\,\bar{q}(s)$$

gives

$$C_{q_{\text{stk}}}(s) = \frac{3.2116(s+2.33)(s+0.1349)}{s(s+0.4348)} = \left[\begin{array}{cc|c} -0.43478 & 0 & -7.5 \\ 0 & 0 & 2.321 \\ \hline -0.55973 & 1 & 3.2116 \end{array}\right]$$

and

$$C_q(s) = 0.42821 + \frac{0.7227}{s} = \left[\begin{array}{c|c} 0 & 0.30947 \\ \hline 1 & 0.42821 \end{array}\right]$$

Conversion from V_{T} to V_{C}

There are three 'air speeds' in common usage:

- **True air speed, V_{T}.** This is the actual speed of the aircraft.
- **Calibrated Air Speed, V_{C}.** This is the speed of the aircraft measured, e.g. by a pitot tube installation and corrected for any errors in the instrument. At sea level, it is the same as the true air speed. However, as altitude increases, the atmosphere thins and an aircraft travelling at a given speed will experience a lower impact pressure, giving rise to a reading lower than the true air speed.
- **Indicated Air Speed.** This is essentially the same quantity as the true air speed but is not corrected for sensor errors. (Sources at QinetiQ say that the error in the VAAC Harrier is not usually significant, so the indicated air speed has been assumed equal to the calibrated air speed.)

It is rare in practice to convert directly between calibrated air speed V_{C} and true air speed V_{T} air speed; on board an aircraft, the calculations are more efficiently performed using the scheme shown in Figure D.4.

In cases where it is absolutely necessary to convert directly—such as the controller trimming model— it is possible to convert between them using the impact

pressure Q_C. At sub-sonic speeds (from [Col95] p. 36):

$$Q_C = P_S \left\{ \left[1 + 0.2 \left(\frac{V_T}{A} \right)^2 \right]^{3.5} - 1 \right\} \tag{D.1}$$

where P_S is the static pressure and A is the speed of sound. Also (from [Col95] p. 38)

$$Q_C = P_{S0} \left\{ \left[1 + 0.2 \left(\frac{V_C}{A_0} \right)^2 \right]^{3.5} - 1 \right\} \tag{D.2}$$

Re-arranging (D.2) to make V_C the subject gives

$$V_C = A_0 \left\{ 5 \left[\left(1 + \frac{Q_C}{P_{S0}} \right)^{1/3.5} - 1 \right] \right\}^{1/2} \tag{D.3}$$

Simulink implementations of (D.1) and (D.3) are shown in Figure D.5. It is easy to connect these together using atmospheric data from 'Atmosphere Model' block supplied with Simulink to get a height-based conversion.

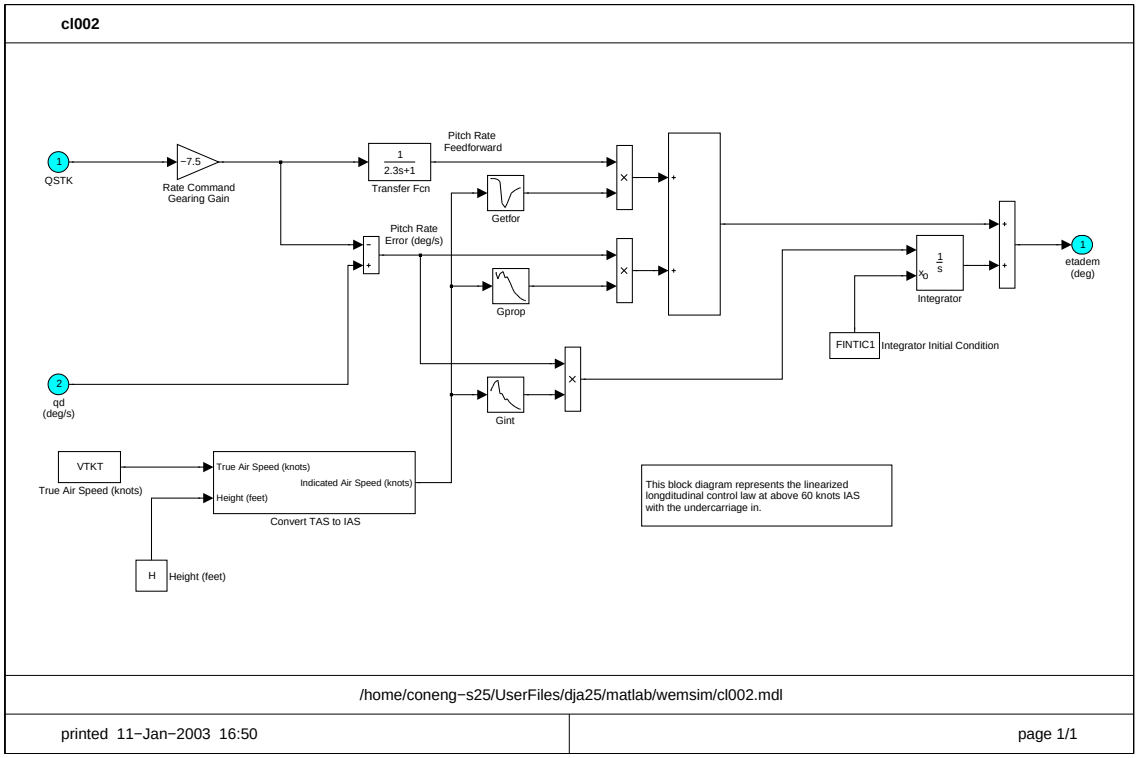

Figure D.3: Simplified Longitudinal Control Law from CL002

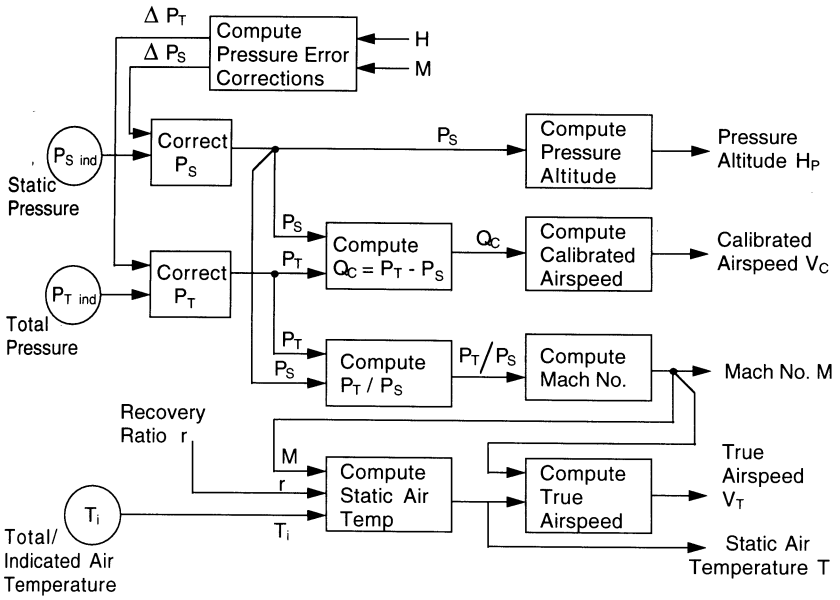

Figure D.4: Air data computation flow diagram (from [Col95] p. 53)

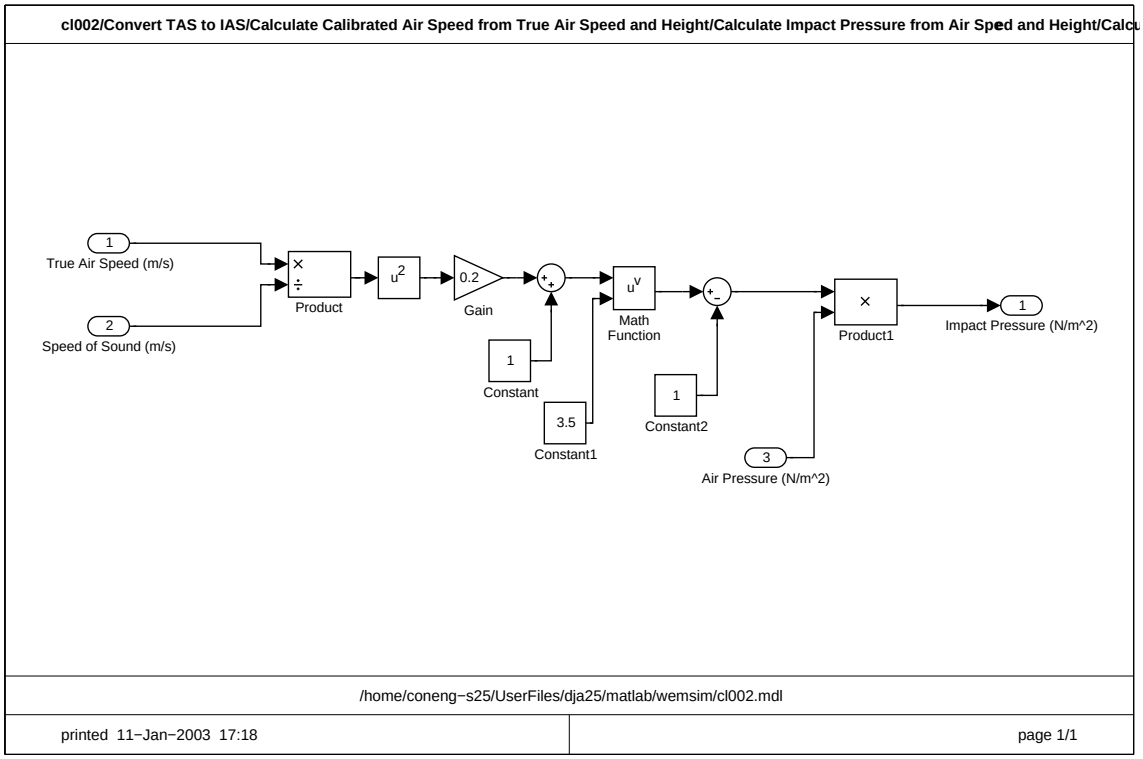

(a) Conversion from V_{T} to Q_{C}

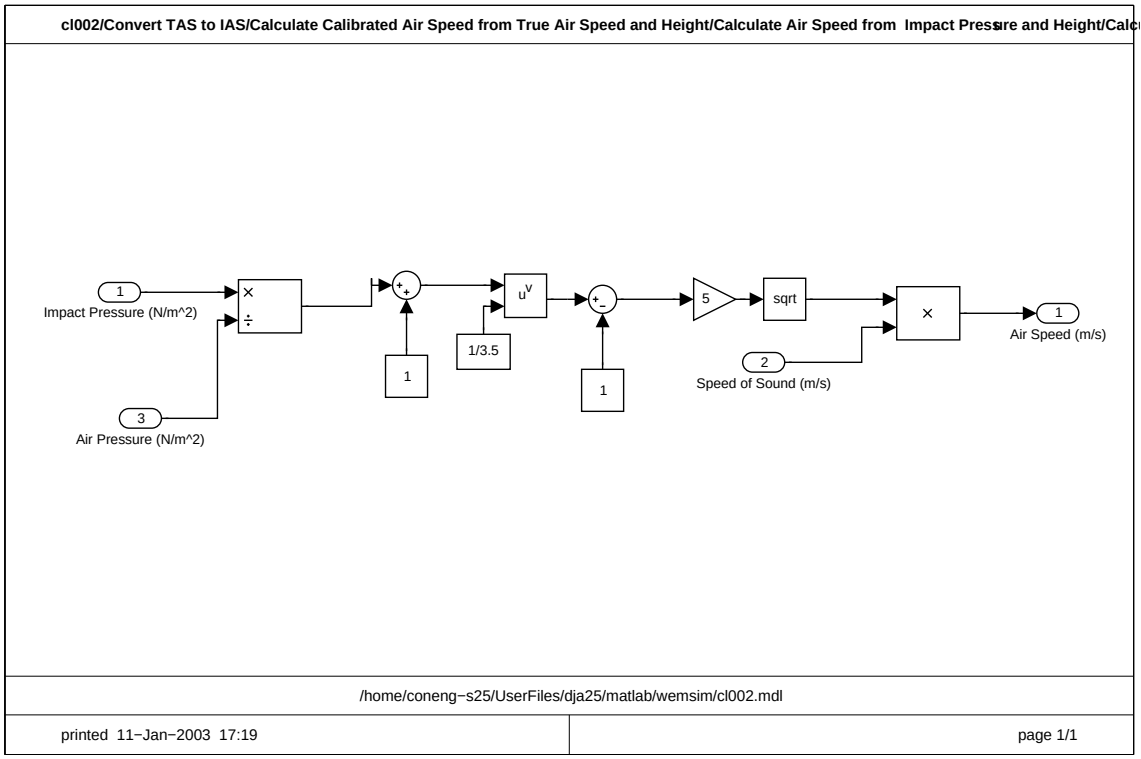

(b) Conversion from Q_{C} to V_{C}

Figure D.5: Converting between air speed and impact pressure

MATLAB function for calculation of W_o and W_i

```
function [Wo,Wi] = wopt(P,C,W)
%WOPT      Calculate optimal weightings for stability analysis.
%   [Wo,Wi] = wopt(P,C,W) calculates optimal weightings for stability
%   analysis.  P and C must be SYSTEM/CONSTANT matrices.
%
%   SEE ALSO: ISCONS, ISSYST, TPC, VRECIP.

% Check that we have correct number of inputs and outputs.
if (nargin ~= 3) | (nargout ~= 2)
  usage
  return
end

% Check that everything is a system matrix.
if ~(issyst(P) | iscons(P)) | ~(issyst(C) | iscons(C))
  error('P and C must be SYSTEM/CONSTANT matrices.')
end

% Find plant input-output dimensions.
Ny = ynum(P); Nu = unum(P);
Nz = Nu + Ny;

% Find optimal weights using mu-analysis functions.
T = tpc(P,C);
Tjw = frsp(T,W);
blk = [ones(Nz,1) zeros(Nz,1)];
[bnds,dvec,sens,pvec,gvec] = mu(Tjw, blk,'U');
[dl,dr] = muunwrap(dvec,blk);

% Extract the relevant bits of each matrix.
Wo = [];Wi = [];
for loop = 1:Ny
  Wo = daug(Wo, sel(dr, loop, loop));
  Wo = checkcons(Wo);
end
for loop = (Ny+1):(Nu+1)
  Wi = daug(Wi, vrecip(sel(dr, loop, loop)));
  Wi = checkcons(Wi);
end

return

function out = checkcons(mat)
[mattype,rowd,cold,num] = minfo(mat);
[data,rowpoint,indv,err] = vunpck(mat);
carryon = 1;
radjust = 0:(rowd - 1);
M1 = data(rowpoint(1) + radjust, :);
```

```
n = 1;
vary = 0;
while carryon
  n = n + 1;
  Mn = data(rowpoint(n) + radjust, :);
  if Mn ~= M1
    vary = 1;
    carryon = 0;
  end
  if n == num, carryon = 0; end
end
if vary
  out = mat;
else
  out = M1;
end
return


function usage
help wopt
return
```

Numerical values of weighting functions

The near-optimal weights W_{i} described in Section 7.3 have the following values:

Test Point 1

$$W_{\mathrm{i}}(s) = \frac{1.1532(s+1.7)(s+0.1056)(s^2+2.475s+4.204)}{s(s+4.207)(s+3.39)(s+0.3125)}$$

Test Point 2

$$W_{\mathrm{i}}(s) = \frac{1.1389(s+1.837)(s+0.1079)(s^2+2.517s+4.252)}{s(s+0.322)(s^2+7.735s+15.34)}$$

Mathematics for non-invalidation

Proposition D.1 (sufficient condition for non-invalidation (LTV perturbations)) *Given a nominal plant $P(z)$, input weight $W_{\mathrm{i}}(z)$ and validation data ($u \in \mathcal{S}_k^q, y \in \mathcal{S}_k^p$), all sampled with the same period, $\gamma > 0$ and a ν-gap radius β, let M be the central controller satisfying*

$$b\left(PW_{\mathrm{i}}, C\right) \geq \beta \ \forall \ C \in \left\{\hat{C} : \hat{C} = \mathcal{F}_\ell(M, Q), Q \in \mathcal{RH}_\infty, \|Q\|_\infty \leq 1\right\} \tag{D.4}$$

Given any sequences $w_{u0} \in \mathcal{S}_k^q, w_{y0} \in \mathcal{S}_k^p$, let

$$\begin{pmatrix} s \\ t \end{pmatrix} = \mathrm{ch}\left(M\right)^{-1} \begin{bmatrix} W_{\mathrm{i}}^{-1} & 0 \\ 0 & I \end{bmatrix} \begin{pmatrix} u + w_{u0} \\ y + w_{y0} \end{pmatrix} \tag{D.5}$$

Then there exists a system $\hat{P}(z) \in \mathcal{B}_\nu^{\mathrm{LTV}}\left(PW_{\mathrm{i}}, \beta\right)$, $w_u \in \mathcal{S}_k^q$, $w_y \in \mathcal{S}_k^p$, $y_{\mathrm{offset}} \in \mathbb{R}^p$ such that (7.1) holds if there exist $w_s \in \mathcal{S}_k^q$, $w_t \in \mathcal{S}_k^p$ and $y_{\mathrm{offset}} \in \mathbb{R}^p$ simultaneously satisfying

$$\begin{bmatrix} ||\Pi_j s||_2^2 + \mathrm{vec}\left(\Pi_j w_s\right)^* \mathrm{vec}\left(\Pi_j s\right) + \mathrm{vec}\left(\Pi_j s\right)^* \mathrm{vec}\left(\Pi_j w_s\right) & \mathrm{vec}\left(\Pi_j (t + w_t)\right)^* \\ \mathrm{vec}\left(\Pi_j (t + w_t)\right) & I \end{bmatrix} \geq 0$$

for all $j = 1, 2, \ldots, k$, and (7.2) where ξ is given by (7.3).

When these exist, realizations of w_u and w_y are given by $\begin{pmatrix} w_u \\ w_y \end{pmatrix} = \xi$.

Outline of proof. The proof follows exactly the same lines as that of Proposition 7.1 except that the LTV interpolation condition if Theorem 5.3 holds in place of the LTI one from Theorem 5.1. □

Test Point 1: Numerical validation results

Figure D.6 shows the numerical points used to produce the plots of Figure 7.12) (p. 132).

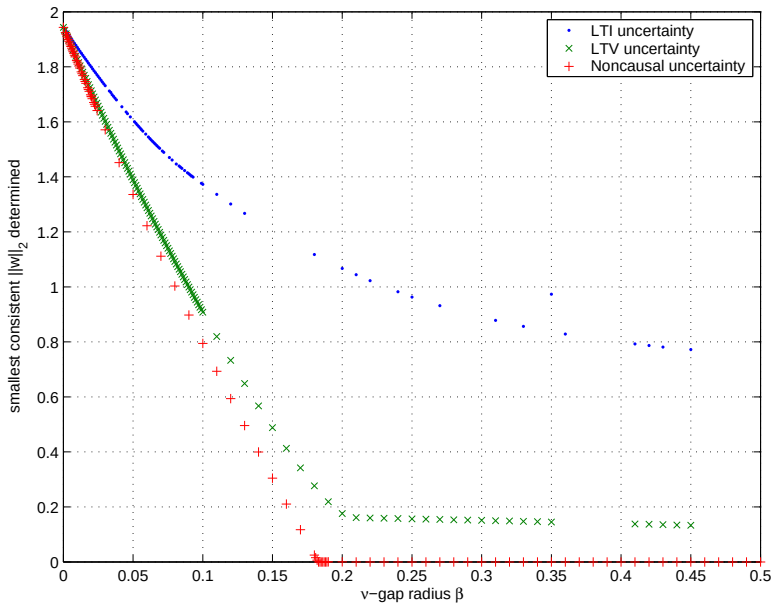

(a) β vs. $||w||_2$ trade-off with initial state fixed to zero

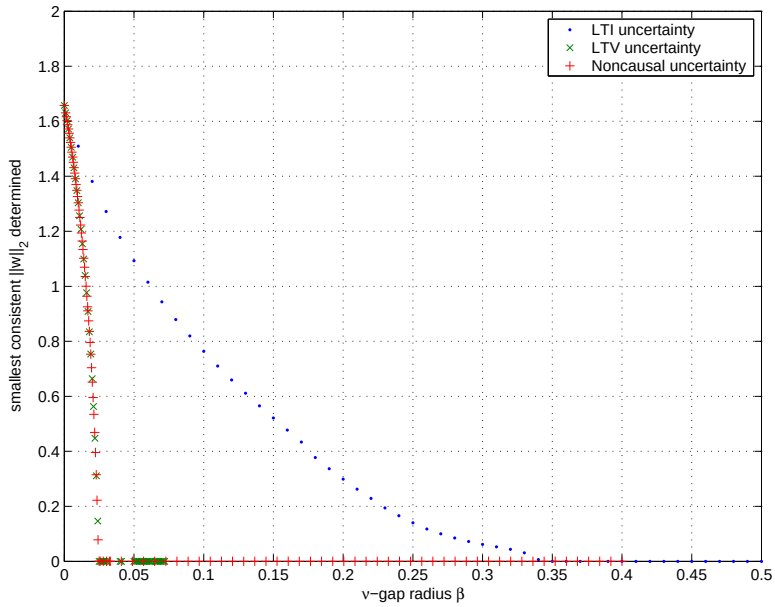

(b) β vs. $||w||_2$ trade-off with initial state free

Figure D.6: (Test Point 1) These graphs show the points returned by the optimizations that were used to produce the plots of Figures 7.12.Apparent outliers were attributed to numerical problems, and smooth lines were produced using MATLAB's (cubic) `spline` command.

Computing the first lower bound

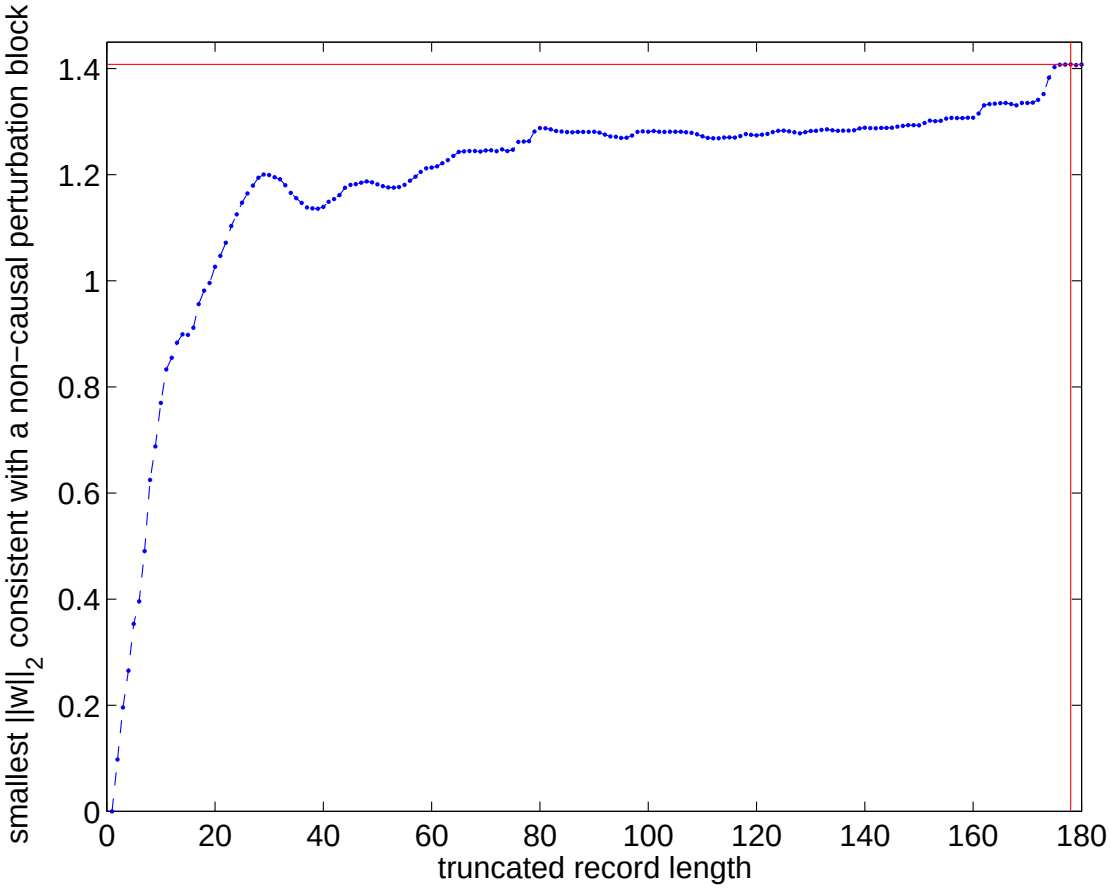

Figure D.7: Computing the first LTV lower bound for $\beta = 0.07$ (Test Point 2, no initial state). This shows clearly that the largest γ value obtained by applying non-causal invalidation criterion to truncated data records does not always correspond to the final truncation. In this case, the value for the 178th truncation is the maximum. The absence of monotinicity is particularly evident for truncations in the range 20–40.